



**RESTARTED HOLOMORPHIC EMBEDDING POWER
FLOW METHOD**

ALUISIO CESAR DOS SANTOS JUNIOR

ORIENTADOR: FRANCISCO DAMASCENO FREITAS
COORIENTADOR: LUIS FILOMENO DE JESUS FERNADES

DISSERTAÇÃO DE MESTRADO EM ENGENHARIA ELÉTRICA
DEPARTAMENTO DE ENGENHARIA ELÉTRICA

FACULDADE DE TECNOLOGIA
UNIVERSIDADE DE BRASÍLIA

UNIVERSIDADE DE BRASÍLIA
FACULDADE DE TECNOLOGIA
DEPARTAMENTO DE ENGENHARIA ELÉTRICA

RESTARTED HOLOMORPHIC EMBEDDING POWER
FLOW METHOD

ALUISIO CESAR DOS SANTOS JUNIOR

ORIENTADOR: FRANCISCO DAMASCENO FREITAS
COORIENTADOR: LUIS FILOMENO DE JESUS FERNANDES

DISSERTAÇÃO DE MESTRADO EM
ENGENHARIA ELÉTRICA

PUBLICAÇÃO: PPGEE.DM – 692/2018

BRASÍLIA/DF: 09 DE MARÇO - 2018

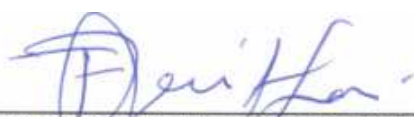
UNIVERSIDADE DE BRASÍLIA
FACULDADE DE TECNOLOGIA
DEPARTAMENTO DE ENGENHARIA ELÉTRICA

RESTARTED HOLOMORPHIC EMBEDDING POWER
FLOW METHOD

ALUISIO CESAR DOS SANTOS JUNIOR

DISSERTAÇÃO DE MESTRADO SUBMETIDA AO DEPARTAMENTO
DE ENGENHARIA ELÉTRICA DA FACULDADE DE TECNOLOGIA
DA UNIVERSIDADE DE BRASÍLIA, COMO PARTE DOS REQUISITOS
NECESSÁRIOS PARA A OBTENÇÃO DO GRAU DE MESTRE EM
ENGENHARIA ELÉTRICA.

APROVADA POR:



FRANCISCO DAMASCENO FREITAS, Dr., ENE/UNB
(ORIENTADOR)



KLEBER MELO E SILVA, Dr., ENE/UNB
(EXAMINADOR INTERNO)



RODRIGO ANDRADE RAMOS, Dr., USP
(EXAMINADORA EXTERNO)

BRASÍLIA/DF, 09 DE MARÇO DE 2018

FICHA CATALOGRÁFICA

SANTOS JUNIOR, ALUISIO CESAR DOS

RESTARTED HOLOMORPHIC EMBEDDING POWER
FLOW METHOD

[Distrito Federal] 2018.

xiv, 109 páginas, 297 mm (ENE/FT/UnB, Mestre, Engenheiros Eletricistas,
2018). Dissertação de Mestrado – Universidade de Brasília.

Faculdade de Tecnologia. Departamento de Engenharia Elétrica.

- | | |
|---------------------------|---------------------------------|
| 1. Fluxo de Potência | 2. Métodos Numéricos |
| 3. Métodos Não-Iterativos | 4. Método Holomorphic Embedding |
| I. ENE/FT/UnB | II. Título |

REFERÊNCIA BIBLIOGRÁFICA

Santos Junior, A. C. (2018). RESTARTED HOLOMORPHIC EMBEDDING POWER FLOW METHOD. Dissertação de Mestrado em Engenharia Elétrica, Publicação PPGEE.DM-692/2018, Departamento de Engenharia Elétrica, Faculdade de Tecnologia, Universidade de Brasília, Brasília, DF, 109 páginas.

CESSÃO DE DIREITOS

AUTOR: Aluisio Cesar dos Santos Junior

TÍTULO: RESTARTED HOLOMORPHIC EMBEDDING POWER FLOW METHOD

GRAU / ANO: Mestre em Engenharia Elétrica / 2018

É concedida à Universidade de Brasília permissão para reproduzir cópias desta dissertação de mestrado e para emprestar tais cópias somente para propósitos acadêmicos e científicos. O autor reserva outros direitos de publicação e nenhuma parte desta dissertação de mestrado pode ser reproduzida sem a autorização por escrito do autor.



Aluisio Cesar dos Santos Junior
Brasília – DF

AGRADECIMENTOS

∞

Agradeço a Deus por tudo.

Agradeço aos meus pais, Aluizio (in memoriam) e Nairdes, pelo esforço para que nada me faltasse e, sobretudo, por batalharem para que pudesse ter uma boa educação.

Agradeço a minha esposa Mychelle pela paciência nos momentos ausentes e imenso apoio e a minha filha Liz pela fonte de inspiração.

Agradeço ao Departamento de Engenharia Elétrica da Universidade de Brasília (UnB) pela oportunidade que me foi concedida em poder cursar um Mestrado Acadêmico conduzido por professores altamente qualificados e comprometidos com o programa.

Agradeço imensamente ao professor e orientador Francisco Damasceno pela grande motivação e apoio incondicional, porque sem o qual este trabalho não teria sido possível. Igualmente agradeço ao professor Filomeno.

Aluisio Junior

RESUMO

Esta dissertação apresenta uma formulação básica do método de fluxo de carga com adaptação holomórfica, do inglês *Holomorphic Embedding Load-flow Method* (HELM), com reinicialização, uma abordagem não-iterativa proposta para resolver o problema do fluxo de carga. A formulação básica do método é implementada computacionalmente realizando-se modificações na ferramenta MATPOWER tradicional. A nova abordagem para o HELM foi denominada nesta dissertação de Restarted Holomorphic Embedding Load-flow Model (RHELM). Na sua concepção básica, propõe-se uma técnica alternativa ao HELM que visa acelerar a convergência do método HELM original. Nesta proposta, uma "solução semente" adotada no HELM é atualizada a partir de valores iniciais, que por sua vez são atualizados a partir de valores parciais aproximados de tensão nodal, a cada reinicialização. Na técnica proposta neste trabalho, é suficiente uma aproximação de Padé de baixa ordem como técnica de continuação analítica, para atingir a precisão necessária para a série de potências de tensão nodal. O método requer o cálculo de alguns poucos termos da aproximação de Padé em oposição a uma aproximação de mais alta ordem usada para resolver pelo método HELM original. O desempenho do modelo proposto é avaliado para uma grande variedade de sistemas-teste, incluindo uma rede de 9241 barras. Os resultados obtidos revelam que, em comparação com métodos iterativos tradicionais, como o método de Newton Raphson, a formulação proposta é bastante eficiente para cálculos envolvendo sistemas de grande porte e pode ser uma ferramenta eficaz para solucionar sistemas com elevado nível de carregamento. O método proposto sempre apresenta convergência numérica para a solução, quando esta existe, diferentemente do HELM, que pode estagnar em um valor limite, mas sem a precisão numérica esperada.

Palavras-chave: Holomorphic Embedding Load-flow Method, fluxo de carga, continuidade analítica, aproximação de Padé, séries de potência

ABSTRACT

This work presents the basic formulation of the Holomorphic Embedding Load Flow Method (HELM), with restarting, a non-iterative approach proposed in order to solve the power flow problem. The basic formulation of the method is implemented computationally by carrying out a modification on the traditional MATPOWER tool. A new approach for the HELM, called Restarted Holomorphic Embedding Load-flow Model (RHELM), is proposed to accelerate the convergence of the original HELM. In this proposal, a "germ solution" adopted in the HELM is updated from initial values, which in turn are updated from approximate nodal voltage partial values, with each restart. The proposed method requires low order Padé approximant as an analytic continuation technique to reach the required precision to the voltage power series. The method requires the computation of a few terms of the Padé approximation as opposed to a higher order approximation used to solve the original HELM. The performance of the proposed method is evaluated for a wide variety of test systems including a 9241-bus network. The obtained results reveal that, in comparison with the traditional iterative methods (based on Newton Raphson method) and the original HELM, the proposed formulation is very efficient and robust for computations involving low- and large- scale systems and may be an effective tool for dealing with computation for stressed systems. The proposed method always presents numerical convergence for the solution, when it exists, unlike the HELM, which can stagnate in a limit value, but without the expected numerical precision.

Index terms: Holomorphic Embedding Load-flow Method, power flow, analytic continuation, Padé approximant, power series

Contents

| | | |
|----------|--|-----------|
| 1 | INTRODUCTION | 1 |
| 1.1 | OVERVIEW AND CONTEXTUALIZATION | 1 |
| 1.2 | STUDY MOTIVATION | 3 |
| 1.3 | OBJECTIVE | 4 |
| 1.4 | RELATED PUBLICATIONS | 4 |
| 1.5 | ORGANIZATION | 5 |
| 2 | ITERATIVE POWER FLOW SOLUTION METHODS | 6 |
| 2.1 | INTRODUCTION | 6 |
| 2.2 | POWER FLOW STUDY REASONS | 6 |
| 2.3 | THE POWER FLOW PROBLEM CHARACTERISTICS | 7 |
| 2.3.1 | Computation of Bus Admittance Matrix | 8 |
| 2.3.2 | Bus Classification | 14 |
| 2.3.3 | Power Balance Equations | 15 |
| 2.4 | SOLVING POWER BALANCE EQUATIONS | 17 |
| 2.4.1 | The Gauss-Seidel Family Methods | 17 |
| 2.4.2 | The Newton-Raphson Method | 19 |
| 2.4.3 | The Fast Decoupled Load Flow Method | 23 |
| 2.4.4 | Complexity Analysis Related to GS, NR and FDLF | 25 |
| 2.4.5 | Motivation for Non-Iterative Methods Development | 26 |
| 2.5 | NON-ITERATIVE METHODS | 27 |
| 2.5.1 | The Series Load Flow Method | 27 |
| 2.6 | CONCLUSION OF THE CHAPTER | 28 |
| 3 | THE HOLOMORPHIC EMBEDDING METHOD | 29 |
| 3.1 | INTRODUCTION | 29 |
| 3.2 | HOLOMORPHIC FUNCTION AND POWER SERIES COMPUTATION | 29 |
| 3.2.1 | Holomorphic Functions | 30 |
| 3.2.2 | Power Series Expansion of Holomorphic Functions | 30 |

| | | |
|----------|--|-----------|
| 3.3 | THE BASIC POWER BALANCE EQUATIONS USING HOLOMORPHIC EMBEDDING METHOD | 31 |
| 3.3.1 | Modeling for <i>slack</i> , PQ- and PV-buses | 31 |
| 3.3.2 | <i>Slack</i> -Bus HEM | 32 |
| 3.3.3 | Load Bus (PQ-bus) HEM | 33 |
| 3.3.4 | Generator Bus (PV-bus) HEM | 36 |
| 3.3.5 | Power Series Expansion Resulting After Applying HEM | 39 |
| 3.4 | HEM MATRIX REPRESENTATION | 41 |
| 3.5 | ANALYTIC CONTINUATION AND PADÉ APPROXIMANT | 42 |
| 3.6 | 2-BUS TUTORIAL CASE | 47 |
| 3.7 | CONCLUSION OF THE CHAPTER | 50 |
| 4 | STATE OF THE ART ON SOME HELM APPROACHES | 51 |
| 4.1 | INTRODUCTION | 51 |
| 4.2 | BIBLIOGRAPHICAL REVIEW | 51 |
| 4.3 | BIBLIOGRAPHICAL REVIEW SYNTHESIS | 57 |
| 4.4 | CONCLUSION OF THE CHAPTER | 59 |
| 5 | RESTARTED HOLOMORPHIC EMBEDDING POWER FLOW METHOD | 60 |
| 5.1 | INTRODUCTION | 60 |
| 5.2 | THE RESTARTED HOLOMORPHIC EMBEDDING METHOD | 60 |
| 5.2.1 | Situation for $n = 1$ | 62 |
| 5.2.2 | Situation for $n = 2$ | 64 |
| 5.2.3 | Situation for $n > 2$ | 65 |
| 5.3 | THREE-BUS TUTORIAL SYSTEM | 67 |
| 5.3.1 | General coefficient recursive relation for $n > 1$ | 69 |
| 5.3.2 | Linear System Variables Reduction | 70 |
| 5.3.3 | Padé approximant | 72 |
| 5.3.4 | Summary of RHELM Solution Process | 73 |
| 5.4 | CONCLUSION OF THE CHAPTER | 74 |
| 6 | EXPERIMENTS AND RESULTS | 76 |
| 6.1 | INTRODUCTION | 76 |
| 6.2 | COMPUTATIONAL ENVIROMENT | 77 |
| 6.2.1 | MATPOWER Structure as a Simulation Tool for Developing HELM and RHELM Models | 77 |
| 6.3 | A 3-BUS ILLUSTRATIVE GENERAL SYSTEM STUDY | 77 |

| | | |
|----------|---|------------|
| 6.3.1 | Description of the system model | 77 |
| 6.4 | 2-BUS TEST-SYSTEM STUDY | 82 |
| 6.4.1 | Study for Different Loadings | 83 |
| 6.4.2 | Study with Different Parameters for the Interconnection Circuit | 86 |
| 6.5 | ANALYSIS FOR MULTIBUS TEST SYSTEMS | 88 |
| 6.5.1 | 9-Bus System | 89 |
| 6.5.2 | 14-Bus System | 89 |
| 6.5.3 | 39-Bus System | 90 |
| 6.5.4 | 118-Bus System | 91 |
| 6.5.5 | 300-Bus System | 92 |
| 6.5.6 | 1354-Bus System | 93 |
| 6.5.7 | 9241-Bus System | 93 |
| 6.5.8 | Other Experiments with Smaller Number of Restarting | 94 |
| 6.6 | EXECUTION TIME CHARACTERISTICS | 96 |
| 6.7 | CONCLUSION OF THE CHAPTER | 99 |
| 7 | CONCLUSION | 101 |
| 7.1 | GENERAL CONCLUSIONS | 101 |
| 7.2 | FUTURE WORK SUGGESTIONS | 104 |
| | BIBLIOGRAPHY | 105 |

List of Tables

| | | |
|------|---|----|
| 2.1 | Bus classification summary | 15 |
| 4.1 | Bibliographical Review Synthesis | 58 |
| 6.1 | Transmission Line Branch Data Specification for the 3-bus System . . . | 78 |
| 6.2 | Bus Data Specification for the 3-bus System | 78 |
| 6.3 | Results for the 3-bus System | 81 |
| 6.4 | Convergence results by NR \times HELM \times RHELM for different load levels | 85 |
| 6.5 | Convergence results by NR \times HELM \times RHELM for different line reactances | 87 |
| 6.6 | Results of experiments for different restarting evaluated on the 300-, 1354- and 9241-bus models | 95 |
| 6.7 | Execution time relative to the computational burden performed by RHELM for the 39-, 118-, 300-, 1354- and 9241-bus systems | 97 |
| 6.8 | Execution time relative to the computational burden performed by HELM for the 39-, 118-, 300-, 1354- and 9241-bus systems | 98 |
| 6.9 | Execution time relative to the computational burden performed by NR method for the 39-, 118-, 300-, 1354- and 9241-bus systems | 98 |
| 6.10 | Ratio of the execution time with relation to the execution time of the NR method | 99 |

List of Figures

| | | |
|------|--|----|
| 2.1 | 3-bus transmission system one-line diagram | 9 |
| 2.2 | Two winding in-phase tap transformer model | 12 |
| 2.3 | Equivalent π -model for in-phase transformer | 13 |
| 2.4 | Components of a n -bus power system connected to a generic bus i | 16 |
| 3.1 | 3-bus system for illustrating the application of the Holomorphic Embedding Method | 41 |
| 3.2 | Original holomorphic embedding power flow solution flowchart | 47 |
| 3.3 | 2-bus test-system for illustrating the HEM application | 48 |
| 5.1 | Restarted-HELM power flow solution flowchart | 74 |
| 6.1 | MATPOWER's input data for the 3-bus system | 79 |
| 6.2 | MATPOWER's output data for the 3-bus system | 81 |
| 6.3 | 2-bus system for analysis of convergence and existence of solutions by NR, HELM and RHELM | 82 |
| 6.4 | Errors obtained for different load levels by the RHELM and HELM for case 1 to 3 for a maximum Padé order $L = M = 35$ | 86 |
| 6.5 | Errors obtained for different transmission line configurations by the RHELM and HELM for case 1 to 3 for a maximum Padé approximant order $L = M = 35$ | 87 |
| 6.6 | Solution convergence results by the RHELM and the original HELM methods for the 9-bus system | 89 |
| 6.7 | Solution convergence results by the RHELM and the original HELM methods for the 14-bus system | 90 |
| 6.8 | Solution convergence results by the RHELM and the original HELM methods for the 39-bus system with $N_0 = 2$, $R_n = 0$ and $N_R = 0$ | 90 |
| 6.9 | Solution convergence results by the RHELM and the original HELM methods for the 39-bus system with $N_0 = 2$, $R_n = 1$ and $N_R = 2$ | 91 |
| 6.10 | Solution convergence results by the RHELM and the original HELM methods for the 118-bus system | 92 |

| | | |
|------|---|----|
| 6.11 | Solution convergence results by the RHELM and the original HELM methods for the 300-bus system | 92 |
| 6.12 | Solution convergence results by the RHELM and the original HELM methods for the 1354-bus system | 93 |
| 6.13 | Solution convergence results by the RHELM and the original HELM methods for the 9241-bus system | 94 |
| 6.14 | Solution convergence results by the RHELM when $R_n = 1$ for the 300-bus system | 95 |
| 6.15 | Solution convergence results by the RHELM when $R_n = 1$ for the 1354-bus system | 96 |
| 6.16 | Solution convergence results by the RHELM when $R_n = 2$ for the 9241-bus system | 96 |

SYMBOL LIST AND ABBREVIATION

| | |
|--------------|---|
| α | Complex variable used in holomorphic embedding |
| a | Unknown coefficients in the numerator polynomial of the Padé approximant |
| A | A Matrix in a system $Ax = \gamma$ |
| a_{km} | Transformer Ratio between transformer nodes k and m |
| b | Unknown coefficients in the denominator polynomial of the Padé approximant |
| B | Shunt susceptance (\mathcal{U}) |
| δ | Phase angle |
| $f'(\alpha)$ | i^{th} derivative of the function $f(\alpha)$ |
| $f[n]$ | Power series coefficient of degree n for a function f |
| $f(\alpha)$ | Power series representation of function f using parameter α |
| G | Conductance (\mathcal{U}) |
| γ | γ vector in a system $Ax = \gamma$ |
| HE | Holomorphic Embedding |
| HEM | Holomorphic Embedding Method |
| $HELM$ | Holomorphic Embedding Load Flow Method |
| $HEPF$ | Holomorphic Embedding Power Flow Method (the same as HELM) |
| HV | High Voltage (pu) |
| I | Electric Current (A) |
| I_{km} | Electric Current between transformer nodes k and m |
| I_{mk} | Electric Current between transformer nodes m and k |
| L | Degree of numerator polynomial in the Padé approximant |
| λ | Imaginary part in a statement $\rho + j\lambda$ |
| $[L/M]$ | Notation in Padé approximant, where the power series are truncated in a numerator L and a denominator M |
| LV | Low Voltage (pu) |
| M | Degree of denominator polynomial in the Padé approximant |
| MTP | MATPOWER |
| n | Degree of α in the power series |

| | |
|---------------|--|
| N | Number of buses in a power system |
| P | Active Power (W) |
| P_i | Real power injection at bus i |
| PBE | Power Balance Equations |
| pu | <i>Per Unit</i> |
| Q | Reactive Power (var) |
| Q_i | Reactive power injection at bus i |
| R | Transmission Line Resistance (Ω) |
| $RHELM$ | Restarted Holomorphic Embedding Load Flow Method |
| $RHEM$ | Restarted Holomorphic Embedding Method |
| $RHEPF$ | Restarted Holomorphic Embedding Power Flow Method (the same as RHELM) |
| ρ | Real part in a statement $\rho + j\lambda$ |
| S | Complex Power (VA) |
| S_i | Complex power injection at bus i |
| V | Voltage (V) |
| V_i | Per unit voltage at bus i |
| V_j | Per unit voltage at bus j |
| V_k | Voltage at transformer node k |
| V_m | Voltage at transformer node m |
| V_p | Voltage at internal transformer non physical node p |
| V_i^{sp} | Specified voltage at bus i |
| $V_i(\alpha)$ | Voltage power series for bus i |
| $V_i(0)$ | Voltage function for bus i evaluated at $\alpha = 0$ (germ solution) |
| $V_i(1)$ | Voltage series for bus i evaluated at $\alpha = 1$ |
| $V_i re[n]$ | Real part of the voltage series coefficient of degree n |
| $V_i im[n]$ | Imaginary part of the voltage series coefficient of degree n |
| $V_i[n]$ | n^{th} order voltage series coefficients of bus i |
| $W_i(\alpha)$ | Inverse voltage power series for bus i |
| X | Transmission Line Reactance (Ω) |
| Y | Transmission Line Admittance (\mathcal{U}) |
| Y_{bus} | Bus admittance matrix |
| Y_{ij} | Admittance bus matrix entry between bus i and bus j |
| $Y_i sh$ | Shunt component of the bus admittance matrix at bus i |
| $Y_i tr$ | Non-shunt component of the bus admittance matrix between buses i and j |
| Z | Transmission Line Impedance (Ω) |

Chapter 1 INTRODUCTION

1.1 OVERVIEW AND CONTEXTUALIZATION

In Brazil, a large amount of electrical energy sources is located far away from the main loads. Also, there is a considerable growing of renewable energy sources in the networks. Therefore, the power network will have to change in order to be able to allow the energy transportation from the sources to the loads in general [1].

The power flow study is a numerical analysis for evaluating some quantities in an interconnected power system. This mathematical tool continues to be the focus of several investigations [2, 4–7], taking into account aspects of the modern transformations of the electrical networks.

This kind of study is required for planning and designing of future expansion of power systems as well as for determining operational conditions of existing systems. The goal of the power flow algorithm is to find an equilibrium point also known as steady state operation of the electric power system. The main information obtained from a power flow study is the magnitude and phase angle of the voltage at each bus and the active and reactive power flowing at each branch of the grid. To solve the nonlinear Power Balance Equations (PBE), for many decades, only several traditional iterative methods have been widely used, including the Gauss-Seidel (GS) method, the Newton-Raphson (NR) method, and the Fast Decoupled Load Flow (FDLF) method [3]. These techniques appear to work well for operating points near nominal system conditions. Furthermore, the numerical performance of these methods is dependent on the choice of the initial voltage guess. With an improper estimate of the starting point, these methods may converge to an unstable equilibrium point. Consequently, they neither guarantee to find a solution if one exists nor guarantee to find the “operable solution”. These techniques may diverge or converge to Low Voltage (LV) solutions [4]. One major concern with these methods is that numerical divergence of iterations does not necessarily mean the non-existence of a stable (from the point of view of voltage stability) power flow solution, namely High Voltage (HV) solution [5].

In 1981 Sauer [6] proposed to calculate an approximated solution of bus voltage based on its Taylor series expansion. On the other hand, it is not guaranteed that the series will converge to a value that expresses the bus voltage [7].

In 2012, based on a Holomorphic Embedding Method (HEM), which is a recursive and non-iterative mathematical tool to solve nonlinear equations, Trias [7] proposed to apply this technique to the power flow problem solution. The approach was called by the author as Holomorphic Embedding Load Flow Method (HELM). Despite the reliance on a Taylor series calculation, the approach is completely different from that proposed by Sauer. The series computed by using HELM has a too small radius of convergence. Then, Trias proposed to use an analytical continuation [8] adjustment in order to improve the radius of convergence. The improvement is based on the construction of a Padé approximant (continued analytical function) [8]. The following properties are aimed when an analytical function is used: it is guaranteed that the technique finds a solution if it exists; it will find only the operational solution; and will unequivocally signal if no solution exists through oscillations in the rational Padé approximation values for the voltage power series coefficients.

The HEM and its associated theory open up new perspectives on the power flow study. It provides a novel and recent approach on the problems of existence or multiplicity of solutions, and voltage collapse. In order to do that, advanced concepts on algebraic geometry and complex analysis are used [9].

The HELM original implementation was demonstrated on systems with pure PQ-buses and a slack-bus [7]. After this, some models also including PV-buses were proposed [10], [11].

On the HELM formulation, the voltages at all buses and the reactive power at the PV-buses are expressed as Maclaurin series of a complex embedding parameter α [8]. The solution of the original problem is verified when $\alpha = 1$. On the other hand, several strategies can be used to achieve the solution. But, the user must employ one which provide the best numerical performance to find the results. Hence, this is a challenge for dealing with HELM. An advantage is that, if an operation point exists at a given loading level, the correct voltage solution will be obtained by using a Padé approximant of the holomorphic series.

To generate the power series by using HELM, it is necessary to determine a germ

solution. This is the solution when the parameter α is null. The germ solution for the HELM is not analogous to the initial estimate of the solution in the NR method. Unlike the NR initial estimate, the germ solution is obtained by evaluating a set of equations [12].

1.2 STUDY MOTIVATION

Several works have reported advantages from the HELM approach (non-iterative or recursive method) [7,9,39] over the iterative family methods, such as the traditional NR. The main aspects are related to the searching for a solution on the boundary of the maximum loading point or even for a situation when NR diverges. For instance, due to an inadequate initial estimate. The HELM does not suffer of this constraining. On the other hand, as this technique was proposed recently (see [7] and other references on the subject), some works have presented contributions to improve the performance of the technique. The best strategy to compute the voltage power series dominates the investigations.

In some cases, a problem verified on the HELM approach is the amount of the power series coefficients needed for computing an adequate analytic function for a given quantity. In general, contributions of the high order power series terms are so small that floating point precision must be greatly extended. Even so, obtaining the final solution is quite slow. In [39] it is reported studies demonstrating that even for a very simple system, a mantissa of a 64-bit (double-precision or round-off of the order 10^{-15}) floating point is not sufficient to benefit from the theoretically perfect convergence of HELM.

In general the calculus are carried out taking into account handling scripts in a given programming language. For instance, MATLAB has double-precision as default. The computational aspects might be independent of this procedure. But, depending on the loading level of the system the found solution can stagnate for the HELM.

1.3 OBJECTIVE

This work proposes to use the HELM approach to solve a power flow problem, but considering that the germ solution is dependent of an initial bus (node) voltage and this dependence is exploited to reduce greatly the number of coefficients of the power series. This first germ solution then is used to generate a small number of coefficients of the power series needed by HELM and the result is employed to compute a partial analytical solution for the problem. As in general this first analytical solution has inadequate accuracy for the required result of the power flow problem, we propose to turn it as a new initial voltage to compute an updated germ solution. Following, an updated analytical solution is obtained. Again, for a very small number of coefficients for a voltage variable. This process goes on until a required accuracy be achieved. In view of this characteristic of updating the germ solution we call this new method as Restarted HELM (RHELM). The method and their variants found in the literature do not use this strategy, since they employ only a single initial germ solution. To demonstrate the efficacy of the proposed method, the following specific objectives are presented and investigated:

- description of the traditional power flow method: this introductory content aims to present main concepts associated to the classical power flow formulation, which is also adopted for the proposed method in this work;
- description of the original HELM and its variants: the original HELM is presented and shown its main aspects;
- description of the RHELM: a mathematical description of the method is made highlighting the main contributions of the purpose;
- experiments: several experiments are used to demonstrate the method performance compared to the original HELM and NR method.

1.4 RELATED PUBLICATIONS

The investigations related to the theme of this dissertation made possible the publication/acceptance of the following research papers in international and national conferences, respectively:

- A. C. Santos, F. D. Freitas and L. F. J. Fernandes, “Holomorphic Embedding Approach as an Alternative Method for Solving the Power Flow Problem,” 2017 in *Workshop on Communication Networks and Power Systems (WCNPS)*, Brasília, Brazil, 2017, pp. 1-4.
- A. C. Santos, F. D. Freitas and L. F. J. Fernandes, “Load Flow Problem Formulation as a Holomorphic Embedding Method,” 2018 in *VII Simpósio Brasileiro de Sistemas Elétricos (SBSE)*, Niterói, Brazil, 2018, pp. 1-6 (accepted paper).

1.5 ORGANIZATION

In addition to chapter 1, the text of this work is organized as follows:

- **Chapter 2**, where is presented the basic formulation for the general power flow problem and some adopted solution methodologies with focus on some well known iterative methods;
- **Chapter 3**, where is presented a detailed exposition on the HELM and how the embedding problem is considered for a traditional power flow problem;
- **Chapter 4**, where is presented a basic bibliographical review about the theme discussed in this work;
- **Chapter 5**, where is detailed the formulation for the RHELM, a new approach HELM based, proposed for improving the convergence for the original HELM;
- **Chapter 6**, in which the main computational results are presented and comparisons and performance reviews are performed to the NR, HELM and RHELM model approaches; and
- **Chapter 7**, in which the conclusions of this work are highlighted and suggestions for future works are presented.

Chapter 2 ITERATIVE POWER FLOW SOLUTION METHODS

2.1 INTRODUCTION

In this chapter, it is presented a description of the basic model for the general power flow problem and some adopted iterative methods to solve it. Firstly, some well known iterative methods are presented. Subsequently, a non-iterative technique which did not have success due its several restrictions is mentioned. Then, these conventional methods are compared and it is introduced the motivation to apply an investigation for non-iterative model aiming to solve the power flow problem, called Holomorphic Embedding Load-flow Method.

2.2 POWER FLOW STUDY REASONS

Power flow studies are undertaken for various reasons, some of which are well known [15]:

- quantification of line flows and bus voltages in the system (voltage profile);
- effect investigation of change in configuration and incorporation of changing due to system loading;
- study of the effect of temporary loss of transmission capacity and(or) generation on system loading and monitored effects;
- study of the effect of in-phase and quadrature boost voltages on system loading;
- economic system operation study;
- system loss minimization;
- transformer tap setting for economic operation;

- possible improvements to an existing power system by change of conductor sizes and system voltages;
- support for system planning, operation and control as well as for contingency analysis;
- estimate of system conditions before faults.

2.3 THE POWER FLOW PROBLEM CHARACTERISTICS

Under normal conditions electrical systems operate in their steady-state mode and the basic calculation required to determine the characteristics of this state is a kind of study denominated power flow (or load flow) problem. Therefore, the power flow problem consists in finding the steady-state operating point of an interconnected electric power system. More specifically, providing the load demanded at consumption buses and the power supplied by generators, the aim is to obtain all bus voltage phasors (for a given frequency, in general 60 Hz or 50 Hz) and complex power flowing through all network components. These information are essential for the continuous evaluation of the loading of a power system and for analyzing the effectiveness of alternative plans for system expansion to meet increased load demand [16].

The power flow solver is the most widely used application both in operating and in planning environments, either as a standalone tool or as a subroutine within more complex processes (stability analysis, optimization problems, training simulators, etc.). During the daily grid operation, the load flow constitutes the basic tool for security analysis, by identifying unacceptable voltage deviations or potential component overloading, as a consequence of both natural load evolution and sudden structural changes. It also allows the planning engineer to simulate different future scenarios that may arise for a forecast demand.

The power flow solution can be obtained in two stages. The first and most critical one is aimed at finding the complex voltage at all buses, for which conventional linear circuit analysis techniques have limitations. This is a consequence of complex powers, rather than impedances and sources, being specified as binding constraints, leading to a set of nonlinear equations. The second step simply consists of computing the remaining variables of interest, such as active and reactive power flows, ohmic losses, etc., which is a trivial problem since all bus voltages are available [17].

The load flow problem consists of the calculation of power flows and voltages of a network for specified terminal or bus conditions. A single-phase representation is adequate since power systems are usually assumed as balanced for normal operation. Four quantities are associated with each bus: the real and reactive power, the voltage magnitude, and the phase angle. Based on assumptions of these quantities, three types of buses are defined in the load flow calculation and at a bus, two of the four quantities are specified. To solve the problem, one reference bus must be selected (the slack-bus), to provide the additional real and reactive power to supply the transmission losses, since these are unknown until the final solution be obtained. At this bus the voltage magnitude and phase angle are known. The remaining buses of the system are designated either as voltage controlled buses or load buses. The real power and voltage magnitude are specified at a voltage controlled bus (PV-bus), while the real and reactive power are specified at a load bus (PQ-bus) [18].

The mathematical formulation of the power flow problem results in a system of algebraic nonlinear equations. The form of the equations depends on the selection of the independent variable set, i.e., voltages or currents. Thus, either the admittance or impedance network matrices can be used. The solution of the algebraic equations describing the power system are based, primarily, on an iterative technique because of their nonlinearity. The solution must fulfill Kirchhoff's laws, i.e., the algebraic sum of all flows at a bus must be equal zero. From a dual form, the algebraic sum of all voltages in a closed-loop (mesh) must be equal zero [18].

2.3.1 Computation of Bus Admittance Matrix

The first step in developing the mathematical model describing the power flow in the network is the computation of a bus admittance matrix. The bus admittance matrix is a complex $n \times n$ matrix (where n is the number of buses in the system) constructed from admittances of the equivalent circuit elements (shunt and series) of the circuit models of the power system. Most component models are represented by a combination of shunt elements (connected between a bus and the reference node) and series elements (connected between two system buses). The computation of the bus admittance matrix follows two simple rules [19]:

- The admittance of elements connected between node i and reference is added to the (i, i) entry of the admittance matrix;

- The admittance of elements connected between nodes i and j is added to the (i, i) and (j, j) entries of the admittance matrix. In general, the negative of the admittance is added to the (i, j) and (j, i) entries of the admittance matrix (one exception occurs for transformer with phase-shift).

For simple illustration on the admittance matrix construction, consider the 3-bus transmission system shown in Figure 2.1:

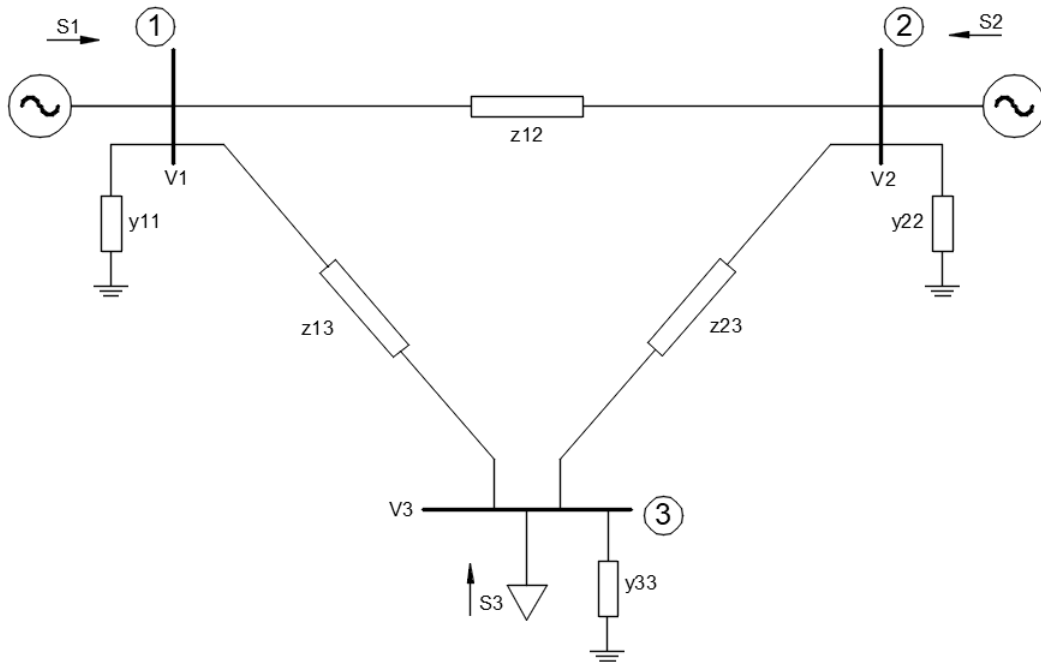


Figure 2.1: 3-bus transmission system one-line diagram

Each line impedance connecting buses 1, 2 and 3 are denoted by z_{12} , z_{23} and z_{31} , respectively. The corresponding line admittances are y_{12} , y_{23} and y_{31} . The shunt admittance at each bus is represented, as totally capacitive, by y_{11} , y_{22} and y_{33} , since they represent contributions of transmission lines.

According to the Kirchhoff's Current Law (KCL), the sum of all current contributions that leaves a node is equal to the sum of the currents that arrives to the same node. Considering the case of Figure 2.1, the branch admittances between the bus i and j can be defined as $y_{ij} = \frac{1}{z_{ij}} = \frac{1}{r_{ij} + jx_{ij}}$, where z_{ij} is the branch impedance, and r_{ij} and x_{ij} are the resistance and reactance composing the impedance, respectively [20].

Applying KCL at each bus and thus rearranging these equations, the current

injected into each node leads to the set of equations [21]:

$$\begin{cases} I_1 = V_1 y_{11} + (V_1 - V_2) y_{12} + (V_1 - V_3) y_{13} \\ I_2 = V_2 y_{22} + (V_2 - V_1) y_{21} + (V_2 - V_3) y_{23} \\ I_3 = V_3 y_{33} + (V_3 - V_1) y_{31} + (V_3 - V_2) y_{32} \end{cases} \quad (2.1)$$

which can be represented as a matrix form:

$$\begin{bmatrix} I_1 \\ I_2 \\ I_3 \end{bmatrix} = \begin{bmatrix} y_{11} + y_{12} + y_{13} & -y_{12} & -y_{13} \\ -y_{12} & y_{22} + y_{12} + y_{23} & -y_{23} \\ -y_{13} & -y_{23} & y_{33} + y_{13} + y_{23} \end{bmatrix} \begin{bmatrix} V_1 \\ V_2 \\ V_3 \end{bmatrix} \quad (2.2)$$

which is also equivalent to:

$$\begin{bmatrix} I_1 \\ I_2 \\ I_3 \end{bmatrix} = \begin{bmatrix} Y_{11} & Y_{12} & Y_{13} \\ Y_{21} & Y_{22} & Y_{23} \\ Y_{31} & Y_{32} & Y_{33} \end{bmatrix} \begin{bmatrix} V_1 \\ V_2 \\ V_3 \end{bmatrix} \quad (2.3)$$

The diagonal entries are calculated as:

$$\begin{cases} Y_{11} = y_{11} + y_{12} + y_{13} \\ Y_{22} = y_{22} + y_{12} + y_{23} \\ Y_{33} = y_{33} + y_{13} + y_{23} \end{cases} \quad (2.4)$$

while the off-diagonal entries are (for networks without phase-shift transformer):

$$\begin{cases} Y_{12} = Y_{21} = -y_{12} \\ Y_{13} = Y_{31} = -y_{13} \\ Y_{23} = Y_{32} = -y_{23} \end{cases} \quad (2.5)$$

For an n -bus system, the elements of the bus admittance matrix can be written down merely by inspection of the network. The diagonal terms are determined as:

$$Y_{ii} = \sum_{j=1}^n y_{ij} \quad (2.6)$$

where Y_{ii} (calculated when $j = i$) means the sum of all admittances connected to the bus, while y_{ii} is the equivalent shunt admittance connected to the bus i .

The off-diagonal terms are assumed to be of the form:

$$Y_{ij} = Y_{ji} = -y_{ij} \quad (2.7)$$

Extending the (2.3) to an n -bus system, the node equation for the system is formulated in a general matrix form as [21]:

$$\begin{bmatrix} I_1 \\ I_2 \\ \vdots \\ I_i \\ \vdots \\ I_n \end{bmatrix} = \begin{bmatrix} Y_{11} & Y_{12} & \dots & Y_{1i} & \dots & Y_{1n} \\ Y_{21} & Y_{22} & \dots & Y_{2i} & \dots & Y_{2n} \\ \vdots & \vdots & & \vdots & & \vdots \\ Y_{i1} & Y_{i2} & \dots & Y_{ii} & \dots & Y_{in} \\ \vdots & \vdots & & \vdots & & \vdots \\ Y_{n1} & Y_{n2} & \dots & Y_{ni} & \dots & Y_{nn} \end{bmatrix} \begin{bmatrix} V_1 \\ V_2 \\ \vdots \\ V_i \\ \vdots \\ V_n \end{bmatrix} \quad (2.8)$$

The matrix representation is useful for enabling the use of computational tools in the resolution of linear systems. The representation in (2.8) can also be written as in (2.9) or (2.10), since the objective is to find the voltages in each power grid node [20].

$$I_{bus} = Y_{bus} V_{bus} \quad (2.9)$$

$$V_{bus} = Y_{bus}^{-1} I_{bus} \quad (2.10)$$

where I_{bus} is the vector of the injected bus currents (i.e, external current sources). But in case of using (2.10), if Y_{bus} is singular, the set of equation must be determined by using other strategy instead of computing the inverse of this matrix.

The following can be adopted in (2.9) and (2.10): the current is positive when flowing towards the bus, and negative if it is flowing away from the bus. V_{bus} is the vector of nodal bus voltages measured from the reference node (i.e., node voltages). Y_{bus} is known as the *bus admittance matrix*.

From the resolution of (2.10) it is possible to find the nodal voltages of the system. However, the values of injected currents into the buses are also not known, resulting in a problem of nonlinear equations that are usually solved by iterative methods. In a real-world power system network, there are a large number of buses and each one is connected to only the nearest ones, so that many of the elements outside the diagonal matrix are null, characterizing it as a highly sparse matrix [20].

2.3.1.1 Off-nominal in-phase Tap Transformer Model

Off-nominal transformer taps (transformers with transformation ratios different from the system voltage bases at the terminals) present some special difficulties. Figure

2.2 shows a representation for a type of an off-nominal turns ratio transformer [19], where Z_{km} is the series impedance of the transformer at nominal operation conditions and I_{km} and I_{mk} are currents flowing from each bus of the transformer; $V_k = |V_k|e^{j\theta_k}$ and $V_m = |V_m|e^{j\theta_m}$ are nodal voltages at physical buses k and m of the transformer, while $V_p = |V_p|e^{j\theta_p}$ is a nodal voltage for an internal and fictitious node p ; a_{km} is the off-nominal turn ratio in pu. This a complex-valued parameter, but in this work we consider it assuming just a positive real value.

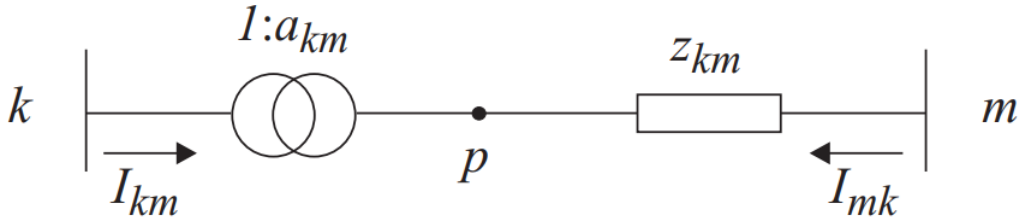


Figure 2.2: Two winding in-phase tap transformer model

For this model the ideal transformer voltage magnitude ratio (turns ratio) must satisfy:

$$\frac{V_p}{V_k} = a_{km} \quad (2.11)$$

Since the transformer is assumed to have taps in phase, the condition in the ideal transformer in (2.11) leads to $\theta_k = \theta_p$, where θ_k and θ_p are the phases of V_k and V_p , respectively. Therefore, in this situation, a_{km} is a real number.

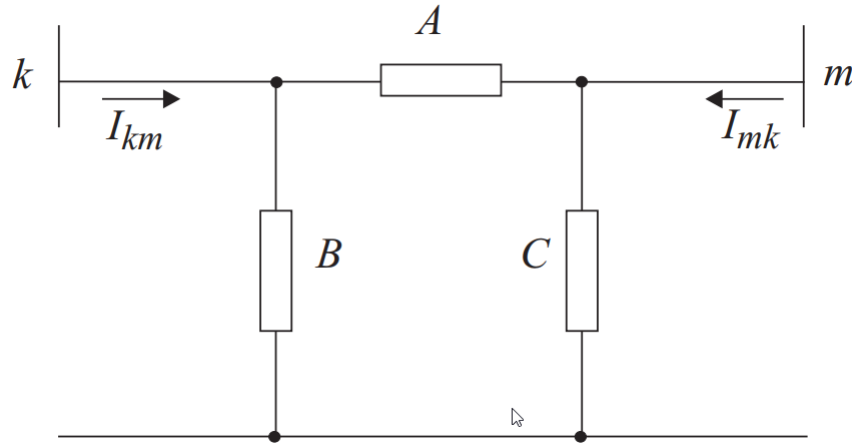
The ideal transformer (the k - p part of the model) yields:

$$V_k I_{km}^* + V_p I_{mk}^* = 0 \quad (2.12)$$

Then, by using (2.11) gives

$$\frac{I_{km}}{I_{mk}} = -\frac{|I_{km}|}{|I_{mk}|} = -a_{km} \quad (2.13)$$

which means that the complex currents I_{km} and I_{mk} are out of phase by 180° since $a_{km} \in \mathbb{R}$. The Figure 2.3 represents the equivalent π -model for the in-phase tap transformer in Figure 2.2.

Figure 2.3: Equivalent π -model for in-phase transformer

Parameters A, B, and C of this model can be obtained by identifying the coefficients of the expressions for the complex currents I_{km} and I_{mk} associated with the models of Figure 2.2 and 2.3.

$$I_{km} = -a_{km}y_{km}(V_m - V_p) = (a_{km}^2y_{km})V_k + (-a_{km}y_{km})V_m \quad (2.14)$$

$$I_{mk} = y_{km}(V_m - V_p) = (-a_{km}y_{km})V_k + (y_{km})V_m \quad (2.15)$$

or in matrix form:

$$\begin{bmatrix} I_{km} \\ I_{mk} \end{bmatrix} = \begin{bmatrix} a_{km}^2y_{km} & -a_{km}y_{km} \\ -a_{km}y_{km} & y_{km} \end{bmatrix} \begin{bmatrix} V_k \\ V_m \end{bmatrix} \quad (2.16)$$

As seen the matrix on the right hand side of (2.16) is symmetric. Figure 2.3 provides now the following:

$$I_{km} = (A + B)V_k + (-A)V_m \quad (2.17)$$

$$I_{mk} = (-A)V_k + (A + C)V_m \quad (2.18)$$

or in matrix form:

$$\begin{bmatrix} I_{km} \\ I_{mk} \end{bmatrix} = \begin{bmatrix} A + B & -A \\ -A & A + C \end{bmatrix} \begin{bmatrix} V_k \\ V_m \end{bmatrix} \quad (2.19)$$

Identifying the matrix elements from the matrices in equations (2.16) and (2.19) yields [24]:

$$A = a_{km}y_{km} \quad (2.20)$$

$$B = a_{km}(a_{km} - 1)y_{km} \quad (2.21)$$

$$C = (1 - a_{km})y_{km} \quad (2.22)$$

A remark should be done on the off-nominal tap position with relation to the side of the transformer (winding at the side of bus k or m). The off-nominal tap can be assumed at the side of the bus m , as adopted in the previous model or at the side of the bus k as adopted in the Matpower model default [14]. However, even in the case of using Matpower, expressions (2.20)-(2.22) are still valid. But the user need to consider the value $1/a_{km}$ in these equations. This means that Matpower's tap \bar{a} is at the side of the bus k and $\bar{a} = 1/a_{km}$. Therefore, for this situation the same model in Figure 2.3 must be used.

2.3.2 Bus Classification

A bus is a point or node at which transmission lines, loads, generators or other devices are connected. In a power system study, every bus is associated with four quantities, such as magnitude of voltage, $|V|$, phase angle of voltage, δ , active power, P , and reactive power, Q . Two of these bus quantities are specified and the remaining two variables are unknown. The bus types are categorized depending on its two specified variables. Thus, the system buses are generally classified into three categories [25]:

Load bus: at this bus type the active and reactive powers are specified. The magnitude and the phase angle of the bus voltages are unknown. This bus type is denominated PQ-bus. This is classified as a non-generator bus whose information about the powers can be obtained from historical data records, measurement or forecast. In this type of bus the real and reactive power supplied to the bus (or injected power) is assumed to be positive, while the power consumed at the bus is defined as negative. Hence, the net power consumed at this bus is known and the specified variables are P and Q . Finally, the unknown variables are $|V|$ and δ ;

Generator bus: This type of bus is known as *regulated voltage bus*, because the voltage magnitude at the bus is specified. As a consequence it is known as *voltage controlled bus*. At this bus type, the real power and voltage magnitude are specified. The bus voltage phase angle and the reactive power are to be determined. The limits on the value of the reactive power should also be specified, but this constraining has

no influence on the classification of the bus type. This bus type is called PV-bus. In general this bus is associated to a generator unit in which output active power generated is controlled by adjusting the prime mover and the voltage can be regulated by adjusting the excitation system set-point of the generator. Often, limits are given to the values of the reactive power depending upon the characteristics of individual machine. As for PQ-bus, net injected power into the bus assumes a positive value, while consumed power (case of motor) has negative values. The known variables in this bus are P and $|V|$ and the unknowns are Q and δ ; and

Slack-bus: This bus is taken as angular reference for the system. So, the magnitude and phase angle of the voltage are specified. This bus makes up the difference between the scheduled loads and generated power that are caused by losses in the network. Hence, this bus is used as a reference in order to meet the power balance condition at the network. The slack-bus is usually selected as a power station with a huge capacity. This is justified since it must supply the power unbalance of the system. The known variables on this bus are $|V|$ and δ and the unknowns are P and Q .

For the basic 3-bus transmission system shown in Figure 2.1, bus 1 is set as slack-bus, bus 2 is a PV-bus and bus 3 is a PQ-bus. Table 2.1 summarizes the classification of the bus system.

Table 2.1: Bus classification summary

| ID number | Type of Bus | Variables | | | |
|-----------|--------------------|-----------|---------|---------|----------|
| | | P | Q | $ V $ | δ |
| 1 | Slack Bus | Unknown | Unknown | Known | Known |
| 2 | Generator Bus (PV) | Known | Unknown | Known | Unknown |
| 3 | Load Bus (PQ) | Known | Known | Unknown | Unknown |

2.3.3 Power Balance Equations

Consider a typical bus of a power system network as shown in Figure 2.4. In this partial one-line diagram, the transmission lines are represented by their equivalent π models where series impedances have been converted to per unit (pu) admittances on a common MVA base [21].

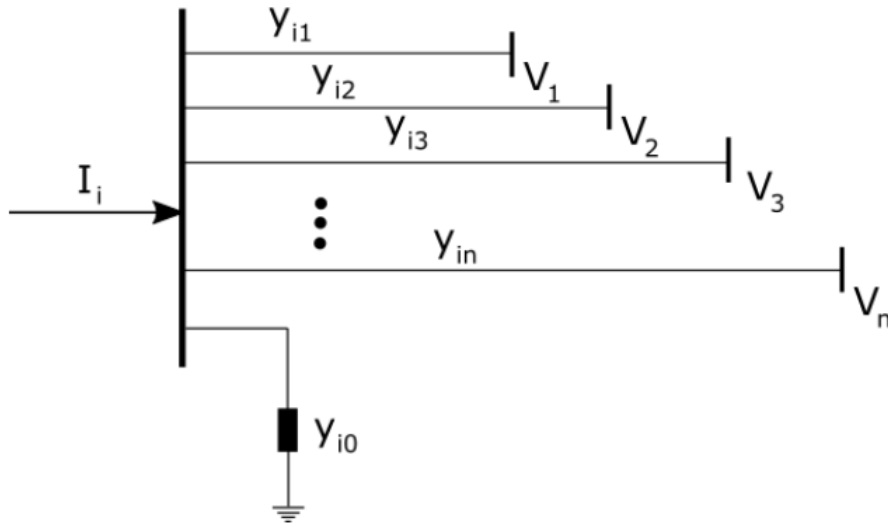


Figure 2.4: Components of a n -bus power system connected to a generic bus i

The application of the KCL to this system and specifically to the bus i yields:

$$\begin{aligned} I_i &= y_{i0}V_i + y_{i1}(V_i - V_1) + y_{i2}(V_i - V_2) + \dots + y_{in}(V_i - V_n) \\ &= (y_{i0} + y_{i1} + y_{i2} + \dots + y_{in})V_i - y_{i1}V_1 - y_{i2}V_2 - \dots - y_{in}V_n \end{aligned} \quad (2.23)$$

which can also be represented as:

$$I_i = V_i \sum_{j=0}^n y_{ij} - \sum_{j=1}^n y_{ij}V_j, \quad j \neq i \quad (2.24)$$

Rewriting (2.24), yields:

$$I_i = \sum_{j=1}^n Y_{ij}V_j \quad (2.25)$$

In equation (2.25), j includes bus i . Expressing this equation in polar form, it can be represented as [21]:

$$I_i = \sum_{j=1}^n |Y_{ij}||V_j|\angle(\theta_{ij} + \delta_j) \quad (2.26)$$

where θ_{ij} is the phase angle of the admittance matrix entry Y_{ij} .

The complex power at bus i is given by:

$$P_i - jQ_i = V_i^* I_i \quad (2.27)$$

Substituting (2.26) for I_i in (2.27) it is obtained the next equation:

$$P_i - jQ_i = |V_i| \angle -\delta_i \sum_{j=1}^n |Y_{ij}| |V_j| \angle (\theta_{ij} + \delta_j) \quad (2.28)$$

Breaking up the complex equation in (2.28) into their real and imaginary parts, it is obtained a set of nonlinear algebraic equations (also known as Power Balance Equations) in terms of the independent variables, voltage magnitude, in pu, and phase angle, in radians:

$$P_i = \sum_{j=1}^n |V_i| |V_j| |Y_{ij}| \cos(\theta_{ij} - \delta_i + \delta_j) \quad (2.29)$$

$$Q_i = - \sum_{j=1}^n |V_i| |V_j| |Y_{ij}| \sin(\theta_{ij} - \delta_i + \delta_j) \quad (2.30)$$

2.4 SOLVING POWER BALANCE EQUATIONS

Currently, the most widely applied Power Flow solvers are the Newton-Raphson and the Fast Decoupled Load-Flow methods. The Gauss-Seidel method for solving the Power Flow problem was popular in the 1960s. The performance of different power flow solution methods can be affected by the characteristics of the power systems, including topology, branch parameters, load profile and size [22].

2.4.1 The Gauss-Seidel Family Methods

The Gauss-Seidel (GS) is the earliest proposed method used to solve the power flow problem. This method is developed based on the Gauss method. It is an iterative

method used for solving a set of nonlinear algebraic equations. The method makes use of an initial guess for value of voltage, to obtain a calculated value of a particular variable. The initial guess value is replaced by a calculated value. The process is then repeated until the iteration solution converges. The convergence is quite sensitive to the starting values assumed [23].

This scheme sequentially sweeps each node, updating its complex voltage in terms of the voltages of adjacent buses until the infinity norm of the difference of the voltage values from consecutive iterations is smaller than a specified tolerance [26].

Assuming that a system has a slack-bus (bus 0) and N load buses, the power injection at bus i can be written as:

$$S_i = V_i I_i^* = V_i \left(\sum_{j=0}^N Y_{ij} V_j \right)^* = V_i \sum_{j=0}^N Y_{ij}^* V_j^* \quad (2.31)$$

where the index for the slack-bus is assigned as 0; S_i is the complex power injection at bus i ; V_i is the nodal voltage at bus i , and $Y_{ij} = (G_{ij} + jB_{ij})$ is the $(i,j)^{th}$ admittance matrix entry. Then the above equation can be written as:

$$S_i^* = V_i^* \sum_{j=0}^N Y_{ij} V_j = V_i^* \left(Y_{ii} V_i + \sum_{j=0, j \neq i}^N Y_{ij} V_j \right) \quad (2.32)$$

Rearranging (2.32), the voltage at each load bus is given by:

$$V_i = \frac{1}{Y_{ii}} \left(\frac{S_i^*}{V_i^*} - \sum_{j=0, j \neq i}^N Y_{ij} V_j \right) \quad (2.33)$$

The process of updating values for the unknown voltages is illustrated in the sequel.

$$\left\{ \begin{array}{l} V_1^{(n+1)} = \frac{1}{Y_{11}} \left(\frac{S_1^*}{V_1^{(n)*}} - Y_{10} V_0 - \sum_{j=2}^N Y_{1j} V_j^{(n)} \right) \\ V_2^{(n+1)} = \frac{1}{Y_{22}} \left(\frac{S_2^*}{V_2^{(n)*}} - Y_{20} V_0 - Y_{21} V_1^{(n+1)} - \sum_{j=3}^N Y_{2j} V_j^{(n)} \right) \\ \vdots \\ V_i^{(n+1)} = \frac{1}{Y_{ii}} \left(\frac{S_i^*}{V_i^{(n)*}} - Y_{i0} V_0 - \sum_{j=1}^{i-1} Y_{ij} V_j^{(n+1)} - \sum_{j=i+1}^N Y_{ij} V_j^{(n)} \right) \\ \vdots \\ V_N^{(n+1)} = \frac{1}{Y_{NN}} \left(\frac{S_N^*}{V_N^{(n)*}} - Y_{N0} V_0 - \sum_{j=1}^{N-1} Y_{1j} V_j^{(n+1)} \right) \end{array} \right. \quad (2.34)$$

where the superscript n in $V_i^{(n)}$ represents the updated result of V_i after the n^{th} iteration and will be used in the $(n+1)^{\text{th}}$ iteration. Then the infinity norm of the difference of the voltage values is used to decide whether the iteration process should be terminated or not.

The implementation of the GS-based algorithm is relatively easy to do. In this algorithm an LU factorization of the associated matrix is not needed. Thus, it takes a relatively small amount of memory and has low computational complexity. Although the computational effort per iteration is moderate, the convergence of this method is linear, which means that the tolerance decreases more or less linearly with the number of iterations (and tends to increase as the dimension N of the system increases). This represents an important limitation for large systems, as the total computational cost, and hence solution time, increases considerably as larger systems are solved [17].

2.4.2 The Newton-Raphson Method

The Newton-Raphson method is one largely employed for solving nonlinear equation systems. The method is iterative and needs an initial estimate to initialize the iterations. Its convergence is achieved when a specified tolerance is obtained for the mismatch of the balance equations.

To illustrate the method applied to a nonlinear equations represented by $f(x) = 0$, $x \in \mathbb{R}$, and $f(x) \in \mathbb{R}$, consider an initial estimates $x^{(0)}$ for a set of roots of $f(x) = 0$. A perturbation around the point $x^{(0)}$ is defined as $\Delta x^{(0)}$. Then, a first updated solution for the roots can be defined as $x^{(1)} = x^{(0)} + \Delta x^{(0)}$. A new updating of this solution leads to $x^{(2)} = x^{(1)} + \Delta x^{(1)}$ and so on. Essentially, the problem consists in finding the true roots by a linear approximation of $f(x)$ by causing small disturbances on the obtained partial solutions. These numerical perturbations become smaller as the result of the iterative process converges to a root set of the problem. So, the problem is iterative in nature, because small disturbances are needed until the specified tolerance for convergence is reached.

For an estimate $x = x^{(0)}$ and a disturbance $\Delta x^{(0)}$, there is a mismatch $c \in \mathbb{R}$ on the root approximation in such way that

$$f(x^{(0)} + \Delta x^{(0)}) = c. \quad (2.35)$$

On the other hand, the function $f(x)$ can be expanded in a Taylor series around $x^{(0)}$ [21] giving the approximation

$$f(x^{(0)}) + \left(\frac{df}{dx}\right)^{(0)} \Delta x^{(0)} + \frac{1}{2!} \left(\frac{d^2f}{dx^2}\right)^{(0)} (\Delta x^{(0)})^2 + \dots \approx c \quad (2.36)$$

Assuming the root $x^{(0)}$ is so close to the correct solution that $\Delta x^{(0)}$ is a very small value, then the terms of higher orders can be neglected. Thus, (2.36) can be approximated linearly, as in (2.37), where $\Delta c^{(0)} = c - f(x^{(0)})$, is the mismatch for the solution $x^{(0)}$ or the residue.

$$\Delta c^{(0)} = c - f(x^{(0)}) \simeq \left(\frac{df}{dx}\right)^{(0)} \Delta x^{(0)} \Rightarrow \Delta x^{(0)} \simeq \left[\left(\frac{df}{dx}\right)^{(0)}\right]^{-1} \Delta c^{(0)} \quad (2.37)$$

Thus, the initial estimate added to increment $\Delta x^{(0)}$ results in the updated solution approximation $x^{(1)}$, given by

$$x^{(1)} = x^{(0)} + \Delta x^{(0)} \quad (2.38)$$

The iterative process repeats itself until x converges, which happens when the value of the increment becomes too small, or less than a value $\epsilon > 0$, the *specified tolerance* for convergence. Equations (2.39), (2.40) and (2.41) can be used for describing a general form of the Newton-Raphson method algorithm [20].

$$\Delta c^{(k)} = c - f(x)^{(k)} \quad (2.39)$$

$$\Delta x^{(k)} = \left[\left(\frac{df}{dx}\right)^{(k)}\right]^{-1} \Delta c^{(k)} \quad (2.40)$$

$$x^{(k+1)} = x^{(k)} + \Delta x^{(k)} \quad (2.41)$$

The term $\left(\frac{df}{dx}\right)^{(k)}$ of (2.40) defines the Jacobian matrix for $f(x)$ at $x = x^{(k)}$.

2.4.2.1 Jacobian Matrix

The Jacobian matrix for a problem with n functions and variables x_i , for $i = 1, 2, \dots, n$, i.e., $f(x) \in \mathbb{R}^n$, $x \in \mathbb{R}^n$, around an initial estimate, $x^{(0)} \in \mathbb{R}^n$, just as in

(2.16), is calculated as

$$\begin{cases} f_1^{(0)} + \left(\frac{\partial f_1}{\partial x_1}\right)^{(0)} \Delta x_1^{(0)} + \left(\frac{\partial f_1}{\partial x_2}\right)^{(0)} \Delta x_2^{(0)} + \dots + \left(\frac{\partial f_1}{\partial x_n}\right)^{(0)} \Delta x_n^{(0)} = c_1 \\ f_2^{(0)} + \left(\frac{\partial f_2}{\partial x_1}\right)^{(0)} \Delta x_1^{(0)} + \left(\frac{\partial f_2}{\partial x_2}\right)^{(0)} \Delta x_2^{(0)} + \dots + \left(\frac{\partial f_2}{\partial x_n}\right)^{(0)} \Delta x_n^{(0)} = c_2 \\ \vdots \\ f_n^{(0)} + \left(\frac{\partial f_n}{\partial x_1}\right)^{(0)} \Delta x_1^{(0)} + \left(\frac{\partial f_n}{\partial x_2}\right)^{(0)} \Delta x_2^{(0)} + \dots + \left(\frac{\partial f_n}{\partial x_n}\right)^{(0)} \Delta x_n^{(0)} = c_n \end{cases} \quad (2.42)$$

Equation (2.43) is another form of (2.42). Essentially, again the goal is to find the increment $\Delta x_i^{(0)}$, for $i = 1, 2, \dots, n$. In the same way, it is possible to find the increments for the k^{th} iteration. Equations (2.44), (2.45) and (2.46) describe expressions at the k^{th} iteration of the Newton-Raphson method for the case when exist n functions with n variables.

$$\begin{bmatrix} c_1 - (f_1)^{(0)} \\ c_2 - (f_2)^{(0)} \\ \vdots \\ c_n - (f_n)^{(0)} \end{bmatrix} = \begin{bmatrix} \left(\frac{\partial f_1}{\partial x_1}\right)^{(0)} & \left(\frac{\partial f_1}{\partial x_2}\right)^{(0)} & \dots & \left(\frac{\partial f_1}{\partial x_n}\right)^{(0)} \\ \left(\frac{\partial f_2}{\partial x_1}\right)^{(0)} & \left(\frac{\partial f_2}{\partial x_2}\right)^{(0)} & \dots & \left(\frac{\partial f_2}{\partial x_n}\right)^{(0)} \\ \vdots & \vdots & \ddots & \vdots \\ \left(\frac{\partial f_n}{\partial x_1}\right)^{(0)} & \left(\frac{\partial f_n}{\partial x_2}\right)^{(0)} & \dots & \left(\frac{\partial f_n}{\partial x_n}\right)^{(0)} \end{bmatrix} \begin{bmatrix} \Delta x_1^{(0)} \\ \Delta x_2^{(0)} \\ \vdots \\ \Delta x_n^{(0)} \end{bmatrix} \quad (2.43)$$

$$\Delta C^{(k)} = J^{(k)} \Delta X^{(k)} \quad (2.44)$$

$$\Delta X^{(k)} = [J^{(k)}]^{-1} \Delta C^{(k)} \quad (2.45)$$

$$X^{(k+1)} = X^{(k)} + \Delta X^{(k)} \quad (2.46)$$

where $\Delta X^{(k)}$, $\Delta C^{(k)}$ and $J^{(k)}$ correspond to:

$$\Delta X^{(k)} = \begin{bmatrix} \Delta x_1^{(k)} \\ \Delta x_2^{(k)} \\ \vdots \\ \Delta x_n^{(k)} \end{bmatrix} \quad (2.47)$$

$$\Delta C^{(k)} = \begin{bmatrix} c_1 - (f_1)^{(k)} \\ c_2 - (f_2)^{(k)} \\ \vdots \\ c_n - (f_n)^{(k)} \end{bmatrix} \quad (2.48)$$

$$J^{(k)} = \begin{bmatrix} \left(\frac{\partial f_1}{\partial x_1}\right)^{(k)} & \left(\frac{\partial f_1}{\partial x_2}\right)^{(k)} & \cdots & \left(\frac{\partial f_1}{\partial x_n}\right)^{(k)} \\ \left(\frac{\partial f_2}{\partial x_1}\right)^{(k)} & \left(\frac{\partial f_2}{\partial x_2}\right)^{(k)} & \cdots & \left(\frac{\partial f_2}{\partial x_n}\right)^{(k)} \\ \vdots & \vdots & \ddots & \vdots \\ \left(\frac{\partial f_n}{\partial x_1}\right)^{(k)} & \left(\frac{\partial f_n}{\partial x_2}\right)^{(k)} & \cdots & \left(\frac{\partial f_n}{\partial x_n}\right)^{(k)} \end{bmatrix} \quad (2.49)$$

and $J^{(k)}$ is again called *Jacobian matrix* at the k^{th} iteration.

2.4.2.2 Newton-Raphson Power Flow Solution

The Newton-Raphson iterative method can be used to calculate the power flow solution by taking the power balance equations as the starting point, since both are nonlinear. The bus 1 is assumed as the slack-bus. Then it is omitted to form the linear system involving Jacobian and residues (mismatches).

Considering the basic nonlinear power balance equations expanded in Taylor's series about the initial estimate and neglecting all higher order terms, results in the following set of linear equations:

$$\begin{bmatrix} \Delta P_2^{(k)} \\ \vdots \\ \Delta P_n^{(k)} \\ \Delta Q_2^{(k)} \\ \vdots \\ \Delta Q_n^{(k)} \end{bmatrix} = \begin{bmatrix} \frac{\partial P_2}{\partial \delta_2} & \cdots & \frac{\partial P_2}{\partial \delta_n} & \frac{\partial P_2}{\partial |V_2|} & \cdots & \frac{\partial P_2}{\partial |V_n|} \\ \vdots & \ddots & \vdots & \vdots & \ddots & \vdots \\ \frac{\partial P_n}{\partial \delta_2} & \cdots & \frac{\partial P_n}{\partial \delta_n} & \frac{\partial P_n}{\partial |V_2|} & \cdots & \frac{\partial P_n}{\partial |V_n|} \\ \hline \frac{\partial Q_2}{\partial \delta_2} & \cdots & \frac{\partial Q_2}{\partial \delta_n} & \frac{\partial Q_2}{\partial |V_2|} & \cdots & \frac{\partial Q_2}{\partial |V_n|} \\ \vdots & \ddots & \vdots & \vdots & \ddots & \vdots \\ \frac{\partial Q_n}{\partial \delta_2} & \cdots & \frac{\partial Q_n}{\partial \delta_n} & \frac{\partial Q_n}{\partial |V_2|} & \cdots & \frac{\partial Q_n}{\partial |V_n|} \end{bmatrix} \begin{bmatrix} \Delta \delta_2^{(k)} \\ \vdots \\ \Delta \delta_n^{(k)} \\ \Delta |V_2^{(k)}| \\ \vdots \\ \Delta |V_n^{(k)}| \end{bmatrix} \quad (2.50)$$

The Jacobian matrix gives the linearized relationship between small changes in voltage angle $\Delta \delta_i^{(k)}$ and voltage magnitude $\Delta |V_i^{(k)}|$ with the small changes in real and reactive power $\Delta P_i^{(k)}$ and $\Delta Q_i^{(k)}$. Entries of the Jacobian matrix are the partial derivatives of the equations for PQ- and PV-buses, evaluated, respectively, at $\Delta \delta_i^{(k)}$ (for buses unless the slack-bus) and $\Delta |V_i^{(k)}|$ (only for PQ-bus). Considering a simplified form, (2.50) can be written as:

$$\begin{bmatrix} \Delta P \\ \Delta Q \end{bmatrix} = \begin{bmatrix} J_1 & J_2 \\ J_3 & J_4 \end{bmatrix} \begin{bmatrix} \Delta \delta \\ \Delta |V| \end{bmatrix} \quad (2.51)$$

Once the Jacobian matrix is calculated, the residues $\Delta P_i^{(k)}$ and $\Delta Q_i^{(k)}$ must be found as:

$$\Delta P_i^{(k)} = P_i^{sp} - P_i^{(k)}, \quad i \in PQ - \text{ and } PV - \text{ buses} \quad (2.52)$$

$$\Delta Q_i^{(k)} = Q_i^{sp} - Q_i^{(k)}, \quad i \in PQ - \text{ buses} \quad (2.53)$$

where $P_i^{(k)}$ and $Q_i^{(k)}$ are the active and reactive power calculated at k^{th} iteration and P_i^{sp} and Q_i^{sp} are the known (specified) values for the active and reactive power at bus i . In the PV-bus case, the variables related to reactive power are disregarded [20].

Finally, using (2.30), it is possible to find the increments for the phase angle and for the voltage magnitude and also add them to the initial estimate, as represented in (2.54) and (2.55).

$$\delta_i^{(k+1)} = \delta_i^{(k)} + \Delta \delta_i^{(k)}, \quad i \in PQ - \text{ and } PV - \text{ buses} \quad (2.54)$$

$$|V_i^{(k+1)}| = |V_i^{(k)}| + \Delta |V_i^{(k)}|, \quad i \in PQ - \text{ buses} \quad (2.55)$$

New iterations are performed until $\max \left[|\Delta P_i^{(k)}|, |\Delta Q_i^{(k)}| \right] \leq \epsilon$, with ϵ being the specified convergence tolerance [20].

2.4.3 The Fast Decoupled Load Flow Method

The Fast Decoupled Load Flow (FDLF) method is a variant of the NR method. The FDLF is one of the improved methods, which is based on a simplification of the NR method and reported by Stott and Alsac in 1974 [22].

This method, like the NR method, offers calculation simplifications, fast convergence and reliable results. As a consequence, it became a widely used method in load flow analysis. However, fast decoupling for some cases, for example where high resistance-to-reactance (R/X) ratios or heavy loading (low voltage) at some buses are present, may cause divergence in the process. This is justified because the technique besides be an approximation method, it also assumes simplifications on forming the Jacobian matrix. In view of this, many efforts and developments have been made

to overcome these convergence obstacles. Some of them targeted the convergence of systems with high X/R ratios, and others with low voltage buses. Three assumptions are used to derive this method from the NR approach [26], [21]:

- 1) The branch conductance values are zero;
- 2) The magnitudes of all voltages are close to 1 pu;
- 3) The voltage angles across all branch are close to zero, namely $\sin \theta_{ij} \approx 0$ and $\cos \theta_{ij} \approx 1$.

Using these assumptions, the power balance equations can be written as follows:

$$\frac{\partial \Delta P_i}{\partial |V_j|} = -|V_i|(G_{ij} \cos \theta_{ij} + B_{ij} \sin \theta_{ij}) \approx 0 \quad (2.56)$$

$$\frac{\partial \Delta Q_i}{\partial \theta_j} = |V_i||V_j|(G_{ij} \cos \theta_{ij} + B_{ij} \sin \theta_{ij}) \approx 0 \quad (2.57)$$

The equations (2.56) and (2.57) justify to neglect the off-diagonal sub-matrices of the Jacobian matrix. This method is a modification of NR, taking advantage of the weak coupling between P - δ and Q - $|V|$ due to the high X/R ratios. The Jacobian matrix of (2.51) is reduced to half by ignoring the element of J_2 and J_3 . The equation (2.51) is simplified as showed in (2.58) [21] [25]:

$$\begin{bmatrix} \Delta P \\ \Delta Q \end{bmatrix} = \begin{bmatrix} J_1 & 0 \\ 0 & J_4 \end{bmatrix} \begin{bmatrix} \Delta \delta \\ \Delta |V| \end{bmatrix} \quad (2.58)$$

The equation (2.58) can be broken into two independent parts, related to ΔP and ΔQ as

$$\Delta P = J_1 \Delta \delta = \left[\frac{\partial P}{\partial \delta} \right] \Delta \delta \quad (2.59)$$

$$\Delta Q = J_4 \Delta |V| = \left[\frac{\partial Q}{\partial |V|} \right] \Delta |V| \quad (2.60)$$

which can still be represented in a reduced form as:

$$\frac{\Delta P}{|V_i|} = -B' \Delta \delta \quad (2.61)$$

$$\frac{\Delta Q}{|V_i|} = -B'' \Delta |V| \quad (2.62)$$

The terms B' and B'' are the imaginary parts of the bus admittance matrix Y_{bus} . It is equivalent to ignore all shunt connected elements for construction of J_1 and J_4 . Therefore, in the Fast Decoupled Load Flow method, the successive voltage magnitude and phase angle changes are computed as [21]:

$$\Delta \delta = -[B']^{-1} \frac{\Delta P}{|V|} \quad (2.63)$$

$$\Delta |V| = -[B'']^{-1} \frac{\Delta Q}{|V|} \quad (2.64)$$

The Fast Decoupled Load Flow method exploits the approximate decoupling of the real and the reactive power equations, and keeps the Jacobian matrix as a constant matrix throughout the entire iteration process. This means that the Jacobian matrix for this method is factorized only once. Thus the FDLF solution requires more iterations than the Newton-Raphson method, but requires considerably less time per iteration, and a power flow solution is obtained very rapidly. This technique is very useful in contingency analysis where numerous outages are simulated or a power flow solution is required for online control. Thus, this method is widely applied in real-time power system operations. Even though the FDLF method has superior calculation speed over the NR method, it is initial guess dependent. Hence, it presents convergence problems, including those ones near the Saddle Node Bifurcation Point (SNBP) [21], [26].

2.4.4 Complexity Analysis Related to GS, NR and FDLF

GS and NR methods are compared considering both use Y_{bus} as the network model. The GS method requires the fewest number of arithmetic operations to complete an iteration. This is because the sparsity of the network matrix and the simplicity to obtain the solution of the nonlinear system. Consequently, this method requires less time per iteration. For the NR method, the Jacobian matrix needs to be computed at each iteration. For typical large systems, the time per iteration in the NR method is roughly equivalent to 7 times that of the GS method. The time per iteration in both these methods increases almost directly according to the buses of the network.

The rate of convergence of the GS method is slow (linear convergence characteristic), requiring a considerably greater number of iterations to obtain a solution than the NR method, which has quadratic convergence characteristics and is the best among all methods from the standpoint of convergence. In addition, the number of iterations for the GS method increases directly as the number of buses of the network increases. On the other hand, the number of iterations for the NR method remains practically constant, independent of system size.

In general, the NR method needs three to five iterations to reach an acceptable solution for a large-scale system. In the GS method and other iterative methods, convergence is affected by the choice of slack-bus and the presence of series capacitor, but the sensitivity of the NR method is minimal to these factors which cause poor convergence. Therefore, for large systems the NR method is faster, more accurate and more reliable than the GS method or any other known iterative method. In fact, it works for any size and kind of problem and is able to solve a wider variety of ill-conditioned problems. Its programming logic is considerably more complex and it has the disadvantage of requiring a large computational memory even when a compact storage scheme is used for the Jacobian and admittance matrices. In fact, it can be made even faster by adopting the scheme of optimally renumbered buses [28], [25].

For FDLF, the convergence is geometric, two to five iterations are normally required for practical accuracies, and it is faster than the formal NR method. This is due to the fact that the elements of B' and B'' are fixed approximation to the tangents of the defining functions $\delta P/|V|$ and $\delta Q/|V|$. If $\delta P/|V|$ and $\delta Q/|V|$ are calculated efficiently, then the speed for iterations of the FDLF is nearly five times that of the formal NR or about two-thirds that of the GS method. Storage requirements are around 60 percent of the formal NR, but slightly more than the decoupled NR method [28].

2.4.5 Motivation for Non-Iterative Methods Development

The three mainstream PF methods work very well when the system operates under near nominal conditions. Unfortunately, these three methods become less robust when the system operates with a voltage profile far from nominal, such as under a severe contingency condition. Furthermore, these iterative methods need an appropriate guess of the initial values. Promisingly, several non-iterative PF methods have been proposed, though they have not been thoroughly tested [26].

2.5 NON-ITERATIVE METHODS

Since the traditional iterative methods depend of an initial estimate and have convergence issues, emerging non-iterative methods have been studied. In the sequel it is discussed on the non-iterative approaches for solving the power flow problem.

2.5.1 The Series Load Flow Method

A non-iterative method called the Series Load-Flow method was proposed by Sauer [6]. This technique consists on determining voltage variables as a function of explicit power series. Two different approaches for computing the voltage power series were proposed by Sauer. One of them is the explicit voltage function in terms of the Taylor series obtained via a series recursion technique. Another, is based on a fixed-point iteration series with initial guess of voltages zero. The method may be considered a problem that consists in solving a nonlinear equation $V = f(V)$. Thus, it has the near-Newton properties [6].

Even though the derived voltage power series from both approaches provides an explicit form of the PF solution, thus the work developed by Sauer was essentially an analytical representation for the iteration process. The work was extended in [29] and the series was derived by expanding the solution function using Taylor series theory around a feasible operating point. The solution could be explicitly expressed by the Taylor series expansion. Hence, the load sensitivity could be performed easily by checking the first-order-term coefficient of the Taylor series. Unlike other iterative methods, the voltage solution could be derived by one substitution once the series was established with non-iterative characteristics. However, the solution was still initial point dependent. A reasonable feasible point that had small PBE's mismatches was required, otherwise the convergence of the Taylor series was not guaranteed. Finally, the calculation of the coefficients in the Taylor series could be computationally intensive and impractical for large-scale system applications [4], [26].

2.6 CONCLUSION OF THE CHAPTER

In this chapter an overview on modeling the network considering the admittance matrix has been presented. This representation, involving the connection between currents and nodal voltage, are essential to develop the power flow techniques evaluated in this work. They were introduced three conventional methods (the GS, the NR and the FDLF methods) and a discussion on a non-iterative method (the Series Load Flow method). The conventional methods perform reliably for the meshed system operating at near nominal conditions, but they are initial estimate dependent, and they face convergence issues when the system is under contingency or heavily loaded. Non-iterative methods claim to present advantages. They help overcome the convergence issues. As they are much less researched than the conventional methods, they beg adequate study and are open to further development. The next chapter exploits a subject on the direction of non-iterative method study.

Chapter 3 THE HOLOMORPHIC EMBEDDING METHOD

3.1 INTRODUCTION

In this chapter, a non-iterative method called Holomorphic Embedding Method (HEM) is presented and applied to solve the power flow problem. This model is based on the mathematical complex analysis topic and aims to find a solution for a nonlinear problem in a recursive way rather than iterative.

The method is applied to the nonlinear power flow problem in such way that models for PQ-buses, PV-buses and a *slack*-bus are incorporated. In this way, it is ensured that the equations describing the power flow are holomorphic, which is done with the inclusion of a complex-valued parameter α .

The analytical properties of the holomorphic functions are used to approximate the variables as power series which is a function of an embedding parameter α . A reference solution (*germ solution*) is defined for $\alpha = 0$ and enables the calculation of the coefficients of the power series in a recursive way. Finally, a Padé approximation is used in order to extend the series radius of convergence. The effective value of the original function is recovered when the Padé approximant is computed for $\alpha = 1$.

3.2 HOLOMORPHIC FUNCTION AND POWER SERIES COMPUTATION

The formulation of the problem discussed in this chapter requires the presentation of some definitions concerning holomorphic function properties which are the basis for the expansion of these functions in power series.

3.2.1 Holomorphic Functions

A holomorphic function is a complex-valued analytic function that is infinitely complex differentiable around every point within its domain. One important property of it is that it can be represented by its Taylor series around a neighborhood of each point in its domain [9].

The term holomorphic function is often used interchangeably with analytic function. The word "analytic" is defined in a broader sense to denote any function (real, complex, or of more general type) that can be written as a convergent power series in a neighborhood of each point in its domain. The fact that all holomorphic functions are complex analytic functions, and vice-versa, is a major theorem in complex analysis. Holomorphic functions are also sometimes referred to as *regular* functions [30].

Because the fact that complex differentiation is linear and obeys the product, quotient, and chain rules, it implies that the sums, products and compositions of holomorphic functions are holomorphic, and the quotient of two holomorphic functions is also holomorphic wherever the denominator is not zero.

3.2.2 Power Series Expansion of Holomorphic Functions

The Maclaurin series of a generic function $f(\alpha) \in \mathbb{C}$ is generated when a Taylor series is expanded about α equal zero [8]. Using the Maclaurin series expansion, an holomorphic function $f(\alpha)$ can be expanded as a power series with an infinite number of terms as presented by [26]:

$$f(\alpha) = \sum_{i=0}^{\infty} f[i]\alpha^i = \sum_{i=0}^{\infty} \frac{f^{(i)}(\alpha)}{i!}, \text{ for } |\alpha| \leq r \quad (3.1)$$

where $f^{(i)}(\alpha)$ is the i^{th} derivative of the function $f(\alpha)$, $f[i]$ is the i^{th} coefficient of the power series of the function $f(\alpha)$, and r is a convergence radius. Assuming the voltage function is holomorphic, it can be expanded and approximated for n terms as a power series [8]:

$$V(\alpha) = \sum_{i=0}^n V[i]\alpha^i, \text{ for } |\alpha| < r \quad (3.2)$$

Thus the generated voltage power series contains all of the properties of the analytic function $V(\alpha)$. It is need to consider that to be analytic, any function $f(\alpha)$

must satisfy the Cauchy-Riemann equations [30]. An equivalent condition in complex domain known as Wirtinger's derivative [30] requires that:

$$\frac{\partial f(\alpha)}{\partial \alpha^*} = 0 \quad (3.3)$$

The embedding process can retain the holomorphicity only when V^* is embedded with variable α^* instead of α . This statement can be proved using the Wirtinger's derivative. The truncated Maclaurin series expansion of the $V^*(\alpha)$ and $V^*(\alpha^*)$ are expressed as [4]:

$$\begin{aligned} V^*(\alpha) &= V[0]^* + V[1]^* \alpha^* + \dots + V[n]^* (\alpha^*)^n \\ V^*(\alpha^*) &= V[0]^* + V[1]^* \alpha + \dots + V[n]^* (\alpha)^n \end{aligned} \quad (3.4)$$

The variable $V^*(\alpha)$ in (3.4) is a function of α^* . Therefore, the Wirtinger equations will not be satisfied. The expansion of $V^*(\alpha^*)$ indeed is independent of α^* such that $\frac{\partial V^*(\alpha^*)}{\partial \alpha^*} = 0$, which implies that $V^*(\alpha^*)$ in (3.4) is a holomorphic function. Thus, the model must use the expression of $V_i^*(\alpha^*)$ instead of $V_i^*(\alpha)$ for embedding the power balance equations holomorphically for the case of the power flow problem [26].

The power series of the voltage as shown in (3.2), when evaluated at $\alpha = 1$, gives the solution to the original nonlinear equation set. However, if the power series has a radius of convergence less than 1.0, then the sum of power series terms evaluated at $\alpha = 1$ will not converge. However, an analytic continuation technique may be applied to extend this radius of convergence. This topic will be better introduced in Section 3.5.

3.3 THE BASIC POWER BALANCE EQUATIONS USING HOLOMORPHIC EMBEDDING METHOD

3.3.1 Modeling for *slack*, PQ- and PV-buses

In a generic system with $(N + 1)$ buses composed of a *slack* bus, a set of load buses (PQ-bus) and generator buses (PV-bus), the basic models can be represented

by a set of nonlinear equations called PBEs. For this set of bus, an index of bus i is assigned to each one. The bus index number $i = 0$ is reserved to the slack-bus. V_j is the voltage phasor of bus j and Y_{ij} is the $(i, j)^{th}$ entry of the bus admittance matrix, Y_{bus} , of the power system [9]:

- *Slack-bus*:

The slack-bus voltage, V_{sl} , can be expressed as the specified slack-bus voltage V_0^{sp} in the power system, so:

$$V_{sl} = V_0^{sp} \quad (3.5)$$

- *Load bus (PQ-bus)*:

The basic equation for a load bus at bus i can be represented as:

$$\sum_{j=0}^N Y_{ij} V_j = \frac{S_i^*}{V_i^*}, \quad i \in PQ - bus \quad (3.6)$$

where S_i is the complex power injections at bus i , and V_i is the bus voltage at bus i .

- *Generator bus (PV-bus)*:

For a generator bus, the voltage magnitude, $|V_i|$ and active power output, P_i , are known. The voltage angle and reactive power supply/consumption, Q_i , are unknown, so:

$$P_i = \operatorname{Re} \left(V_i \sum_{j=0}^N Y_{ij}^* V_j^* \right), \quad i \in PV - bus \quad (3.7)$$

$$|V_i| = V_i^{sp}$$

3.3.2 *Slack-Bus HEM*

Applying the embedding parameter α in the basic PBE for a *slack*-bus represented in (3.5) results in a possible HE model for this type of bus [9]:

$$V_{sl}(\alpha) = 1 + \alpha(V_0^{sp} - 1). \quad (3.8)$$

From (3.8), the power series for $V_{sl}(\alpha)$ has just two terms and the series has maximum power α^1 , i.e, $V_{sl}(\alpha) = V_0[0] + V_0[1]\alpha$, where $V_0[0] = 1$ and $V_0[1] = (V_0^{sp} - 1)$.

Then, according to (3.8), when $\alpha = 1$ results in $V_0(1) = V_0^{sp}$ and the original result is recovered.

The power series coefficient, $V_0[n]$, $n = 0, 1$, can be identified considering the Kronecker delta notation [9]

$$V_0[n] = \delta_{n0} + \delta_{n1}(V_0^{sp} - 1) \quad (3.9)$$

where it was used the Kronecker delta notation defined as [9]:

$$\delta_{ni} = \begin{cases} 1, & \text{if } n=i \\ 0, & \text{if } n \neq i \end{cases} \quad (3.10)$$

3.3.3 Load Bus (PQ-bus) HEM

Equation (3.6) describes the power balance equations required for the calculation of state variables V_j referring to PQ-buses. In this equation it is possible to extract the shunt contribution of the network in the bus admittance matrix Y_{bus} . Then, the term Y_{bus} is separated into the sum $Y_{bus} = Y_{i\ sh} + Y_{ij\ tr}$, where $Y_{i\ sh}$ is the total shunt admittance connected at bus i , and $Y_{ij\ tr}$, the remaining of the (i, j) entry of bus admittance matrix associated with only the branch impedance. This way, elements of a connection matrix of branches $Y_{ij\ tr}$ and a diagonal matrix of connections with shunts $Y_{i\ sh}$ elements are introduced [9]. Then, given $Y_{i\ sh}$ and an entry Y_{ij} :

$$Y_{ij\ tr} = \begin{cases} Y_{ii} - Y_{i\ sh}, & \text{if } i=j \\ Y_{ij}, & \text{if } i \neq j \end{cases} \quad (3.11)$$

Note that in (3.11) the diagonal entries of $Y_{ij\ tr}$ are determined simply removing the shunt contribution connected to the bus i from the admittance matrix Y_{bus} .

Thus, the Left Hand Side (LHS) of (3.4) for the bus i ($\sum_{j=0}^N Y_{ij}V_j$) is broken up in [20]:

$$\sum_{j=0}^N Y_{ij}V_j = \sum_{j=0}^N Y_{ij \ tr}V_j + Y_{i \ sh}V_i, \quad i \in PQ - bus \quad (3.12)$$

It is possible to impose a holomorphic condition for(3.6). With this aim, the complex parameter α is included in this equation. In this approach, the term $Y_{i \ sh}V_i$ is transferred to the Right Hand Side (RHS) of the (3.4). In this sense, (3.13) describes the HEM for load buses [26]. It must be noted that it is used the term $V_i^*(\alpha^*)$ instead of $V_i^*(\alpha)$ in order to satisfy the Cauchy-Riemann equations [7]. After this consideration, the basic holomorphic embedding formulation for load buses is given by [9]:

$$\sum_{j=0}^N Y_{ij \ tr}V_j(\alpha) = \frac{\alpha S_i^*}{V_i^*(\alpha^*)} - \alpha Y_{i \ sh}V_i(\alpha), \quad i \in PQ - bus \quad (3.13)$$

There are several ways to make a holomorphic function. It is chosen a way for which if $\alpha = 1$ the (3.6) is recovered from (3.13) [9], [26].

Since the voltages have become holomorphic functions from (3.13), they can be written for their respective expansions in Taylor series around one point. Choosing this point as $\alpha = 0$, the result is a Maclaurin series, which is described for $V(\alpha)$ and $V^*(\alpha^*)$:

$$V(\alpha) = \sum_{n=0}^{\infty} V[n]\alpha^n \quad (3.14)$$

$$V^*(\alpha^*) = V^*[0] + V^*[1]\alpha + \dots + V^*[n]\alpha^n \quad (3.15)$$

Substituting the voltages from (3.13) into the power series in (3.14) and (3.15), results in

$$\begin{aligned} \sum_{j=0}^N Y_{ij \ tr}(V_j[0] + V_j[1]\alpha + V_j[2]\alpha^2 + \dots + V_j[n]\alpha^n) = \\ = \frac{\alpha S_i^*}{(V_i^*[0] + V_i^*[1]\alpha + V_i^*[2]\alpha^2 + \dots + V_i^*[n]\alpha^n)} - \\ - \alpha Y_{i \ sh}(V_i[0] + V_i[1]\alpha + V_i[2]\alpha^2 + \dots + V_i[n]\alpha^n) \end{aligned} \quad (3.16)$$

In the situation of (3.16) and to solve the power flow problem, it is necessary to identify the coefficients of the series considering identity at both RHS and LHS of the equation. But, a first procedure to be done is to compute a series to represent the inverse of $V^*(\alpha^*)$ since this inverse function arises multiplying the term αS_i^* . One strategy which can be used is to define the inverse of $V(\alpha)$ as a power series function denominated $W(\alpha)$ [33]. This procedure is performed as

$$W(\alpha) = \frac{1}{V(\alpha)} = W[0] + W[1]\alpha + W[2]\alpha^2 + \dots + W[n]\alpha^n \quad (3.17)$$

Then the substitution of (3.17) in (3.16) results in

$$\begin{aligned} \sum_{j=0}^N Y_{ij \ tr} (V_j[0] + V_j[1]\alpha + V_j[2]\alpha^2 + \dots + V_j[n]\alpha^n) = \\ = \alpha S_i^* (W_i^*[0] + W_i^*[1]\alpha + W_i^*[2]\alpha^2 + \dots + W_i^*[n]\alpha^n) - \\ - \alpha Y_{i \ sh} (V_i[0] + V_i[1]\alpha + V_i[2]\alpha^2 + \dots + V_i[n]\alpha^n) \end{aligned} \quad (3.18)$$

From equation (3.17), $W(\alpha) \times V(\alpha) = 1$, thus this equation can also be written as:

$$(W[0] + W[1]\alpha + W[2]\alpha^2 + \dots + W[n]\alpha^n) \times (V[0] + V[1]\alpha + V[2]\alpha^2 + \dots + V[n]\alpha^n) = 1 \quad (3.19)$$

It is possible to solve (3.19) by multiplying the power series term-by-term and then equating the coefficients of the same power in α . This way, as the voltage coefficients $V[i]$, $i = 0, 1, 2, \dots, n$ are computed before determining $W[i]$, then the coefficients $W[i]$ are found explicitly from the coefficients of $V(\alpha)$ as:

$$\left\{ \begin{array}{ll} W[0]V[0] = 1 \implies W[0] = 1/V[0] & (for \alpha^0) \\ W[0]V[1] + W[1]V[0] = 0 & (for \alpha^1) \\ W[0]V[2] + W[1]V[1] + W[2]V[0] = 0 & (for \alpha^2) \\ \vdots & \\ W[0]V[n] + W[1]V[n-1] + \dots + W[n]V[0] = 0 & (for \alpha^n) \end{array} \right. \quad (3.20)$$

Thus, it is possible to find the n^{th} coefficient of the series of the function $W(\alpha)$ for each $n \geq 1$ through the expression [9]:

$$W[\alpha] = -\frac{\sum_{j=0}^{n-1} W[j]V[n-j]}{V[0]}, \quad n \geq 1 \quad (3.21)$$

Finally, for PQ-buses, considering identity at the RHS and LHS of (3.18) and taking into account previous $(n-1)$ known coefficients, the unknown n -th coefficient for the voltage $V_i(\alpha)$ is calculated as

$$\sum_{j=0}^N Y_{ij \ tr} V_j[n] = S_i^* W_i^*[n-1] - Y_{i \ sh} V_i[n-1] \quad (3.22)$$

3.3.4 Generator Bus (PV-bus) HEM

For a generator bus the reactive power is an unknown variable. Therefore, in (3.6) the complex power is separated into its real and imaginary parts. Thus, by separating the terms referring to the admittance matrix and including the embedding parameter α , it is obtained the equation [9]:

$$\sum_{j=0}^N Y_{ij \ tr} V_j(\alpha) = \frac{\alpha P_i - jQ_i(\alpha)}{V_i^*(\alpha^*)} - \alpha Y_{i \ sh} V_i(\alpha), \quad i \in PV - bus \quad (3.23)$$

The reactive power $Q_i(\alpha)$ is a variable and so has an expansion in function of the embedding parameter α . As matter of fact, this variable also has operational limits (superior and inferior). On the other hand, this constraining will not be focus of this dissertation. Therefore, the variable with free limits can be represented by a power series

$$Q(\alpha) = Q[0] + Q[1]\alpha + \dots + Q[n]\alpha^n. \quad (3.24)$$

The PV-bus has controlled voltage. The idea for this kind of control is to keep the magnitude of voltage at the bus i in a constant magnitude value, V_i^{sp} . A possible way

for considering the embedded equation (3.23) and also meeting the imposed voltage constraint is to adopt the procedure proposed in [9]:

$$|V_i(\alpha)|^2 = V_i(\alpha)V_i^*(\alpha^*) = 1 + (|V_i^{sp}|^2 - 1)\alpha, \quad i \in PV - bus \quad (3.25)$$

Interesting to note in (3.25) that the function $|V_i(\alpha)|^2$ is analytic, but $|V_i(\alpha)|$ alone does not meet the criteria to be an analytic function, i.e., it does not satisfy the Cauchy-Riemann equations or Wirtinger's derivative (see (3.3)).

Equations (3.23) and (3.25), then characterize the basic HEM for the power balance equation of typical generator buses.

Repeating the methodology used for load buses, the voltages $V_j(\alpha)$, $V_i(\alpha)$, $V_i^*(\alpha^*)$ and the reactive power $Q_i(\alpha)$ are replaced in (3.23) and (3.25) by their respective Maclaurin power series, so that it is obtained the result [20]:

$$\begin{aligned} & \sum_{j=0}^N Y_{ij \ tr} (V_j[0] + V_j[1]\alpha + V_j[2]\alpha^2 + \dots + V_j[n]\alpha^n) = \\ & = \frac{\alpha P_i - j(Q_i[0] + Q_i[1]\alpha + Q_i[2]\alpha^2 + \dots + Q_i[n]\alpha^n)}{(V_i^*[0] + V_i^*[1]\alpha + V_i^*[2]\alpha^2 + \dots + V_i^*[n]\alpha^n)} - \\ & \quad - \alpha Y_{i \ sh} (V_i[0] + V_i[1]\alpha + V_i[2]\alpha^2 + \dots + V_i[n]\alpha^n) \end{aligned} \quad (3.26)$$

Using (3.17) and evaluating the coefficients of $W(\alpha)$ from (3.21), equation (3.26) becomes:

$$\begin{aligned} & \sum_{j=0}^N Y_{ij \ tr} (V_j[0] + V_j[1]\alpha + V_j[2]\alpha^2 + \dots + V_j[n]\alpha^n) = \\ & = (\alpha P_i - j(Q_i[0] + Q_i[1]\alpha + Q_i[2]\alpha^2 + \dots + Q_i[n]\alpha^n) \times \\ & \quad \times (W_i^*[0] + W_i^*[1]\alpha + W_i^*[2]\alpha^2 + \dots + W_i^*[n]\alpha^n) - \\ & \quad - \alpha Y_{i \ sh} (V_i[0] + V_i[1]\alpha + V_i[2]\alpha^2 + \dots + V_i[n]\alpha^n) \end{aligned} \quad (3.27)$$

The coefficients of same power index from RHS and LHS in (3.27) are matched to compute a generic coefficient n , $V_i[n]$, given that the coefficients until $n-1$ are known. Then a general equation for unknown coefficient of $V_i[n]$ and $Q_i[n]$ is

$$\sum_{j=0}^N Y_{ij \ tr} V_j[n] = P_i W_i^*[n-1] - j \sum_{k=1}^{n-1} Q_i[k] W_i^*[n-k] - Y_{i \ sh} V_i[n-1] \quad (3.28)$$

It can be demonstrated [9] that in (3.28) the germ solution for $Q_i(\alpha)$ is zero, i.e. $Q_i[0] = 0$. This justify the reason why the RHS summation index starts from $k = 1$ instead zero in in (3.28).

Observing (3.28), it is noted that V_i and Q_i are unknown variables. Hence, Q_i appears as an additional variable in the problem formulation. Therefore, it is needed to include an additional expression in the equation system. This requirement is fulfilled by adding the voltage constraint equation [26]:

$$(V_i[0] + V_i[1]\alpha + V_i[2]\alpha^2 + \dots + V_i[n]\alpha^n) \times \\ \times (V_i^*[0] + V_i^*[1]\alpha + V_i^*[2]\alpha^2 + \dots + V_i^*[n]\alpha^n) = 1 + (|V_i^{sp}|^2 - 1)\alpha \quad (3.29)$$

By equating the coefficients of the same power index of α on both side of the equation (3.28), it is possible to find the coefficients from equation (3.30), assuming that $V_i[0] = 1$, $i = 0, 1, \dots, N$, resulting in equation (3.31) [26]:

$$\begin{cases} V_i[0]V_i^*[0] = 1 \\ V_i[0]V_i^*[1] + V_i[1]V_i^*[0] = |V_i^{sp}|^2 - 1 \\ \sum_{k=0}^n V_i[k]V_i^*[n-k] = 0, \text{ for } n = 2, 3, 4, \dots \end{cases} \quad (3.30)$$

$$\begin{cases} V_i[0] = 1 \\ V_i^*[1] + V_i[1] = 2V_{i \text{ re}}[1] = |V_i^{sp}|^2 - 1 \\ V_i^*[n] + V_i[n] = 2V_{i \text{ re}}[n] = -\sum_{k=1}^{n-1} V_i[k]V_i^*[n-k], \text{ for } n = 2, 3, 4, \dots \end{cases} \quad (3.31)$$

The germ solution (for $n = 0$) is then $V_i[0] = 1$, $i = 0, 1, \dots, N$. The very single result is obtained of straightforward way (without no additional computation), because it was adopted the embedded model (3.8) for the slack-bus and the fact that there is no shunt admittance or load for the system [7]. Physically, it means that the system then operates at this state as if there was a single generator with voltage 1 pu and all other bus operating at no load. Evidently, in this state all bus must also operates at voltage of 1 pu. Note also in (3.31) that the real part, $V_{i \text{ re}}[n]$, of the complex quantity $V_i[n]$ is directly calculated based on known coefficient values computed previously. But, the imaginary part of the same voltage phasor, $V_{i \text{ im}}[n]$, stays unknown.

Finally, it is obtained the equation (3.32) which represents the real part of the coefficients of voltage power series for PV-buses [33].

$$V_{i\ re}[n] = \begin{cases} 1, & \text{if } n = 0 \\ \frac{|V_i^{sp}|^2 - 1}{2}, & \text{if } n = 1 \\ -\frac{1}{2} \sum_{k=1}^{n-1} V_i[k] V_i^*[n-k], & \text{for } n = 2, 3, 4, \dots \end{cases} \quad (3.32)$$

3.3.5 Power Series Expansion Resulting After Applying HEM

The final solution for the power balance equations holomorphically embedded is obtained after the calculation of the coefficients for the power series of the functions $V_i(\alpha)$ and $Q_i(\alpha)$ as [26]:

$$V_i(\alpha) = V_i[0] + V_i[1]\alpha + \dots + V_i[n]\alpha^n \quad (3.33)$$

$$i \in PQ - bus \cup PV - bus \cup slack - bus$$

$$Q_i(\alpha) = Q_i[0] + Q_i[1]\alpha + \dots + Q_i[n]\alpha^n, i \in PV - bus \quad (3.34)$$

So, besides the initial terms, $Q_i[0]$ and $V_i[0]$ called *germ* solution, the remaining coefficients need to be calculated until a required precision be reached (this will be signaled by the result to be computed by an analytical approach of Padé). Or a maximum number of coefficients is achieved. These coefficients are then used by an analytic continuation technique in order to improve the convergence radius of the power series.

3.3.5.1 The *Germ* Solution

The germ solution for a general system with $(N + 1)$ buses is calculated establishing $\alpha = 0$ (3.8), (3.13) and (3.23) for PQ-buses, PV-buses and slack-bus, respectively. Thus, in summary, the germ solution can be obtained by solving this set of equations [26]:

$$\begin{aligned}
\sum_{j=0}^N Y_{ij} \operatorname{tr} V_j[0] &= 0, \quad i \in PQ - bus \\
\sum_{j=0}^N Y_{ij} \operatorname{tr} V_j[0] &= -jQ_i[0]W_i^*[0], \quad i \in PV - bus \\
V_i[0]V_i^*[0] &= 1, \quad i \in PV - bus \\
V_0[0] &= 1, \quad slack - bus
\end{aligned} \tag{3.35}$$

Considering (3.35), the germ solution is then represented by the coefficients [26]:

$$\begin{aligned}
V_i[0] &= 1, \quad i \in PQ - bus \cup PV - bus \cup slack - bus \\
W_i^*[0] &= 1, \quad i \in PQ - bus \cup PV - bus \\
Q_i[0] &= 0, \quad i \in PV - bus
\end{aligned} \tag{3.36}$$

3.3.5.2 General Coefficients for the Power Series

The general holomorphic embedding formulation for each value of a coefficient related to a degree n of α is given by [9]:

- Slack bus (slack):

$$V_0[n] = \begin{cases} 1, & \text{if } n=0 \\ V_i^{sp} - 1, & \text{if } n=1 \\ 0, & \text{if } n=2,3,4,\dots \end{cases} \tag{3.37}$$

- Load bus (PQ-bus):

$$\sum_{j=0}^N Y_{ij} V_j[n] = S_i^* W_i^*[n-1] - Y_{i\ sh} V_i[n-1], \quad \text{for } n \geq 1, \quad i \in PQ - bus \tag{3.38}$$

- Generator bus (PV-bus):

$$\sum_{j=0}^N Y_{ij} \operatorname{tr} V_j[n] = P_i W_i^*[n-1] - j \sum_{k=1}^{n-1} Q_i[k] W_i^*[n-k] - Y_{i\ sh} V_i[n-1] \tag{3.39}$$

$$V_{i\ re}[n] = \begin{cases} 1, & \text{if } n=0 \\ \frac{(V_i^{sp})^2 - 1}{2}, & \text{if } n=1, i \in PV - bus \\ -\frac{1}{2} \sum_{k=1}^{n-1} V_i[k] V_i^*[n-k], & \text{if } n=2,3,4,\dots \end{cases} \tag{3.40}$$

with $V_i[n] = V_{i\ re}[n] + jV_{i\ im}[n]$.

The set of equations (3.38)-(3.40) is separated into real, $V_{i\ re}[n]$, and imaginary parts, $V_{i\ im}[n]$, generating a linear system that have to be solved recursively for a given number of terms until getting a required precision. After this, the result must be transformed by using an analytic continuation technique as will be demonstrated later.

3.4 HEM MATRIX REPRESENTATION

In the previous sections models for the power flow by the Holomorphic Embedding Method for the three types of buses were presented for an electrical power system. In this section the purpose is to lump the models into a single matrix representation. For the sake of simplicity, the three bus system of Figure 3.1 is considered. In this system, bus 1 is the slack-bus; bus 2 is a PV-bus; and bus 3 is a PQ-bus.

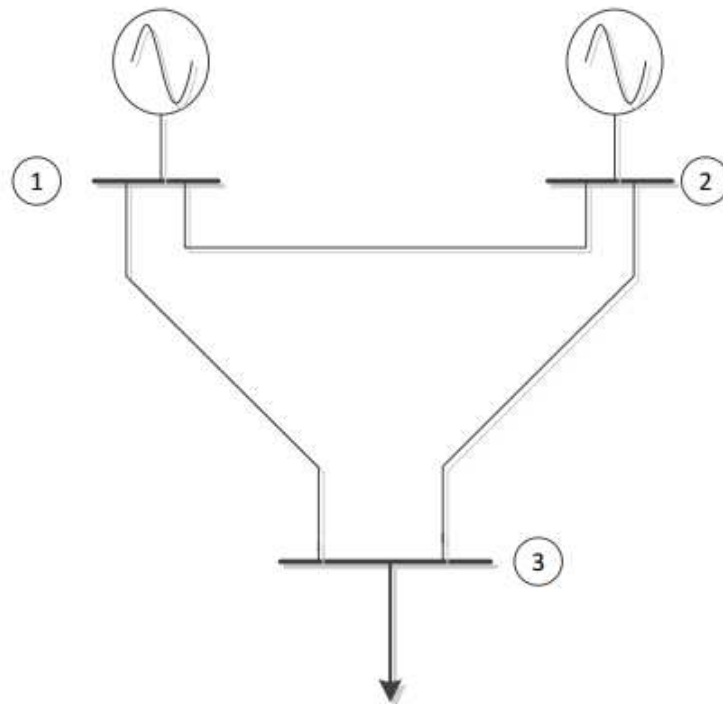


Figure 3.1: 3-bus system for illustrating the application of the Holomorphic Embedding Method

Initially, the bus admittance matrix, containing only branch elements (no shunt connection) is formed. An entry of this matrix, $Y_{ij\ tr}$, is separated into real and imaginary parts as:

$$Y_{ij\ tr} = G_{ij} + B_{ij} \quad (3.41)$$

where G_{ij} and B_{ij} are the conductance and susceptance of the entry Y_{ij} *tr*, respectively.

The power balance equations holomorphically embedded and the bus admittance matrix are separated into real and imaginary parts and the unknown variables are moved to the left hand side. After this consideration, the recursive relation for determining the general coefficients for the basic three-bus system of Figure 2.1 is represented in a matrix form as showed in equation (3.42).

$$\begin{bmatrix} 1 & 0 & 0 & 0 & 0 & 0 \\ 0 & 1 & 0 & 0 & 0 & 0 \\ G_{21} & -B_{21} & 0 & -B_{22} & G_{23} & -B_{23} \\ B_{21} & G_{21} & 1 & G_{22} & B_{23} & G_{23} \\ G_{31} & -B_{31} & 0 & -B_{32} & G_{33} & -B_{33} \\ B_{31} & G_{31} & 0 & G_{32} & B_{33} & G_{33} \end{bmatrix} \begin{bmatrix} V_{1 \text{ re}}[n] \\ V_{1 \text{ im}}[n] \\ Q_2[n] \\ V_{2 \text{ im}}[n] \\ V_{3 \text{ re}}[n] \\ V_{3 \text{ im}}[n] \end{bmatrix} = \begin{bmatrix} \delta_{n0} + \delta_{n1}(V_i^{sp} - 1) \\ 0 \\ re \{ P_2 W_2^*[n-1] - j \sum_{k=1}^{n-1} Q_2[k] W_2^*[n-k] - Y_{2 \text{ sh}} V_2[n-1] \} \\ im \{ P_2 W_2^*[n-1] - j \sum_{k=1}^{n-1} Q_2[k] W_2^*[n-k] - Y_{2 \text{ sh}} V_2[n-1] \} \\ re \{ S_3^* W_3^*[n-1] - Y_{3 \text{ sh}} V_3[n-1] \} \\ im \{ S_3^* W_3^*[n-1] - Y_{3 \text{ sh}} V_3[n-1] \} \end{bmatrix} - \begin{bmatrix} 0 \\ 0 \\ G_{22} \\ B_{22} \\ G_{32} \\ B_{32} \end{bmatrix} V_{2 \text{ re}}[n], n = 0, 1, \dots \quad (3.42)$$

where $V_{2 \text{ re}}[n]$ is calculated using (3.32).

Note that after splitting the equations into real and imaginary parts, for a system with N buses, $2N$ holomorphically embedded equations are necessary. Hence, the admittance matrix, Y_{tr} , has dimension $2N \times 2N$.

3.5 ANALYTIC CONTINUATION AND PADÉ APPROXIMANT

The Power Balance Equations in their basic form, as presented by (3.5) to (3.7) do not satisfy Cauchy-Riemann equations. Hence, they are non-holomorphic. In HEM the voltage or reactive power function is embedded using a complex parameter, α , such that the resultant system of equations is holomorphic. This allows the voltage or reactive power function to be expressed as Taylor's series whose radius of convergence

are unknown. Analytic continuation techniques need to be applied to extend the convergence radius. Analytic continuation is studied in complex analysis and is defined as the technique for extending the domain of a given analytic function. When the power flow problem is evaluated using HEM, analytic continuation must be used to represent the voltage power function outside the radius of convergence of the power series representation [33].

When solving the power balance equations holomorphically embedded according to (3.8), (3.13) and (3.23) for a system of $(N + 1)$ buses as suggested in previous topics, basically two problems are handled. The first one is to determine the amount of terms (power series coefficients) needed to achieve the correct solution at $\alpha = 1$. The second one concerns the convergence of the voltage power series: if the convergence radius is less than 1, which is generally true, the power series do not converge to the desired values [7]. Then, it is not enough to make $\alpha = 1$ and replace this value in the power series equations to find the solution of the power flow problem.

In order to circumvent this situation, there are some methods employed for analytic continuation which can be used to increase the radius of convergence of the power series function. An appropriated technique widely used is the Padé approximant method. The maximal analytic continuation of a power series can be achieved by calculating its diagonal or near-diagonal Padé approximant (depending the number of poles and zeros of the continued fraction). The Padé approximant can be written as a rational function of two polynomials which is computed from the finite power series truncated at a maximum number of terms. An analytical identity for this rational fraction is defined as [9], [27]:

$$[L/M]_{\alpha} = \frac{a[0] + a[1]\alpha + \dots + a[L]\alpha^L}{1 + b[1]\alpha + \dots + b[M]\alpha^M} = \sum_{n=0}^{L+M} f[n]\alpha^n \quad (3.43)$$

where L and M are related to the numerator (zeros) and denominator (poles) of the rational function in α , respectively, and n is the degree of the power series; the power series maximum number of terms required to match with the the Padé approximant is $(L + M)$.

From Stahl's convergence theory, the diagonal or near-diagonal Padé approximants yields the maximal analytic continuation (analytic continuation over the maximal domain of the function). Hence, it provides the convergence guarantee relied

on by the Holomorphic Embedding Load Flow Method [35]. In other words, if a solution of the power balance equations exists, the Padé approximant is guaranteed to converge. Otherwise, if the Padé approximant does not converge, the system of PBE does not have a solution. This means that the power system is beyond the voltage collapse point and is non-operable [4]. One advantage of this method is that the power series of the variable α is approximated by a rational approximant as a function of α . This rational approximant may then be evaluated for an arbitrary value of α , giving that $f(\alpha)$ is known [34], [35].

A near-diagonal Padé approximant is a rational approximant whose the module of the difference between the numerator and denominator polynomial degree are equal 1, i.e. $(|L - M| = 1)$, whereas in diagonal Padé approximant the numerator and denominator polynomial degree are equal, i.e. $(L = M)$. Both diagonal or near-diagonal sequence of Padé approximants have been proved to converge to the desired solution [7], [11], but in this work the approximation to the diagonal of the Padé matrix (diagonal Padé approximant) was the method chosen. This method, in addition to generally not needing many terms to achieve good accuracy for the convergence of the power series, also makes it possible to reach the maximum analytical continuation for a power series function [32].

Then, for finding the analytic continuation for a voltage power series, for example, firstly the basic problem consists in computing the coefficients $V[n]$ of the voltage power series. Secondly, from the power series it is needed to determine the coefficients $a[i], i = 0, 1, 2, \dots, L$ and $b[j], j = 1, 2, \dots, M$ of the polynomial rational fraction. Finally, the voltage $V(1)$ is computed, i.e., the value when $\alpha = 1$ is the voltage value of interest [7], [32].

The function $V(\alpha)$ is approximated by the truncated power series in (3.44) until the degree $L + M$. So $L + M + 1$ coefficients are known (LHS of the equation). However, there are $L + M + 2$ coefficients due to the polynomials at numerator and denominator on the RHS of the equation (unknown variables). Then, in order to find these unknown coefficients, one of the variables at the RHS is chosen as being a free variable. Then, $b[0] = 1$ is chosen [33].

$$V(\alpha) = V[0] + V[1]\alpha + \dots + V[L + M]\alpha^{L+M} = \frac{a[0] + a[1]\alpha + \dots + a[L]\alpha^L}{b[0] + b[1]\alpha + \dots + b[M]\alpha^M} \quad (3.44)$$

Multiplying both sides of (3.44) by the polynomial $b(\alpha)$ and assuming $b[0] = 1$, it is obtained the relation

$$(1 + b[1]\alpha + \dots + b[M]\alpha^M) \times (V[0] + V[1]\alpha + \dots + V[L + M]\alpha^{L+M}) = a[0] + a[1]\alpha + \dots + a[L]\alpha^L \quad (3.45)$$

By identifying the coefficients of α at both sides of (3.45), a general relation among the variables is obtained as

$$\begin{cases} V[0] = a[0] \\ V[1]b[0] + V[0]b[1] = a[1] \\ V[2]b[0] + V[1]b[1] + V[0]b[2] = a[2] \\ \vdots \\ \sum_{k=0}^L V[k]b[L - k] = a[L] \end{cases} \quad (3.46)$$

By equating the coefficients from $L + 1$ to $L + M$ in (3.43) results in

$$\begin{cases} b[M]V[L - M + 1] + b[M - 1]V[L - M + 2] + \dots + b[1]V[L] + V[L + 1] = 0 \\ b[M]V[L - M + 2] + b[M - 1]V[L - M + 3] + \dots + b[1]V[L + 1] + V[L + 2] = 0 \\ \vdots \\ b[M]V[L] + b[M - 1]V[L + 1] + \dots + b[1]V[L + M - 1] + V[L + M] = 0 \end{cases} \quad (3.47)$$

The system in (3.47) can be represented into a matrix form by [26]:

$$\begin{bmatrix} V[L - M + 1] & V[L - M + 2] & \dots & V[L] \\ V[L - M + 2] & V[L - M + 3] & \dots & V[L + 1] \\ \vdots & \vdots & \ddots & \vdots \\ V[M]V[L] & V[L + 1] & \dots & V[L + M - 1] \end{bmatrix} \begin{bmatrix} b[M] \\ b[M - 1] \\ \vdots \\ b[1] \end{bmatrix} = - \begin{bmatrix} V[L + 1] \\ V[L + 2] \\ \vdots \\ V[L + M] \end{bmatrix} \quad (3.48)$$

Analytic continuation applied to power series through using Padé approximation leads to the handling of matrix which can be severely ill-conditioned. Especially, when the order of the Padé approximant is increased [34]. Other drawback is that the Padé

approximant introduces spurious poles on the transfer function represented by the rational fraction and these poles do not correspond to the singularities of the original function. The results evaluated near such poles are misleading [8]. Furthermore, the Padé matrix becomes too large to yield an accurate result in such way that many terms in the series needs to be included [26]. Despite these drawbacks a great impact on expanding the convergence radius of the problem is the key point which justify the use of the Padé approximant.

In summary the original Holomorphic Embedding model applied for solving the power flow problem follows this solution process:

1. Construct the bus admittance matrix Y_{bus} using sparsity techniques;
2. Split the Y_{bus} into shunt (Y_{sh}) and series (Y_{tr}) matrices, composed of only shunt and branch connection, respectively;
3. Generate the Power Balance Equations for Slack-, PQ- and PV-buses holomorphically embedded;
4. Use the germ solution $V_i[0] = 1$, $W_i[0] = 1$ and $Q_i[0] = 0$ as the initial term for the power series in α ;
5. Construct the matrix of the recursive relation with the PBE holomorphically embedded separated into real and imaginary parts for finding the other coefficients $[n]$ of the power series;
6. Apply an analytic continuation technique to the power series, as Padé approximant, and make $\alpha = 1$ to get the solution; if the major voltage mismatch is less than a specified tolerance error, the final solution was reached; otherwise, calculate extra terms to the power series until getting the final solution.

It is important to mention that if the Padé approximation does not converge for $\alpha = 1$, unequivocally, the power flow problem does not have solution [33].

The Figure 3.2 illustrates a flowchart about the original holomorphic embedding power flow implementation solution method.

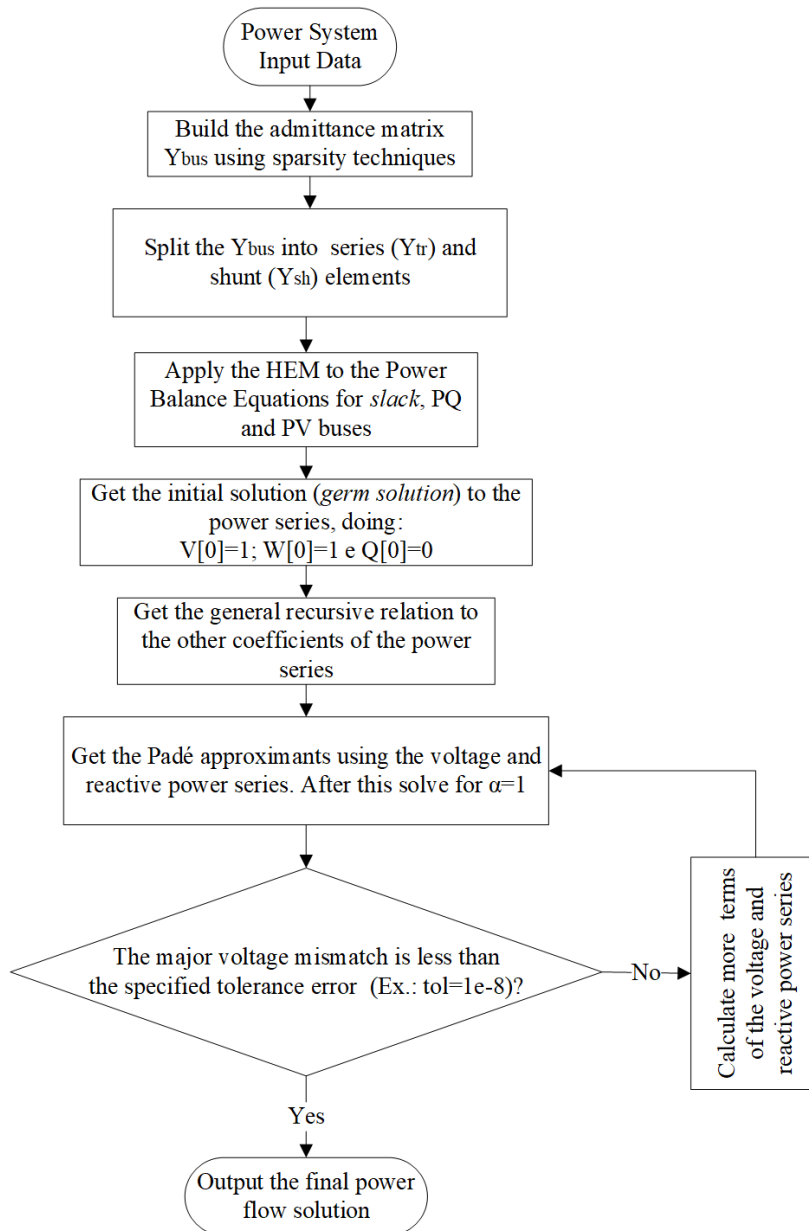


Figure 3.2: Original holomorphic embedding power flow solution flowchart

3.6 2-BUS TUTORIAL CASE

The electric network in Figure 3.3, taken from [33], consists of a two-bus system and is presented here to illustrate step-by-step the application of the method of adapting the load flow equations using the parameter holomorphic α , as described in the previous sections. In this system, the active power consumed at bus 2, P_2 , is dependent of the voltages V_1 and V_2 , and also to the transmission line impedance. The following data are known: the source voltage, V_1 , and the impedance which is assumed purely resistive, R . The active power, P_2 , is also given. The voltage V_2 is the unknown

variable in the problem.

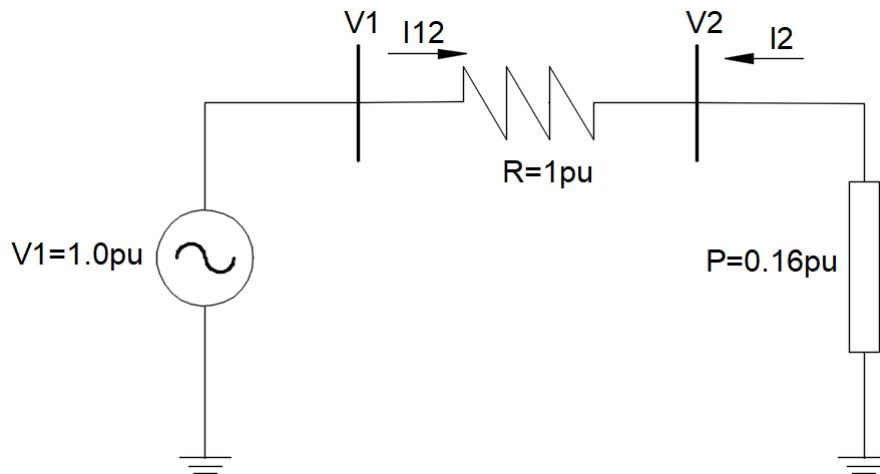


Figure 3.3: 2-bus test-system for illustrating the HEM application

Thus, the power balance equation in this example is simply given by [33]:

$$P_2 = V_2 I_2 = \frac{V_2 (V_1 - V_2)}{R} \quad (3.49)$$

Therefore, it is necessary to solve the following nonlinear equation for the unknown variable V_2 :

$$V_2^2 - V_2 V_1 + R P_2 = 0 \quad (3.50)$$

Considering that $R = 1.0$ pu, $P_2 = 0.16$ pu and $V_1 = 1.0$ pu, it is obtained the following equation:

$$V_2^2 - V_2 + 0.16 = 0 \quad (3.51)$$

The exact solution for (3.51) consists of the operating values (*HV*) 0.8 pu or the (*LV*) 0.2 pu. The parameter α is included in (3.51), so that $V_2^2 - V_2 = -0.16\alpha$. Note that by setting α at the unit value, equation (3.51) is retrieved in its original form.

Now, by expressing the voltage V_2 as a holomorphic function of the complex parameter α , it is obtained:

$$V_2(\alpha) = 1 - \frac{0.16\alpha}{V_2(\alpha)} \quad (3.52)$$

Since $V_2(\alpha)$ is holomorphic in α , this variable can be represented as a power series: $V_2(\alpha) = V_2[0] + V_2[1]\alpha + \dots + V_2[n]\alpha^n$. The *germ* solution is obtained when $\alpha = 0$.

Therefore, $V_2[0] = 1$. In this sense, $W_2(\alpha)$ is defined as the inverse series of the voltage $V_2(\alpha)$, given by:

$$W_2(\alpha) = \frac{1}{V_2(\alpha)} = (W_2[0] + W_2[1]\alpha + \dots + W_2[n]\alpha^n) \quad (3.53)$$

and $W_2(0) = \frac{1}{V_2(0)} = 1$.

Starting from (3.52) and using the inverse voltage series $W_2(\alpha)$, it is determined [33]:

$$V_2[0] + V_2[1]\alpha + \dots + V_2[n]\alpha^n = 1 - 0.16\alpha (W_2[0] + W_2[1]\alpha + \dots + W_2[n]\alpha^n) \quad (3.54)$$

Then, by equating the coefficients of the two sides of the equation (3.54), it is obtained the coefficients of the voltage power series $V_2(\alpha)$ as a recursive process:

$$\begin{cases} V_2[0] = 1; & W_2[0] = \frac{1}{V_2[0]} = 1, & \text{for } n = 0 \\ V_2[n] = -0.16W_2[n-1], & & \text{for } n \geq 1 \end{cases} \quad (3.55)$$

The coefficients of the voltage power series starting with the *germ* solution obtained for $n = 0$. The terms $W_2[n]$ are calculated from (3.21). The accuracy of the result depends on the amount of terms n calculated. For the problem in question, the terms of the series for $V_2(\alpha)$ up to the fourth degree are:

$$V_2(\alpha) = 1 - 0.16\alpha - 0.0256\alpha^2 - 0.0082\alpha^3 - 0.0033\alpha^4 + \dots \quad (3.56)$$

In general, by making $\alpha = 1$ in (3.56) and summing the coefficients of the series, even for a large number of terms, it is found that the result obtained differs from the solution V_2 of the bus voltage. A Padé approximation of $V_2(\alpha)$ is then calculated and the value of V_2 when $\alpha = 1$ is determined. Assuming an error tolerance of 10^{-8} to the exact HV value $V_2 = 0.8$ pu, 12 coefficients are required to the voltage power series, which leads to a Padé approximation with $L = M = 6$.

The diagonal Padé approximant for bus 2 is evaluated as:

$$V_2(\alpha) = \frac{1 - 1.9200\alpha + 1.4080\alpha^2 - 0.4915\alpha^3 + 0.0826\alpha^4 - 0.0059\alpha^5 + 0.001\alpha^6}{1 - 1.7600\alpha + 1.1520\alpha^2 - 0.3441\alpha^3 + 0.0459\alpha^4 - 0.0022\alpha^5 + 0.0000\alpha^6} \quad (3.57)$$

which, for $\alpha = 1$, gives $V_2(\alpha) = 0.8\angle 0^\circ$ pu.

3.7 CONCLUSION OF THE CHAPTER

In this chapter, the problem formulation based on the holomorphic embedding model (HEM) was presented for evaluating the HEM applied to the load flow (HELM) problem. A general linear system was also determined to evaluate the voltage or reactive power coefficients for the *slack*-, PQ- and PV-buses. For a better understanding of the problem solution using the HEM, the description based on a simple three-bus electric system was presented. It was also demonstrated how to obtain the Padé approximant, which is an analytical continuation technique. This is a process to enlarge greatly the radius of convergence of the power series for HELM. This a required procedure to obtain the final solution to the problem, unless a tolerance error.

In the next chapter a bibliographical review is done on works involving HELM and verified progress in recent years on the subject.

Chapter 4 STATE OF THE ART ON SOME HELM APPROACHES

4.1 INTRODUCTION

The holomorphic embedding procedure for calculating the solution of the power flow problem appeared in 2012 [7]. But even before the subject had been studied however having limited repercussions in the academic environment. In this chapter is presented a bibliographical review concerning some works published in the literature on the theme. Several researches are recent and have motivated this dissertation.

4.2 BIBLIOGRAPHICAL REVIEW

Up to now, some contributions identified to the holomorphic embedding method with application for solving the power flow problem are summarized in the sequel. The presentation was prioritized per year, given that research on the subject is fairly recent. Of course, covering all the works already published on the topic is an arduous task and so the description in question is a standout survey by the author.

- **2009-2011:** There were registered two U.S. Patents, number 7,519,506 B2 (Apr. 14, 2009) and number 7,979,239 B2 (Jul. 12, 2011), which introduced an alternative technique to iterative methods, proposed by Trias for solving the power flow problem [37].
- **2012:** Trias [7] proposed in a paper a novel non-iterative power flow method, known as the Holomorphic Embedding Load Flow Method (HELM). The method allows the determination of the HV/operational solution of the problem (if it exists). The purpose was applied to a simple two-bus system. The method unequivocally signals if no solution exists through oscillations in the rational approximation of the voltage power series [7].

- **2013:** The paper [38] presents an improved method for calculating the unstable equilibrium point for a two-bus system using a holomorphic embedding model. The focus of this paper is to prove mathematically that if a unstable equilibrium point solution exists, the method is guaranteed to arrive at that and only that solution. If no solution exists, then such characteristic is demonstrated by oscillations is the series form of the solution.

The paper [11] introduces a PV-bus model, compatible with the Holomorphic Embedding (HE) approach, for solving the Power Balance Equations (PBE) and suggests a remedy for the precision problems that arises with HE in modeling the PV- bus. Because the PBE in traditional form are non-analytic due to the presence of the complex-conjugate operator, many powerful tools applicable to the analytic functions cannot be used. Holomorphism is obtained by embedding the PBE into a bigger problem in such a way as to render the embedded problem analytic.

- **2014:** The master thesis [33], presented by Muthu Kumar, describes the Holomorphic Embedding Load Flow Method in a detailed approach. Software to implement the HE method was developed using MATLAB and numerical tests were carried out on small and medium sized systems to validate the approach. Implementation of different analytic continuation techniques is included and their relevance in applications such as evaluating the voltage solution and estimating the bifurcation point (BP) is discussed. The ability of the HE method to trace the PV-curve of the system is identified.
- **2015:** The doctoral dissertation [4], presented by Yang Feng, develops a non-iterative algorithm for solving the power flow (PF) problem using the holomorphic embedding method. It was demonstrated that the technique is able of finding the *HV* solution, while avoiding converging to *LV* solutions nearby which is a drawback to all other iterative solutions. The detailed implementation of the HE method is discussed and modified holomorphically embedded formulations are proposed to find the *LV*/large-angle solutions of the PF problem. It is theoretically proven that the proposed method is guaranteed to find a total number of $2N$ solutions to the PF problem and if no solution exists, the algorithm is guaranteed to indicate such by the oscillations in the maximal analytic continuation of the coefficients of the voltage power series obtained.

The master thesis [26], presented by Yuting Li, explains in details the connection between mathematical theory of the Holomorphic Embedding Method and its application to power flow calculation. With the existing bus-type-switching

routine, the models of phase shifters and three-winding transformers are proposed to enable the HE algorithm to solve practical large-scale systems. A study parameter β is introduced in the embedding formula $\beta\alpha + (1 - \beta)\alpha^2$. By varying the value of β , numerical tests of different embedding formulations are conducted on several network systems, and it is demonstrated that the best numerical performance is obtained for β values varying between 0.80 to 1.0.

Trias, in the paper [10], establishes additional details on the theoretical foundations of the Holomorphic Embedding Method. Starting from a fundamental projective invariance of the power-flow equations, it is shown how to devise holomorphicity-preserving embeddings that allows regarding the power flow problem as essentially a study in algebraic curves. Complementing this algebraic-geometric viewpoint, which lays the foundation of the method, it is shown how to apply standard analytic techniques (power series) for practical computation. Stahl's theorem on the maximality of the analytic continuation provided by Padé approximants then ensures the completeness of the method. On the other hand, it is shown how to extend the method to accommodate smooth controls, such as the ubiquitous generator-controlled PV-bus.

The master thesis [39], presented by Benedikt Schmidt, explains how the Holomorphic Embedding Method can be applied to solve the PF problem and compares it to the iterative methods. Experimental results show that the superior convergence behavior of HELM enables the load-flow calculation of grids closer to their border of stability than with any other iterative method. This is made possible by a trade-off with respect to runtime through special settings. With default settings HELM delivers already more accurate results in comparable runtime to the iterative methods. The author describes the importance of taking into account high precision for the variables, since a huge number of coefficients are necessary in order to have an adequate accuracy in the results.

- **2016:** The paper [9] does a complete description of the Holomorphic Embedding Method and its application to the PF problem. It is shown that the HEM represents a distinct class of nonlinear equation solvers that are recursive, rather than iterative. As such, for any given problem, there are an infinite number of HEM formulations, each one with different numerical properties and precision demands. The paper provides an intuitive understanding of HEM and apply one variant to the power-flow problem. It is introduced one possible PV-bus model compatible with the HEM and examines some features of different holomorphic embeddings, giving step-by-step details of model building, *germ*

solution calculation, and recursive algorithm.

The paper [13] from Trias and Marín extends the Holomorphic Embedding Load flow Method from AC to DC-based systems. Through an appropriate embedding technique, the method is shown to extend naturally to DC power transmission systems, preserving all the constructive and deterministic properties that allow it to obtain the white branch solution in an unequivocal way. Its applications extend to nascent meshed HVDC networks and also to power distribution systems in more-electric vehicles, ships, aircraft, and spacecraft. In these latter areas, it is shown how the method can cleanly accommodate the higher-order nonlinearities that characterize an I-V curves of many devices. The case of a photovoltaic array feeding a constant-power load is given as an example. The extension to the general problem of finding DC operating points in electronics is also discussed, and exemplified on a diode model.

The paper [40] exposes the modeling and mathematical fundamentals of the embedded AC power flow problem with voltage control and exponential load model in the complex plane. It is showed that modeling the action of network controllers, that regulate the magnitude of voltage phasors, is a challenging task in the complex plane as it has to preserve the framework of holomorphicity for obtaining of these complex variables with fixed magnitude. The paper presents two distinct approaches to modeling the voltage control of generator nodes. Exponential (or voltage-dependent) load models are crucial for accurate power flow studies under stressed conditions. It is exploited the theory of analytic continuation, especially the monodromy theorem for resolving issues that have plagued conventional numerical methods for decades. The work is focused on the indispensable role of Padé approximant for analytic continuation of complex functions, expressed as power series, beyond the boundary of convergence of the series. Also, it is explained the zero-pole distribution of these rational approximant which serves as a proximity index to voltage collapse identification.

The paper [41] cites that original HELM paper [7] dealt only with PQ buses, while a second paper [11] showed how to include PV-buses but suffered from serious accuracy problems. The work proposes to fill this gap by providing several models capable of solving general networks, with computational results for the standard IEEE test cases provided for comparison. In addition, it is proposed a new derivation of the theory behind the method and investigated some of the claims made in the original HELM paper from Trias [7].

The paper [42] presents three different true non-linear reduction methods to

obtain network equivalents for radial (distribution-type) networks using the holomorphically embedded power flow algorithm. The proposed reduction methods are applied in the paper to reduce a radial distribution system and provide a two-bus-model equivalent which accurately models the real and reactive power load seen at the transmission network due to random changes in the distribution system load. Numerical results are provided for a radial 14-bus system to show the accuracy of the proposed methods in preserving voltages and slack-bus power. The approach is shown to have better performance than Ward reduction, even when the loads are increased in a random manner.

The paper [43] proposes to obtain an optimal loading of the generating units using particle swarm optimization along with Holomorphic Embedded Load Flow technique, under consideration of equality and inequality constraints of different units and power flow. It is considered the IEEE 30-bus system to verify the effectiveness of the proposed approach. The simulation results are compared with the results obtained from NR method.

The paper [12] proposes four different HEM-based methods to estimate the Saddle-Node Bifurcation Point (SNBP) of a power system, and makes a comparison in terms of accuracy as well as computational efficiency. All of these methods rely on an important property of a Padé approximant, which is the maximal analytic continuation of the given function. Predicting the SNBP of a power system has become more critical as the power-system loading has increased in many places without a concomitant increase in transmission resources and the biggest advantage of the HEM is that convergence is guaranteed, even at the SNBP.

- **2017:** The paper [32] presents results of the implementation and description of the basic formulation for the Holomorphic Embedding Load Flow Method (HELM). The basic formulation is implemented by generation of an interface to use the data structure of the traditional MATPOWER, which is a free code tool developed in Matlab. Additionally, the same data files of this tool are used as input data for study carried out in the work. Also, the output results are adapted to have similar characteristics to the MATPOWER's output. Experiments and results for seven power systems demonstrate the validity of the tool HELM based.

The paper [44] presents the results of a comparison of the well-established power-flow algorithms as Gauss-Seidel, Newton-Raphson, Dishonest Newton-Raphson, Decoupled Load Flow, Fast Decoupled Load Flow and the new Holomorphic Embedding Load Flow Method (HELM). The algorithms are assessed using

several PQ-bus power flow test cases. The focus of the analysis is on the precision of the solutions of the algorithms and the required computation time. The comparison shows some disadvantages of HELM and motivates a new Adaptive Hybrid Approach that combines the Holomorphic Embedding Load Flow Method and iterative algorithms to merge the benefits of both techniques. The Adaptive Hybrid Approach is able to calculate precise solutions for every test case without starting values and is on average faster than the Newton-Raphson method while being more flexible than every other algorithm considered. It is also shown that the Adaptive Hybrid Approach yields the correct solution like HELM if it exists. The letter [45] cites that the Holomorphic Embedding Method may encounter the precision issue, i.e. the nontrivial round-off errors caused by the limited digits used in computing the power-voltage (P-V) curve for a heavily loaded power system. The letter proposes a multi-stage scheme to solve such a precision issue and calculate an accurate P-V curve. The scheme is verified on the New England 39-bus power system and benchmarked with the result from the traditional continuation power flow method.

The paper [46] proposes an online steady-state voltage stability assessment scheme to evaluate the proximity to voltage collapse at each bus of a load area. Using a non-iterative holomorphic embedding method (HEM) with a proposed physical germ solution, an accurate loading limit at each load bus can be calculated based on online state estimation on the entire load area and a measurement-based equivalent for the external system. The HEM employs a power series to calculate an accurate Power-Voltage (P-V) curve at each load bus and accordingly evaluates the voltage stability margin considering load variations in the next period. An adaptive two-stage Padé approximants method is proposed to improve the convergence of the power series for accurate determination of the nose point on the P-V curve with moderate computational burden.

The doctoral dissertation [47], presented by Shruti Rao, applies the HEM for estimating the saddle-node bifurcation point (SNBP) of a system and for developing reduced-order network equivalents for distribution systems. Different ways of accelerating the convergence of the power series obtained as a part of HELM, are explored. Also, the local-measurement-based methods of estimating the SNBP are studied.

The paper [48] cites that network reduction is an effective tool for reducing the complexity of many analysis, design and optimization problems. However, many of the conventional reduction methods are only accurate at the base case. When

the operating condition changes, the reduced model does not match the full model performance because linearization is used somewhere in the process. The paper proposes a new reduction method that preserves the model's nonlinear structure using the holomorphic embedding technique to generate network reductions which are accurate over a broader range of operating conditions. When applied to the power flow problem, simulation results show that the proposed method can significantly improve bus-voltage and branch-flow accuracy, matching the full-model power-flow solution exactly when moving along the so-called α -line.

The paper [49] cites that the development of appropriate load flow model of Flexible AC Transmission System (FACTS) devices is an important issue for proper planning, control, and protection of power system. In order to evaluate the effects of FACTS devices in load flow problem by HELM technique, it is necessary to develop HELM modeling of these devices. The paper presents HELM modeling of Thyristor-based FACTS controllers, i.e., Static Var Compensator (SVC), Thyristor Controlled Switched Capacitor (TCSC), Thyristor Controlled Voltage Regulator (TCVR), and Thyristor Controlled Phase Angle Regulator (TCPAR). It is also investigated the modeling, white germ solution along with recursive formula and controlling FACTS devices operation bounds.

The paper [50] proposes a multi-dimensional HEM that derives analytical multivariate power series to approach true power flow solutions. The proposed method embeds multiple independent variables into power flow equations and hence can respectively scale power injections or consumptions of selected buses or groups of buses. Then, via a physical germ solution, the method can represent each bus voltage as a multivariate power series about symbolic variables on the system condition so as to derive approximate analytical power flow solutions. The method has a non-iterative mechanism unlike the traditional numerical methods for power flow calculation. Its solution can be derived offline and then evaluated in real time by plugging values into symbolic variables according to the actual condition, so the method fits better into online applications such as voltage stability assessment.

4.3 BIBLIOGRAPHICAL REVIEW SYNTHESIS

Table 4.1 summarizes some highlighted subjects explored in each reference considered in this chapter.

Table 4.1: Bibliographical Review Synthesis

| Reference | Main Contributions Identified | | | | | | | | | |
|----------------------------------|-------------------------------|-----|-----|------|------|------|------|-----|------|------|
| | PAA | OEF | DCA | LVSS | OACT | PVBC | OLDM | ETC | SNBP | MIUC |
| Trias (2012) | ✓ | - | - | - | - | - | - | - | ✓ | - |
| Feng & Tylavsky (2013) | - | - | - | ✓ | ✓ | ✓ | - | - | ✓ | - |
| Subramanian <i>et al.</i> (2013) | - | - | - | - | ✓ | ✓ | - | - | ✓ | - |
| Subramanian (2014) | ✓ | - | - | - | ✓ | ✓ | - | - | ✓ | - |
| Feng (2015) | ✓ | - | - | ✓ | ✓ | ✓ | - | - | ✓ | - |
| Li (2015) | ✓ | ✓ | - | - | ✓ | ✓ | ✓ | - | - | ✓ |
| Trias (2015) | ✓ | - | - | - | - | ✓ | - | - | - | - |
| Schmidt (2015) | - | - | - | - | ✓ | ✓ | - | ✓ | - | - |
| Rao <i>et al.</i> (2016) | ✓ | ✓ | - | ✓ | - | ✓ | - | ✓ | ✓ | ✓ |
| Trias & Marín (2016) | ✓ | ✓ | ✓ | - | - | - | ✓ | ✓ | ✓ | ✓ |
| Baghsorkhi & Suetin (2016) | ✓ | - | - | - | ✓ | ✓ | - | - | ✓ | - |
| Wallace <i>et al.</i> (2016) | ✓ | - | ✓ | - | - | ✓ | - | ✓ | - | ✓ |
| Rao and Tylavsky (2016) | ✓ | - | - | - | - | ✓ | - | - | ✓ | - |
| Shukla <i>et al.</i> (2016) | ✓ | - | - | - | - | ✓ | - | - | - | - |
| Rao and Tylavsky (2017) | ✓ | ✓ | - | - | - | ✓ | - | - | ✓ | ✓ |
| Santos <i>et al.</i> (2017) | ✓ | - | - | - | - | ✓ | - | - | - | ✓ |
| Sauter <i>et al.</i> (2017) | ✓ | - | - | - | - | ✓ | - | ✓ | - | ✓ |
| Wang <i>et al.</i> (2017) | ✓ | ✓ | - | - | - | ✓ | - | - | - | - |
| Liu <i>et al.</i> (2017) | ✓ | ✓ | - | - | - | ✓ | - | ✓ | ✓ | ✓ |
| Rao (2017) | ✓ | ✓ | - | ✓ | ✓ | ✓ | ✓ | ✓ | ✓ | ✓ |
| Zhu <i>et al.</i> (2017) | ✓ | ✓ | - | - | - | ✓ | ✓ | - | ✓ | - |
| Kejani & Gholipour (2017) | ✓ | ✓ | - | - | - | ✓ | ✓ | ✓ | - | - |
| Liu <i>et al.</i> (2017) | ✓ | ✓ | - | - | - | ✓ | - | - | - | ✓ |

Legend:

PAA: Padé Approximant Application;

OEF: Other Embedding Formulation;

DCA: Direct Current Approach;

LVSS: Low Voltage Solution Study;

OACT: Other Analytic Continuation Techniques;

PVBC: PV-Bus Considered;

OLDM: Other Load/Devices Modelling;

ETC: Execution Time Comparison;

SNBP: Saddle Node Bifurcation Point;

MIUC: MATPOWER Implementation or Used for Comparison

4.4 CONCLUSION OF THE CHAPTER

This chapter has presented a bibliographical review on works related to progress on HELM. A detailed description of references covering works published since 2012 is exhibited.

In the next chapter, it is proposed an alternative method to the original HELM. In this new purpose the germ solution is updated according to the approximated results of the computed voltages.

Chapter 5 RESTARTED HOLOMORPHIC EMBEDDING POWER FLOW METHOD

5.1 INTRODUCTION

An alternative approach to the original HELM is presented and discussed in this chapter. It is proposed a different way of computing the power series terms associated to the HELM in the sense that the germ solution now is updated instead to be considered just once. This strategy allows to handle a reduced number of coefficients of the voltage power series, since they are computed again, but with a higher degree of accuracy than considering just one germ solution. As a result of this procedure, after determining a very few bus voltage power series terms (e.g., we have proposed no more than six terms) this data is used to compute a Padé approximant and partial bus voltages. Then this partial computed voltages are used to restart the process again as if another *germ* solution were generated. In view of this characteristics the technique was denominated as Restarted HELM (RHELM).

5.2 THE RESTARTED HOLOMORPHIC EMBEDDING METHOD

The original HELM applied to a multi-bus system uses a *germ* solution to generate series of complex-valued voltages at PQ- and PV-buses besides reactive power at PV-buses [30]. The series of the quantities are directly used to determine a Padé approximant. In most cases, a Padé approximant of higher order is required. This is a concern with respect to accuracy of high order terms without considering extended precision on computations. Furthermore, it would be valuable to have a *germ* solution but assuming that the system is on load (in the original HELM problem formulation, the germ solution is obtained at no load and only a connected voltage source is on at the slack-bus). Taking into account these two main aspects and following the nice idea of embedding the load flow equations [7], we propose an alternative approach for embedding these equations. In our approach *we have used injected power* for formulating the balancing equations instead of injected current, as adopted in [7], [9].

Again, the system is supposed to have $(N + 1)$ bus and the slack-bus is the number 0. Hence the embedded equations for PQ-buses are modified as follows:

$$V_i(\alpha)I_i^*(\alpha^*) = \alpha S_i - \alpha Y_i^{sh*} |V_i(\alpha)|^2 + (1 - \alpha) \hat{S}_i \quad (5.1)$$

where $I_i(\alpha) = \sum_{j=0}^N Y_{ij} V_j(\alpha)$; $|V_i(\alpha)|^2 = V_i(\alpha) V_i^*(\alpha^*)$; $\hat{S}_i = V_i^{(0)} I_i^{(0)*}$ is an initial complex power injected at bus i ; $I_i^{(0)} = \sum_{j=0}^N Y_{ij} V_j^{(0)}$, is an initial current injected at bus i ; $V_i^{(0)}$ is an estimated voltage adopted in several real world tools as Matpower [14], not necessarily a guess as employed for iterative methods like Newton's method.

Note that in (5.1) $V_i^{(0)}$ is given or loaded from a file as done in MATPOWER as an estimated value for initializing NR method. In other words, when $\alpha = 0$ an initial current injected at each bus $I_i^{(0)}$ is computed and the associated starting (fictitious) power \hat{S}_i can also be computed and this value must be exactly the same one at the LHS of the equation. This also works on as a germ solution for the power in analogy with germ solution for the voltage in the original HELM idea. At the situation when $V_i^{(0)} = 1$ (flat start in classical NR method for power flow), the germ solution of the conventional HELM is used. However, in our work, it is proposed to use a value of voltage not necessarily limited to the value 1, aiming to have greater flexibility in the search for more precise results. For example, using a value very close to the exact one would expect faster convergence. This value close to the exact one could be found by applying the own HELM as a starting process for RHELM.

As obtained for HELM, the equation embedding for PV-buses in RHELM is also not straightforward. Specifically and similarly as for HELM two restrictions need to be satisfied. But, both constraints related to active power and controlled voltage are used.

A possible embedding equation for the constraining active power at PV-bus is proposed as:

$$V_i(\alpha)I_i^*(\alpha^*) + V_i^*(\alpha^*)I_i(\alpha) = 2\alpha [P_i - \text{real}(Y_i^{sh})|V_i(\alpha)|^2] + 2(1 - \alpha)\hat{P}_i \quad (5.2)$$

where $\hat{P}_i = \text{real}(\hat{S}_i)$ at PV-buses and Y_i^{sh} can be interpreted as a shunt admittance due to a contribution of load at the bus i represented by constant impedance.

The voltage magnitude constraint is now proposed as:

$$V_i(\alpha)V_i^*(\alpha^*) = |V_i^{(0)}|^2 + \alpha [(V_i^{sp})^2 - |V_i^{(0)}|^2] \quad (5.3)$$

where V_i^{sp} is the specified voltage magnitude at PV-buses.

The reactive power at bus i also stays implicitly estimated. Say, $\hat{Q}_i = \text{imag}(\hat{S}_i)$. But, this variable is not needed in the sequence of the calculus. Finally, the expression (5.3) is also satisfied, because $V_i[0]V_i^*[0] = |V_i^{(0)}|^2$ was the imposed condition in view of the initial condition. Additionally, when $\alpha = 1$ both terms $(1 - \alpha)\hat{S}_i$ in (5.1) and $(1 - \alpha)\hat{P}_i$ in (5.2) vanish. Therefore, we expect the result numerically agrees with the solution of the power flow problem.

In (5.3), note that $|V_i^{(0)}|$ is not necessarily the unit, as adopted in several HELM approaches [9], [4], [26], [39]. In the HELM case, the no load condition of buses leads to voltages be equal to voltage of the slack-bus. This is not true when the system is under load, as assumed for RHELM. Then, in case of PV-buses as in the embedded equation in (5.3), this model must be evaluated considering voltages with real and imaginary parts (remember that for HELM, just the real part is sufficient), since $V_i^{(0)} = V_{i\ re}^{(0)} + jV_{i\ im}^{(0)}$ and $|V_i^{(0)}|^2 = (V_{i\ re}^{(0)})^2 + (V_{i\ im}^{(0)})^2$. Hence, this additional information works on as an improvement on the solver, because more numerical content is added in the direction of the problem solution.

Once the power series coefficients are known for this initial germ solution (coefficients at $n = 0$), a process to compute the other coefficients, i.e. for $n > 0$, is detailed in the sequel.

5.2.1 Situation for $n = 1$

We start detailing the case where $n = 1$ as for PQ-bus as for PV-bus. Then for PQ-buses and considering (5.1), the power series coefficients have to be deduced from the expression for degree 1 for α :

$$V_i[1]I_i[0]^* + V_i[0]I_i[1]^* = (S_i - Y_i^{sh*}V_i[0]V_i[0]^*) - \hat{S}_i \quad (5.4)$$

with $I_i[1] = \sum_{j=0}^N Y_{ij\ tr} V_j[1]$.

In (5.4) the current $I_i[1]$ can be expressed in function of voltages $V_j[1]$, $j = 0, 1, 2, \dots, N$.

Following (5.2) and (5.3), the PV-buses equations are:

$$V_i[1]I_i[0]^* + V_i[0]I_i[1]^* + V_i[1]^*I_i[0] + V_i[0]^*I_i[1] = 2(P_i - \text{real}(Y_i^{sh*})V_i[0]V_i[0]^*) - 2\hat{P}_i \quad (5.5)$$

$$V_i[1]V_i[0]^* + V_i[0]V_i[1]^* = |V_i^{sp}|^2 - |V_i^{(0)}|^2 \quad (5.6)$$

As verified in (5.4), there also exist products $V_i[1]I_i[0]^*$ and their conjugated terms in (5.3) and (5.6). This means that a common point between equations for PQ- and PV-buses for the power series coefficient calculation in RHELM would be the development of voltage and current in function of power series. We will demonstrate later that the current variables can be eliminated along the solution process in such way that only voltage needs to be handled until finalize the computation of a Padé approximant (process for enlarging the radius of convergence as in HELM). i.e., current power series coefficients are a redundant computational burden. Obviously, the current coefficients can be updated, since currents and voltages are related by the admittance matrix. On the other hand, It is noteworthy to point out that this calculation is unnecessary, because only $I_i^{(0)}$ needs to be used for determining a germ solution. But this solution is necessary only in the initial stage of calculation for new coefficients of an updated power series. This occurs for example when restarting the calculation process again, by using an updated and more accurate germ solution, in order to refine the obtained solution. The idea is to reinitialize the process whenever a maximum allowed number of coefficients of the power series is reached without an acceptable numerical solution being reached.

At first, the equations (5.4)-(5.6) should be solved for real-valued unknowns $V_{i\ re}[1]$, $V_{i\ im}[1]$, $I_{i\ re}[1]$ and $I_{i\ im}[1]$, with $V_i[1] = V_{i\ re}[1] + jV_{i\ im}[1]$ and $I_i[1] = I_{i\ re}[1] + jI_{i\ im}[1]$.

Developing equation (5.4), it is obtained:

$$\begin{aligned} & \{V_{i\ re}[0]I_{i\ re}[1] + V_{i\ im}[0]I_{i\ im}[1]\} + j\{-V_{i\ re}[0]I_{i\ im}[1] + V_{i\ im}[0]I_{i\ re}[1]\} + \\ & + \{V_{i\ re}[1]I_{i\ re}[0] + V_{i\ im}[1]I_{i\ im}[0]\} + j\{-V_{i\ re}[1]I_{i\ im}[0] + V_{i\ im}[1]I_{i\ re}[0]\} = \\ & (S_i - \hat{S}_i) - Y_i^{sh*}V_i[0]V_i[0]^* \end{aligned} \quad (5.7)$$

Equation (5.7) can be put as:

$$\begin{bmatrix} V_{i\ re}[0] & V_{i\ im}[0] & I_{i\ re}[0] & I_{i\ im}[0] \\ V_{i\ im}[0] & -V_{i\ re}[0] & -I_{i\ im}[0] & I_{i\ re}[0] \end{bmatrix} \cdot \begin{bmatrix} I_{i\ re}[1] \\ I_{i\ im}[1] \\ V_{i\ re}[1] \\ V_{i\ im}[1] \end{bmatrix} = \begin{bmatrix} real(\gamma_{1i}[1]) \\ imag(\gamma_{1i}[1]) \end{bmatrix} \quad (5.8)$$

where $\gamma_{1i}[1] = (S_i - \hat{S}_i) - Y_i^{sh*} V_i[0] V_i[0]^* = (S_i - \hat{S}_i) - Y_i^{sh*} |V_i[0]|^2$.

At the same way, (5.6) assumes the following real-valued form:

$$\begin{bmatrix} V_{i\ re}[0] & V_{i\ im}[0] \end{bmatrix} \cdot \begin{bmatrix} V_{i\ re}[1] \\ V_{i\ im}[1] \end{bmatrix} = [\gamma_{2i}[1]] \quad (5.9)$$

where $\gamma_{2i}[1] = \frac{1}{2}(|V_i^{sp}|^2 - |V_i^{(0)}|^2)$ and for (5.5)

$$\begin{bmatrix} V_{i\ re}[0] & V_{i\ im}[0] & I_{i\ re}[0] & I_{i\ im}[0] \end{bmatrix} \cdot \begin{bmatrix} I_{i\ re}[1] \\ I_{i\ im}[1] \\ V_{i\ re}[1] \\ V_{i\ im}[1] \end{bmatrix} = [\gamma_{3i}[1]] \quad (5.10)$$

where $\gamma_{3i}[1] = (P_i - \hat{P}_i) - real(Y_i^{sh*}) |V_i[0]|^2$.

5.2.2 Situation for $n = 2$

Now, consider the case where $n = 2$ as for PQ-bus as for PV-bus. Then for PQ-buses and considering again (5.1), the power series coefficients have to be deduced from the expression for degree 2 for α . Then for the bus i :

$$V_i[2]I_i[0]^* + V_i[1]I_i[1]^* + V_i[0]I_i[2]^* = -Y_i^{sh*}(V_i[1]V_i[0]^* + V_i[0]V_i[1]^*) \quad (5.11)$$

with $I_i[2] = \sum_{j=0}^N Y_{ij\ tr} V_j[2]$.

Keeping only unknowns at the LHS of (5.11), this equation is modified to:

$$V_i[2]I_i[0]^* + V_i[0]I_i[2]^* = -V_i[1]I_i[1]^* - Y_i^{sh*}(V_i[1]V_i[0]^* + V_i[0]V_i[1]^*) \quad (5.12)$$

Developing (5.12) in the same way as in (5.7) it is obtained:

$$\begin{bmatrix} V_{i\ re}[0] & V_{i\ im}[0] & I_{i\ re}[0] & I_{i\ im}[0] \\ V_{i\ im}[0] & -V_{i\ re}[0] & -I_{i\ im}[0] & I_{i\ re}[0] \end{bmatrix} \cdot \begin{bmatrix} I_{i\ re}[2] \\ I_{i\ im}[2] \\ V_{i\ re}[2] \\ V_{i\ im}[2] \end{bmatrix} = \begin{bmatrix} real(\gamma_{1i}[2]) \\ imag(\gamma_{1i}[2]) \end{bmatrix} \quad (5.13)$$

where $\gamma_{1i}[2] = -V_{i[1]}I_{i[1]}^* - Y_i^{sh*}|V_{i[1]}|^2$.

Following (5.2) and (5.3), the PV-buses equations for $n = 2$ are given by:

$$\begin{aligned} V_{i[2]}I_{i[0]}^* + V_{i[1]}I_{i[1]}^* + V_{i[0]}I_{i[2]}^* + V_{i[2]}^*I_{i[0]} + V_{i[1]}^*I_{i[1]} + V_{i[0]}^*I_{i[2]} = \\ -2real(Y_i^{sh*})(V_{i[1]}V_{i[0]}^* + V_{i[0]}V_{i[1]}^*) \end{aligned} \quad (5.14)$$

$$V_{i[2]}V_{i[0]}^* + V_{i[1]}V_{i[1]}^* + V_{i[0]}V_{i[2]}^* = 0 \quad (5.15)$$

Similarly, developing equation (5.15), yields:

$$\begin{bmatrix} V_{i\ re}[0] & V_{i\ im}[0] \end{bmatrix} \cdot \begin{bmatrix} V_{i\ re}[2] \\ V_{i\ im}[2] \end{bmatrix} = \begin{bmatrix} \gamma_{2i}[2] \end{bmatrix} \quad (5.16)$$

where $\gamma_{2i}[2] = -\frac{1}{2}(V_{i[1]}V_{i[1]}^*)$.

At the same way, (5.14) assumes:

$$\begin{bmatrix} V_{i\ re}[0] & V_{i\ im}[0] & I_{i\ re}[0] & I_{i\ im}[0] \end{bmatrix} \cdot \begin{bmatrix} I_{i\ re}[2] \\ I_{i\ im}[2] \\ V_{i\ re}[2] \\ V_{i\ im}[2] \end{bmatrix} = \begin{bmatrix} \gamma_{3i}[2] \end{bmatrix} \quad (5.17)$$

where $\gamma_{3i}[2] = -\frac{1}{2}(V_{i[1]}I_{i[1]}^* + V_{i[1]}^*I_{i[1]}) - real(Y_i^{sh*})(V_{i[1]}V_{i[0]}^* + V_{i[0]}V_{i[1]}^*)$.

5.2.3 Situation for $n > 2$

Considering a generic n , the power series coefficients need to be deduced from the expressions for degree n for α . For PQ-buses and considering again (5.1):

$$V_i[n]I_i[0]^* + V_i[0]I_i[n]^* + \sum_{j=1}^{n-1} V_i[n-j]I_i[j]^* = -Y_i^{sh*} \sum_{j=0}^{n-1} V_i[n-j-1]V_i[j]^* \quad (5.18)$$

with $I_i[n] = \sum_{j=0}^N Y_{ij} \text{tr} V_j[n]$.

The equation (5.18), with only unknowns at the LHS, is modified to:

$$V_i[n]I_i[0]^* + V_i[0]I_i[n]^* = - \sum_{j=1}^{n-1} V_i[n-j]I_i[j]^* - Y_i^{sh*} \sum_{j=0}^{n-1} V_i[n-j-1]V_i[j]^* \quad (5.19)$$

Developing (5.19) in the same way as in (5.7) yields:

$$\begin{bmatrix} V_{i \text{ re}}[0] & V_{i \text{ im}}[0] & I_{i \text{ re}}[0] & I_{i \text{ im}}[0] \\ V_{i \text{ im}}[0] & -V_{i \text{ re}}[0] & -I_{i \text{ im}}[0] & I_{i \text{ re}}[0] \end{bmatrix} \cdot \begin{bmatrix} I_{i \text{ re}}[n] \\ I_{i \text{ im}}[n] \\ V_{i \text{ re}}[n] \\ V_{i \text{ im}}[n] \end{bmatrix} = \begin{bmatrix} \text{real}(\gamma_{1i}[n]) \\ \text{imag}(\gamma_{1i}[n]) \end{bmatrix} \quad (5.20)$$

where $\gamma_{1i}[n] = - \sum_{j=1}^{n-1} V_i[n-j]I_i[j]^* - Y_i^{sh*} \sum_{j=0}^{n-1} V_i[n-j-1]V_i[j]^*$.

Following (5.2) and (5.3), the PV-buses equations for n are given by:

$$\begin{aligned} V_i[n]I_i[0]^* + V_i[0]I_i[n]^* + \sum_{j=1}^{n-1} V_i[n-j]I_i[j]^* + V_i[n]^*I_i[0] + V_i[0]^*I_i[n] + \sum_{j=1}^{n-1} V_i[n-j]^*I_i[j] = \\ - 2\text{real}(Y_i^{sh*}) \sum_{j=0}^{n-1} V_i[n-j-1]V_i[j]^* \end{aligned} \quad (5.21)$$

$$V_i[n]V_i[0]^* + V_i[0]V_i[n]^* + \sum_{j=1}^{n-1} V_i[n-j]V_i[j]^* = 0 \quad (5.22)$$

Similarly, developing equation (5.22), it is obtained:

$$\begin{bmatrix} V_{i \text{ re}}[0] & V_{i \text{ im}}[0] \end{bmatrix} \cdot \begin{bmatrix} V_{i \text{ re}}[n] \\ V_{i \text{ im}}[n] \end{bmatrix} = \begin{bmatrix} \gamma_{2i}[n] \end{bmatrix} \quad (5.23)$$

where $\gamma_{2i}[n] = -\frac{1}{2} \sum_{j=1}^{n-1} V_i[n-j]V_i[j]^*$.

At the same way, (5.21) is represented as:

$$\begin{bmatrix} V_{i \text{ re}}[0] & V_{i \text{ im}}[0] & I_{i \text{ re}}[0] & I_{i \text{ im}}[0] \end{bmatrix} \cdot \begin{bmatrix} I_{i \text{ re}}[n] \\ I_{i \text{ im}}[n] \\ V_{i \text{ re}}[n] \\ V_{i \text{ im}}[n] \end{bmatrix} = \begin{bmatrix} \gamma_{3i}[n] \end{bmatrix} \quad (5.24)$$

where $\gamma_{3i}[n] = -\frac{1}{2}(\sum_{j=1}^{n-1} V_i[n-j]I_i[j]^* + \sum_{j=1}^{n-1} V_i[n-j]^*I_i[j]) - \text{real}(Y_i^{sh*}) \sum_{j=0}^{n-1} V_i[n-j-1]V_i[j]^*$.

5.3 THREE-BUS TUTORIAL SYSTEM

In order to illustrate the construction of the linear system related to the (5.8)-(5.10), consider the 3-bus system presented in Section 3.4. In the illustrative example the bus 1 was chosen as the slack-bus. The equations for this system when $n = 1$ are represented in the form of:

$$\begin{bmatrix}
 0 & 0 & 0 & 0 & 1 & 0 & 0 & 0 & 0 & 0 \\
 0 & 0 & 0 & 0 & 0 & 1 & 0 & 0 & 0 & 0 \\
 -1 & 0 & 0 & 0 & G_{21} & -B_{21} & G_{22} & -B_{22} & G_{23} & -B_{23} \\
 0 & -1 & 0 & 0 & B_{21} & G_{21} & B_{22} & G_{22} & B_{23} & G_{23} \\
 0 & 0 & -1 & 0 & G_{31} & -B_{31} & G_{32} & -B_{32} & G_{33} & -B_{33} \\
 0 & 0 & 0 & -1 & B_{31} & G_{31} & B_{32} & G_{32} & B_{33} & G_{33} \\
 0 & 0 & 0 & 0 & 0 & 0 & V_{2\ re}[0] & V_{2\ im}[0] & 0 & 0 \\
 V_{2\ re}[0] & V_{2\ im}[0] & 0 & 0 & 0 & 0 & I_{2\ re}[0] & I_{2\ im}[0] & 0 & 0 \\
 0 & 0 & V_{3\ re}[0] & V_{3\ im}[0] & 0 & 0 & 0 & 0 & I_{3\ re}[0] & I_{3\ im}[0] \\
 0 & 0 & V_{3\ im}[0] & -V_{3\ re}[0] & 0 & 0 & 0 & 0 & -I_{3\ im}[0] & I_{3\ re}[0]
 \end{bmatrix} \times$$

$$\begin{bmatrix}
 I_{2\ re}[1] \\
 I_{2\ im}[1] \\
 I_{3\ re}[1] \\
 I_{3\ im}[1] \\
 V_{1\ re}[1] \\
 V_{1\ im}[1] \\
 V_{2\ re}[1] \\
 V_{2\ im}[1] \\
 V_{3\ re}[1] \\
 V_{3\ im}[1]
 \end{bmatrix} = \begin{bmatrix}
 (V_0^{sp} - 1) \\
 0 \\
 0 \\
 0 \\
 0 \\
 0 \\
 \gamma_{22}[1] \\
 \gamma_{32}[1] \\
 \text{real}(\gamma_{13}[1]) \\
 \text{imag}(\gamma_{13}[1])
 \end{bmatrix} \quad (5.25)$$

Equation (5.25) can be arranged in a compact form considering only specific blocks according to the type of bus and whether the variable is either current or voltage. In the example, $N = 2$, but for a generalized system with $(N + 1)$ buses, a possible arrangement is:

$$\begin{bmatrix} 0_{2 \times 2N} & I_2 & 0_{2 \times 2N} \\ -I_{2N} & Y_{b0} & Y_{b1} \\ T_1 & 0_{2N \times 2} & T_2 \end{bmatrix} \begin{bmatrix} I_i \text{ re,im}[1] \\ V_i \text{ re,im}[1] \end{bmatrix} = \begin{bmatrix} (V_0^{sp} - 1) \\ 0 \\ 0_{2N \times 1} \\ b_{2N \times 1} \end{bmatrix} \quad (5.26)$$

where I_2 is the identity matrix of order two; Y_{b0} is the two-column matrix generated from the real-valued form of $Y_{b \text{ tr}}$ taking the first two columns and deleting the first two rows (the first bus is assumed as slack-bus); Y_{b1} is equal to the real-valued form of $Y_{b \text{ tr}}$ unless both their first two columns and two rows. T_1 and T_2 are order two block-diagonal matrices, T_{1i} , T_{2i} , $i = 1, 2, \dots, N$ constructed according partition of the system of equations (5.25) and $b_{2N \times 1}$ is a vector formed from the γ 's constant as for instance in equations (5.25).

From (5.26) it is possible to apply a block Kron reduction considering as pivot the block 2×1 (an identity matrix) of the linear system coefficient matrix in that equation. So the reduced linear system is transformed to

$$\begin{bmatrix} I_2 & 0_{2 \times 2N} \\ T_1 Y_{b0} & (T_2 + T_1 Y_{b1}) \end{bmatrix} \begin{bmatrix} V_i \text{ re,im}[1] \end{bmatrix} = \begin{bmatrix} (V_0^{sp} - 1) \\ 0 \\ b \end{bmatrix} \quad (5.27)$$

As matter of fact in (5.27) it is needed to solve just the linear system associated to PQ- and PV-buses, since from this equation we have the result for the slack-bus as $V_0 \text{ re}[1] = (V_0^{sp} - 1)$ and $V_0 \text{ im}[1] = 0$. Therefore, the final linear system which must be solved for $2N$ equations and $2N$ unknowns is:

$$\begin{bmatrix} (T_2 + T_1 Y_{b1}) \end{bmatrix} \begin{bmatrix} V_1 \text{ re}[1] \\ V_1 \text{ im}[1] \\ \vdots \\ V_N \text{ re}[1] \\ V_N \text{ im}[1] \end{bmatrix} = (b - T_1 Y_{b0} \begin{bmatrix} (V_0^{sp} - 1) \\ 0 \end{bmatrix}) \quad (5.28)$$

The set of equations (5.28) has the same dimension as the resulting linear system used to compute the power series coefficients for HELM (see for example (3.42), which is the case where $N = 2$). Also, it has the same sparsity pattern when we consider two-block submatrices, since matrices T_1 and T_2 are block-diagonal. In (3.42) the linear system coefficients is essentially dependent of the entries of the matrix $Y_{b \text{ tr}}$. On the other hand, the linear system coefficients $(T_2 + T_1 Y_{b1})$ in (5.28) works on as a weighted $Y_{b \text{ tr}}$, since it depends on this matrix and the germ solution of voltages and currents.

Therefore, *it can change if the germ solution is restarted* with another set of values. It is quite true that a new LU factorization becomes necessary every time the germ solution is changed. In the original HELM the process always use just a germ solution. This means that only one LU factorization is needed. But, it may be a limitation as will be shown through results of experiments.

5.3.1 General coefficient recursive relation for $n > 1$

We consider now the case of power series coefficients for $n > 1$. Again expressions (5.1) to (5.3) are evaluated.

For $n > 1$, general recursive relations to the expressions of PQ- and PV-buses are identified:

- PQ-buses:

$$\begin{bmatrix} V_{i\ re}[0] & V_{i\ im}[0] & I_{i\ re}[0] & I_{i\ im}[0] \\ V_{i\ im}[0] & -V_{i\ re}[0] & -I_{i\ im}[0] & I_{i\ re}[0] \end{bmatrix} \cdot \begin{bmatrix} I_{i\ re}[n] \\ I_{i\ im}[n] \\ V_{i\ re}[n] \\ V_{i\ im}[n] \end{bmatrix} = \begin{bmatrix} real(\gamma_{1i}[n]) \\ imag(\gamma_{1i}[n]) \end{bmatrix} \quad (5.29)$$

where $\gamma_{1i}[n] = -\sum_{j=1}^{n-1} V_i[n-j]I_i^*[j] - Y_i^{sh*}|V_i[n-1]|^2$.

- Voltage constraint in PV-buses:

$$\begin{bmatrix} V_{i\ re}[0] & V_{i\ im}[0] \end{bmatrix} \cdot \begin{bmatrix} V_{i\ re}[n] \\ V_{i\ im}[n] \end{bmatrix} = [\gamma_{2i}[n]] \quad (5.30)$$

where $\gamma_{2i}[n] = -\frac{1}{2}\sum_{j=1}^{n-1} V_i[n-j]V_i^*[j]$.

- PV-buses:

$$\begin{bmatrix} V_{i\ re}[0] & V_{i\ im}[0] & I_{i\ re}[0] & I_{i\ im}[0] \end{bmatrix} \cdot \begin{bmatrix} I_{i\ re}[n] \\ I_{i\ im}[n] \\ V_{i\ re}[n] \\ V_{i\ im}[n] \end{bmatrix} = [\gamma_{3i}[n]] \quad (5.31)$$

where $\gamma_{3i}[2] = -\frac{1}{2}(V_i[1]I_i[1]^* + V_i[1]^*I_i[1]) - real(Y_i^{sh*})(V_i[1]V_i[0]^* + V_i[0]V_i[1]^*)$.

In view of (5.29), (5.30) and (5.31), the coefficients of the linear system at the LHS of the equations has in common the dependency of the germ solution values ($V_i[0]$ and $I_i[0]$). This means that for a generic power series coefficient associated to a degree n in α , the related linear system is of the type $Ax = \gamma$ and A is kept constant, unless a restarted on the germ solution is activated. Only the vector γ is updated in the computation of each power series coefficient.

The computation of any coefficient can be done by a set of equation as in (5.25) by computing the solution of a linear system $Ax = \gamma$, with A kept constant and by updating the vector γ according to the coefficients associated a given degree in α of interest.

5.3.2 Linear System Variables Reduction

The set of equations (5.29) comprises two real-valued expressions and four-valued unknown variables for PQ-buses only. While (5.30) and (5.31) are other two set of real-valued equations and four-valued unknown variables, but associated specifically to PV-buses. The slack-bus does not contribute with equations along this process. Then, considering the total number of PV- and PQ-buses N , a total of $2N$ equations are formed. In the meantime, $4N$ unknown variables are associated to these equations. Therefore, another set with $2N$ equations is necessary in order to equalize the number of equations with the number of unknowns. This requirement is achieved by joining the current equations to the already highlighted equations for the PV- and PQ-buses.

The injected current equations at each bus i as a function of nodal voltages in the real-valued form can be written as:

$$\begin{bmatrix} I_{i \text{ re}}[n] \\ I_{i \text{ im}}[n] \end{bmatrix} = \sum_{j=0}^{N_b} \begin{bmatrix} G_{ij} & -B_{ij} \\ B_{ij} & G_{ij} \end{bmatrix} [V_{i \text{ re,im}}[n]] \quad (5.32)$$

where $[V_{i \text{ re,im}}[n]]^T = [V_0 \text{ re}[n] \ V_0 \text{ im}[n] \ V_1 \text{ re}[n] \ V_1 \text{ im}[n] \ \dots \ V_N \text{ re}[n] \ V_N \text{ im}[n]]$ is a vector of real and imaginary components of a number n of nodal voltage power series coefficients, respectively. The voltage at slack-bus is $V_0[n] = V_0 \text{ re}[n] + jV_0 \text{ im}[n]$.

5.3.2.1 Algorithm for Reduction of Variables

1. Establish the voltage starting conditions for each bus ($V_i = i, \dots, N$), define the slack bus voltage as V_0^{sp} and calculate $I_i^{(0)} = \sum_{j=0}^N Y_{ij} V_j^{(0)}$, $\hat{S}_i = V_i^{(0)} I_i^{(0)*}$ and $\hat{P}_i = \text{real}(\hat{S}_i)$ at PV-buses;
2. Calculate the coefficients for $n = 1$, since for $n = 0$, the voltages are stipulated and the currents and \hat{S} are calculated from $I^{(0)} = Y_{bus} V^{(0)}$;

- Expressions for PQ-buses:

$$T_{i1} = \begin{bmatrix} V_{i\ re}^0 & V_{i\ im}^0 \\ V_{i\ im}^0 & -V_{i\ re}^0 \end{bmatrix}; \quad T_{i2} = \begin{bmatrix} I_{i\ re}^0 & I_{i\ im}^0 \\ -I_{i\ im}^0 & I_{i\ re}^0 \end{bmatrix} \quad (5.33)$$

$$\gamma_{1i}[n] = \begin{cases} (S_i - \hat{S}_i) - Y_i^{sh*} |V_i[0]|^2, & n = 1 \\ -\sum_{j=1}^{n-1} V_i[n-j] I_i^*[j] - Y_i^{sh*} |V_i[n-1]|^2, & n > 1 \end{cases} \quad (5.34)$$

- Expressions for PV-buses:

$$T_{i0} = \begin{bmatrix} V_{i\ re}^0 & V_{i\ im}^0 \end{bmatrix}; \quad a_{k\ re} = \frac{\gamma_{2i}^{(0)}[n]}{V_{i\ re}^{(0)}}; \quad a_{k\ im} = \frac{V_{k\ im}^{(0)}}{V_{k\ re}^{(0)}}, \quad k \in PV \quad (5.35)$$

$$\gamma_{2i}[n] = \begin{cases} \frac{1}{2} (|V_i^{sp}|^2 - |V_i^{(0)}|^2), & n = 1 \\ -\frac{1}{2} \sum_{j=1}^{n-1} V_i[n-j] V_i^*[j], & n > 1 \end{cases} \quad (5.36)$$

$$\gamma_{3i}[n] = \begin{cases} (P_i - \hat{P}_i) - \text{real}(Y_i^{sh*}) |V_i[0]|^2, & n = 1 \\ -\sum_{j=1}^{n-1} V_i[n-j] I_i^*[j] - \text{real}(Y_i^{sh*}) |V_i[n-1]|^2, & n > 1 \end{cases} \quad (5.37)$$

3. Define the bus type (PQ-bus or PV-bus). The linear system matrix is different, according to this definition;

- Expression for PQ-buses:

$$\begin{aligned} & \sum_{\substack{j=1 \\ j \in PQ, j \neq i}}^N \begin{bmatrix} G_{ij} & -B_{ij} \\ B_{ij} & G_{ij} \end{bmatrix} \begin{bmatrix} V_{j\ re} \\ V_{j\ im} \end{bmatrix} + \left\{ \begin{bmatrix} G_{ii} & -B_{ii} \\ B_{ii} & G_{ii} \end{bmatrix} + T_{i1}^{-1} T_{i2} \right\} \begin{bmatrix} V_{i\ re} \\ V_{i\ im} \end{bmatrix} + \\ & + \sum_{\substack{k=1 \\ k \in PV}}^N \begin{bmatrix} -G_{ik} a_{k\ im} & -B_{ik} \\ -B_{ik} a_{k\ im} & G_{ik} \end{bmatrix} V_{k\ im} = \\ & \begin{bmatrix} \hat{\gamma}_{i1\ re} \\ \hat{\gamma}_{i1\ im} \end{bmatrix} = - \begin{bmatrix} G_{i0} \\ B_{i0} \end{bmatrix} V_{0\ re} - \sum_{\substack{k=1 \\ k \in PV}}^N \begin{bmatrix} G_{ik} \\ B_{ik} \end{bmatrix} a_{k\ re} + T_{i1}^{-1} \begin{bmatrix} \gamma_{i1\ re} \\ \gamma_{i1\ im} \end{bmatrix} \end{aligned} \quad (5.38)$$

- Expression for PV-buses:

$$\begin{aligned}
& \sum_{\substack{j=1 \\ j \in PQ, j \neq i}}^N T_{i0} \begin{bmatrix} G_{ij} & -B_{ij} \\ B_{ij} & G_{ij} \end{bmatrix} \begin{bmatrix} V_{j \text{ re}} \\ V_{j \text{ im}} \end{bmatrix} + \sum_{\substack{k=1 \\ k \in PV}}^N T_{i0} \begin{bmatrix} G_{ik} & -B_{ik} \\ B_{ik} & G_{ik} \end{bmatrix} \begin{bmatrix} -a_{k \text{ im}} \\ 1 \end{bmatrix} V_{k \text{ im}} + \\
& \quad + \left\{ T_{i0} \begin{bmatrix} G_{ii} & -B_{ii} \\ B_{ii} & G_{ii} \end{bmatrix} + I_{i \text{ im}}^0 - I_{i \text{ re}}^0 a_{i \text{ im}} \right\} V_{i \text{ im}} = \\
\gamma_{i1 \text{ im}} - q_i V_{0 \text{ re}} &= -I_{i \text{ re}}^0 a_{i \text{ re}} - T_{i0} \begin{bmatrix} G_{ii} \\ B_{ii} \end{bmatrix} a_{i \text{ re}} - \sum_{\substack{k=1 \\ k \in PV}}^N T_{i0} \begin{bmatrix} G_{ik} \\ B_{ik} \end{bmatrix} a_{k \text{ re}} \quad (5.39)
\end{aligned}$$

$$\text{with } q_i = \begin{bmatrix} V_{i \text{ re}}^0 & V_{i \text{ im}}^0 \\ G_{i0} \\ B_{i0} \end{bmatrix}.$$

4. Actualization

- for bus i as a PQ-bus: keep constant the two lines of $\begin{bmatrix} G_{ij} & -B_{ij} \\ B_{ij} & G_{ij} \end{bmatrix}$, updating only the (i, i) block and the coefficients at PV-buses. The product $\begin{bmatrix} G_{ik} & -B_{ik} \\ B_{ik} & G_{ik} \end{bmatrix} \begin{bmatrix} -a_{k \text{ im}} \\ 1 \end{bmatrix}$ is used to generate the two coefficient elements of $V_{k \text{ im}}$, updating also the elements of the block (i, i) ;
- for bus i as a PV-bus: Firstly, multiply all of the blocks 2×2 by T_{i0} . The coefficients of $V_{k \text{ im}}$ are obtained using this result multiplied by $\begin{bmatrix} -a_{k \text{ im}} \\ 1 \end{bmatrix}$. The (i, i) element have also to be calculated properly.

5.3.3 Padé approximant

After computing the power series coefficient an analytic continuation function is computed based on a determination of a Padé approximant. For the RHELM a reduced number of coefficient is suggested. This avoid to use values of coefficient very small/high. The computation carried out as proposed ensure that high precision required for the computation (as required for HELM when stringent operational conditions are verified) is unnecessary.

Since a Padé approximant is computed, the values for $V_i(\alpha)$ for $\alpha = 1$ are evaluated. We propose to use this partial value as starting value for an updated germ solution in order to restart the computation. Hence, this value is the updated $V_i[0]$,

which is used to compute $I_i[0]$ and \hat{S}_i . This allows that a new power series be computed leading to an associated Padé approximant. The process continues until a prescribed precision is reached. In general, we propose no more than 6 coefficients to be used at each restarted procedure.

5.3.4 Summary of RHELM Solution Process

In summary the proposed Restarted Holomorphic Embedding model applied for solving the power flow problem follows this solution process:

1. Construct the bus admittance matrix Y_{bus} using sparsity techniques;
2. Generate the Power Balance Equations for Slack-, PQ- and PV-buses holomorphically embedded using injected power $\hat{S}_i = V_i^{(0)} I_i^{(0)*}$;
3. Use the germ solution $V_i[0] = V_i^{(0)}$, where $V_i^{(0)}$ is an estimated voltage adopted in several real world tools as Matpower [14], (not necessarily a guess as employed for iterative methods like Newton's method), as the initial term for the power series in α ;
4. Construct the matrix of the recursive relation with the PBE holomorphically embedded separated into real and imaginary parts for finding the other coefficients $[n]$ of the power series contemplating until 3 pairs, chosen by the user ($n = 2$; or $n = 4$; or $n = 6$), as initial coefficients;
5. Apply an analytic continuation technique to the reduced power series, as Padé approximant, and make $\alpha = 1$ to get the solution; if the major voltage mismatch is less than a specified tolerance error, the final solution was reached; otherwise, using the last voltage solution as an updated germ, restart the calculation of extra terms, again chosen by the user ($n = 2$; or $n = 4$; or $n = 6$), as new power series coefficients for each restarting, until getting the final solution.

It is important to mention that if the Padé approximation does not converge for $\alpha = 1$, unequivocally, the power flow problem does not have solution [33].

The Figure 5.1 illustrates a flowchart about the proposed restarted holomorphic embedding power flow implementation solution method.

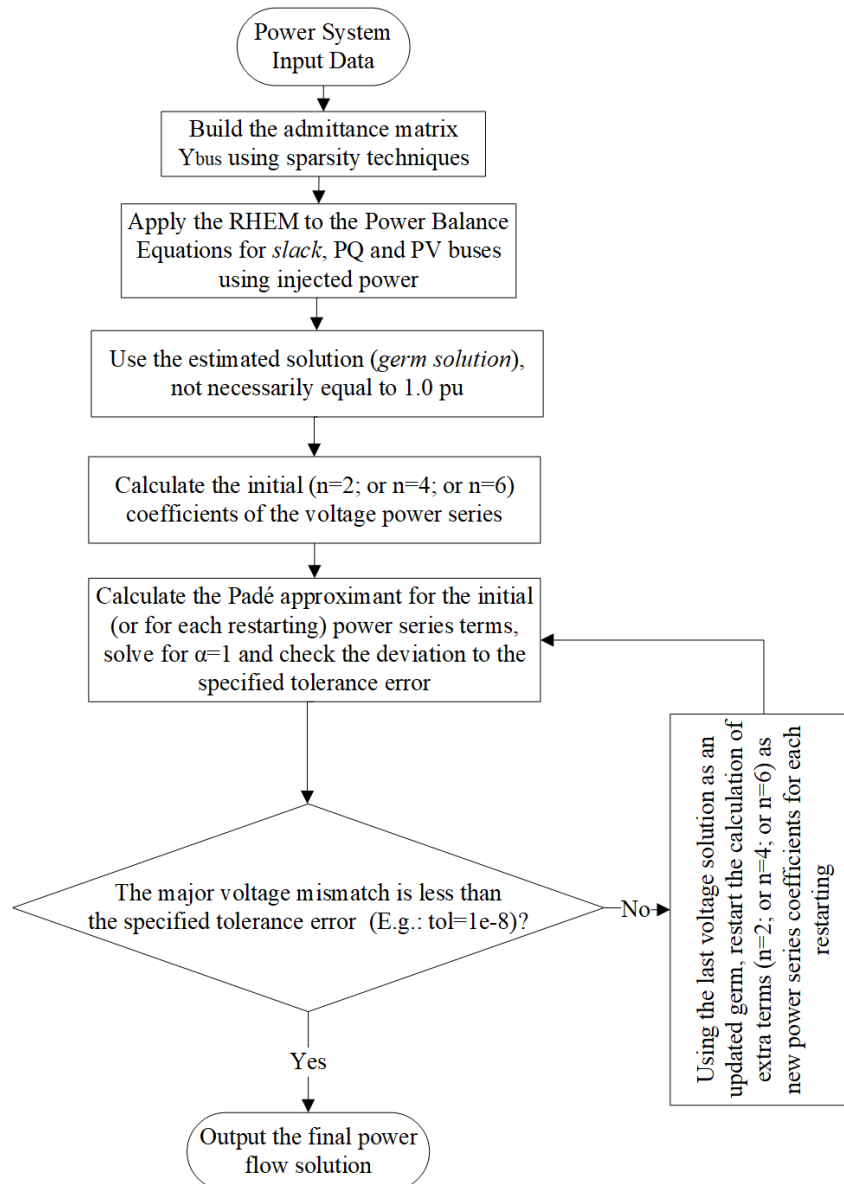


Figure 5.1: Restarted-HELM power flow solution flowchart

5.4 CONCLUSION OF THE CHAPTER

In this chapter, an improving technique to accelerate the convergence of the holomorphic embedding power flow model was presented. A detailed description about the method was highlighted. The alternative method was denominated restarted HELM, because despite to use the conventional HELM approach, it has a characteristic of allowing updating germ solution. This specific updating of partial solution provides properties to the method for better process of convergence.

The main difference on the proposed method was demonstrated in relation to the

HELM idea. In the next chapter, applications are used to demonstrate the effectiveness of the method presented in this chapter and results for comparison with the original Holomorphic Embedding solution model and also with the traditional iterative solution method Newton-Raphson (NR).

Chapter 6 EXPERIMENTS AND RESULTS

6.1 INTRODUCTION

In this chapter, the Restarted Holomorphic Embedded Load-Flow Model (RHELM) is applied for solving the power flow problem. The method is used to compute the power flow solution for different systems and their results are compared with those obtained by the original HELM [7] and the Newton-Raphson method.

The technique was implemented by using the same data pattern (input/output) of MATPOWER tool [14]. The original MATPOWER tool contains the solution technique based on Newton-Raphson method only. Thus, both the formulations of the original Holomorphic Embedding Load Flow Method (HELM) and RHELM were implemented on the MATPOWER. The HELM and NR methods are used in this work as a reference for comparison of results obtained by RHELM. Cases for normal operating conditions and situations in which there is an increase in the load of the buses to verify the variation of the voltage with the load are evaluated.

The MATLAB[®] computing environment was used as a tool to perform the simulations. The MATLAB's default double-precision floating-point mantissa was kept on running MATPOWER (no other type of accuracy with respect to the mantissa length to represent the floating-point number was studied). MATPOWER is a compatible package developed in MATLAB environment that allows the power flow calculation [14].

Several experiments are carried out in order to highlight the benefits of the proposed technique.

6.2 COMPUTATIONAL ENVIROMENT

in this section, the available computational environment is discussed. All computational implementations uses the MATLAB as base.

6.2.1 MATPOWER Structure as a Simulation Tool for Developing HELM and RHELM Models

The power balance equations of the power flow problem holomorphically embedded was implemented by using the same MATPOWER's input and output data format. This structure assures an adequate tool to compare simulation results implemented in the own MATPOWER tool and by using HELM model presented in Chapter 3 and also the proposed Restarted HELM (RHELM) technique presented in Chapter 5.

The MATPOWER is a free and open source code whose script is in MATLAB. Taking advantage of this idea, in this work a script was developed to explore the same MATPOWER's data structure and then incorporated in this free software. Therefore, a new interface to carry out similar computations with respect to bus voltage and power flow computations was unnecessary to develop. The only information transmitted to MATPOWER is a command calling new functions HELM or RHELM. The main difference with relation to the implemented techniques is that the traditional MATPOWER works just on the iterative NR method to solve PBEs, while in the modified code the problem is solved considering the methodology based on HELM and RHELM. All input data are *case.m* files as presented in the MATPOWER's platform. The input data file contains system parameters as transmission line impedance, shunt admittances and other quantities [14].

6.3 A 3-BUS ILLUSTRATIVE GENERAL SYSTEM STUDY

6.3.1 Description of the system model

The electric network in Figure 2.1 presented in Section 2.3, consists of a general three-bus (*Slack*-, PQ-, and PV-buses) system and is used here for illustrating details

of the Holomorphic Embedding Load Flow Method. The study preserves the same basic procedures when applied to real-world large-scale systems [26].

The data of transmission lines (branches) and buses are shown, in Table 6.1 and Table 6.2. In Table 6.1, R , X and B are, respectively, the resistance, reactance and shunt susceptance. In Table 6.2, the bus type follows the same standard from MATPOWER, where bus types 1, 2 and 3 represent load (PQ-bus), generator (PV-bus) bus and *slack*-bus respectively. P_d and Q_d are the active and reactive power demanded by loads connected to each bus. P_g and Q_g are the active and reactive power supplied by generators connected to the *slack*- or PV-buses. The term V^{sp} is the specified voltage in a PV-bus or *slack*-bus.

Table 6.1: Transmission Line Branch Data Specification for the 3-bus System

| From Bus | To Bus | R (pu) | X (pu) | B (pu) |
|----------|--------|--------|--------|--------|
| 1 | 2 | 0.05 | 0.15 | 0.02 |
| 1 | 3 | 0.02 | 0.10 | 0.02 |
| 2 | 3 | 0.08 | 0.40 | 0.01 |

Table 6.2: Bus Data Specification for the 3-bus System

| Bus ID | Bus Type MTP | P_d (MW) | Q_d (Mvar) | P_g (MW) | Q_g (Mvar) | V^{sp} (pu) |
|----------------------|--------------|------------|--------------|------------|--------------|---------------|
| 1- <i>slack</i> -bus | 3 | - | - | - | - | 1.00 |
| 2- <i>PV</i> -bus | 2 | 70 | 30 | 200 | 0 | 1.03 |
| 3- <i>PQ</i> -bus | 1 | 180 | 50 | - | - | - |

The Figure 6.1 shows the MATPOWER's input data (data mask) for the 3-bus System.

The admittance matrix Y_{bus} of this system (all data in pu of the 100 MVA power base and 230 kV, according to Figure 6.1) is given by:

$$Y_{bus} = \begin{bmatrix} 3.9231 - j15.5954 & -2.0000 + j6.0000 & -1.9231 + j9.6154 \\ -2.0000 + j6.0000 & 2.4808 - j8.3888 & -0.4808 + j2.4038 \\ -1.9231 + j9.6154 & -0.4808 + j2.4038 & 2.4038 - j12.0042 \end{bmatrix} pu \quad (6.1)$$

```

function mpc = case3
%CASE3 Power flow data for 3 bus (Slack-PV-PQ).
%% MATPOWER Case Format : Version 2
mpc.version = '2';
%%----- Power Flow Data -----%%
%% system MVA base
mpc.baseMVA = 100;
%% bus data
% bus_i type Pd Qd Gs Bs area Vm Va baseKV zone Vmax Vmin
mpc.bus = [
1 3 0 0 0 0 1 1.00 0 230 1 1.1 0.9;
2 2 70 30 0 0 1 1.03 0 230 1 1.1 0.9;
3 1 180 50 0 0 1 1.00 0 230 1 1.1 0.9;
];
%% generator data
% bus Pg Qg Qmax Qmin Vg mBase status Pmax Pmin Pcl Pc2 Qc1min Qc1max Qc2min Qc2max ramp_agc ramp_i0 ramp_30 ramp_q apf
mpc.gen = [
1 0 0 100 -100 1 100 1 0 0 0 0 0 0 0 0 0 0 0;
2 200 0 100 -100 1.03 100 1 500 0 0 0 0 0 0 0 0 0 0;
];
%% branch data
% fbus tbus r x b rateA rateB rateC ratio angle status angmin angmax
mpc.branch = [
1 2 0.05 0.15 0.02 250 250 250 0 0 1 -360 360;
1 3 0.02 0.10 0.02 250 250 250 0 0 1 -360 360;
2 3 0.08 0.40 0.01 250 250 250 0 0 1 -360 360;
];

```

Figure 6.1: MATPOWER's input data for the 3-bus system

The shunt elements of the Y_{bus} , represented by $Y_{ii\ sh}$ are:

$$Y_{ii\ sh} = \begin{bmatrix} j0.0200 \\ j0.0150 \\ j0.0150 \end{bmatrix} pu \quad (6.2)$$

The matrix $Y_{ij\ tr}$, which is the Y_{bus} , unless the shunt components is

$$Y_{ij\ tr} = \begin{bmatrix} 3.9231 - j15.6154 & -2.0000 + j6.0000 & -1.9231 + j9.6154 \\ -2.0000 + j6.0000 & 2.4808 - j8.4038 & -0.4808 + j2.4038 \\ -1.9231 + j9.6154 & -0.4808 + j2.4038 & 2.4038 - j12.0192 \end{bmatrix} pu \quad (6.3)$$

The power flow problem based on the HELM methodology and the system with the data of Tables 6.1 and 6.2 can be solved from (3.42) and uses terms from $Y_{ii\ sh}$ and $Y_{ij\ tr}$. The coefficients for $n = 0$, as already mentioned, can be found from the *germ* solution. The other coefficients, for generic n terms, are evaluated once the quantities in $n - 1$ and the real components of voltage in the PV buses $V_{i\ re}[n]$ are known. These voltage $V_{i\ re}[n]$, therefore, need to be calculated initially, as described in Section 3.4.

$$\begin{bmatrix} 1 & 0 & 0 & 0 & 0 & 0 \\ 0 & 1 & 0 & 0 & 0 & 0 \\ -2.0000 & -6.0000 & 0 & 8.4038 & -0.4808 & -2.4038 \\ 6.0000 & -2.0000 & 1 & 2.4808 & 2.4038 & -0.4808 \\ -1.9231 & -9.6154 & 0 & -2.4038 & 2.4038 & 12.0192 \\ 9.6154 & -1.9231 & 0 & -0.4808 & -12.0192 & 2.4038 \end{bmatrix} \begin{bmatrix} V_{1 \text{ re}}[n] \\ V_{1 \text{ im}}[n] \\ Q_2[n] \\ V_{2 \text{ im}}[n] \\ V_{3 \text{ re}}[n] \\ V_{3 \text{ im}}[n] \end{bmatrix} = \begin{bmatrix} \delta_{n1}(V_i^{sp} - 1) \\ 0 \\ re \{1.3W_2^*[n-1] - j \sum_{k=1}^{n-1} Q_2[k]W_2^*[n-k] - 0.015V_2[n-1]\} \\ im \{1.3W_2^*[n-1] - j \sum_{k=1}^{n-1} Q_2[k]W_2^*[n-k] - 0.015V_2[n-1]\} \\ re \{(-1.8 + j0.5)W_3^*[n-1] - 0.015V_3[n-1]\} \\ im \{(-1.8 + j0.5)W_3^*[n-1] - 0.015V_3[n-1]\} \end{bmatrix} - \begin{bmatrix} 0 \\ 0 \\ 2.4808 \\ 8.4038 \\ -0.4808 \\ 2.4038 \end{bmatrix} V_{2 \text{ re}}[n], \quad n = 1, 2, \dots \quad (6.4)$$

Once the coefficients are obtained, the resulting series for the voltages at the 3 buses and the reactive power in bus 2 are approximated using (3.44) that corresponds to the analytic continuation by Padé approximant to the power series, resulting in a division of polynomials. The coefficients of these polynomials are found by (3.46) to (3.48). Finally, the solution for each variable can be evaluated in $\alpha = 1$ for a tolerance error of 1×10^{-8} for the voltage mismatch. In MATPOWER this tolerance is a metric to evaluate the accuracy of power mismatch in pu of the the NR method. To reach this tolerance error, 16 coefficients of the power series are calculated. Consequently, the diagonal Padé approximant have 8^{th} order, i.e., $M = N = 8$, which can also be represented as a Padé approximant [8/8].

For illustration, the voltage power series for the voltage at bus 2 is given by:

$$\begin{aligned} V_2(\alpha) = 1 + (0.0304 + j0.1094)\alpha + (-0.0064 - j0.0034)\alpha^2 + (0.0006 + j0.0007)\alpha^3 + \dots \\ + (2.209e^{-12} + j4.616e^{-12})\alpha^{16} \end{aligned} \quad (6.5)$$

The diagonal Padé approximant for bus 2 is evaluated as:

$$V_2(\alpha) = \frac{1 + (-0.5777 + j0.0572)\alpha + \dots + (2.2952e^{-7} + j2.3838e^{-7})\alpha^8}{1 + (-0.6082 - j0.0522)\alpha + \dots + (5.672e^{-8} + j1.7236e^{-7})\alpha^8} \quad (6.6)$$

which, for $\alpha = 1$, gives $V_2(\alpha) = 1.030\angle 5.949^\circ$ pu.

It is important to mention that both coefficients for the power series and for the rational polynomial fraction are complex numbers.

Table 6.3 presents the final results for the 3-bus system.

Table 6.3: Results for the 3-bus System

| Bus | Voltage | | Generation | | Load | |
|--------------|--------------------|---------------------|------------------|---------------------------------|------------------|---------------------------------|
| | <i>Mag</i> (pu) | <i>Ang</i> (deg) | <i>P</i> (MW) | <i>Q</i> (MVA _r) | <i>P</i> (MW) | <i>Q</i> (MVA _r) |
| 1 | 1.000 | 0.000 | 59.43 | 65.83 | - | - |
| 2 | 1.030 | 5.949 | 200.00 | 51.64 | 70.00 | 30.00 |
| 3 | 0.921 | -7.248 | - | - | 180.00 | 50.00 |
| Total | | | 259.43 | 117.47 | 250.00 | 80.00 |

The output data with the results for the 3-bus system provided by MATPOWER is shown in Figure 6.2.

```

=====
|      Bus Data      |
=====
Bus      Voltage      Generation      Load
#      Mag(pu) Ang(deg)      P (MW)      Q (MVAr)      P (MW)      Q (MVAr)
-----
  1  1.000   -0.000*    59.43    65.83         -         -
  2  1.030    5.949   200.00    51.64    70.00    30.00
  3  0.921   -7.248         -         -   180.00    50.00
-----
          Total:    259.43    117.47    250.00    80.00
=====

|      Branch Data      |
=====
Brnch   From   To   From Bus Injection   To Bus Injection   Loss (I^2 * Z)
#       Bus   Bus   P (MW)  Q (MVAr)  P (MW)  Q (MVAr)  P (MW)  Q (MVAr)
-----
  1     1     2   -68.94    5.68    71.34   -0.54    2.399    7.20
  2     1     3   128.37   60.15   -124.32 -41.78    4.044   20.22
  3     2     3    58.66   22.19   -55.68   -8.22    2.984   14.92
-----
                          Total:    9.426    42.33
=====

```

Figure 6.2: MATPOWER's output data for the 3-bus system

The voltages have a fixed modules for buses 1 and 2, as expected. The *slack*-bus and the PV-bus, provide sufficient active and reactive power to supply the loads. The difference between the generated power and the power consumed in the loads correspond to the losses in the lines, which is also obtained in the output of the modified MATPOWER tool for HELM model.

6.4 2-BUS TEST-SYSTEM STUDY

In order to evaluate the results of solutions obtained by the studied methods in comparison to traditional NR, including loading up to near the point of voltage collapse and above this point, a study was made considering the generic 2-bus system of Figure 6.3. The study was conducted of two ways. At the first strategy, the loading at bus 2 was incremented until divergence has been occurred. In the second study, the load was kept constant, but the impedance Z of the interconnection circuit was modified simulating a contingency at the circuit. All experiments aim to evaluate the performance of the non-iterative methods HELM and the proposed one RHELM. The NR method was employed as iterative method.

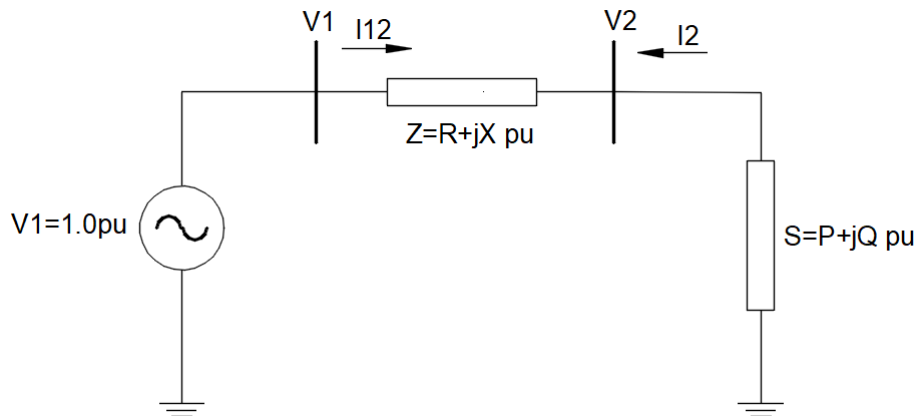


Figure 6.3: 2-bus system for analysis of convergence and existence of solutions by NR, HELM and RHELM

The exact (analytic) value of the voltage at bus 2 was computed in order to be used as reference for comparison of the results of the iterative and non-iterative numerical methods.

The current I_2 injected at bus 2 is $I_2 = (V_2 - V_1)/Z$. The injected complex power at bus 2 is $S = V_2 I_2^*$. Then, the expression $V_2(V_2^* - V_1^*) = Z^* S = \rho + j\lambda$ must be satisfied. In view of this details, we have the complex-valued equation $|V_2|^2 - V_2 V_1^* -$

$\rho - j\lambda = 0$. Assume that $V = V_2$. So, since V_1 is a known real-valued voltage, this can be broken into two real-valued equations given by

$$V_{re}^2 + V_{im}^2 - V_1 V_{re} - \rho = 0 \quad (6.7)$$

$$V_{im} = -\lambda \quad (6.8)$$

From (6.8) the imaginary part of V is always $V_{im} = -\lambda$. Then from (6.7), the real part of V is computed by:

$$V_{re} = \frac{V_1}{2} \pm a, \quad a = \sqrt{(V_1/2)^2 - (\lambda^2 - \rho)} \quad (6.9)$$

From (6.9) it is evident that when a assumes a complex value, the value V_{re} becomes meaningless from the point of view of real numbers. This information can be used to determine whether the numerical problem is divergent for iterative methods or the the result obtained for the voltage Padé approximant oscillates. When a is zero means that the two roots in (6.9) are equals. Then HV and LV solutions coincides. This is equivalent to find the voltage collapse point of the system. However, at this point the classical NR method diverges, since the Jacobian matrix is singular.

6.4.1 Study for Different Loadings

Experiments were carried out by considering three cases. For these cases an impedance $Z = 0.1 + j0.2$ pu was used. The methods NR, HELM and RHELM were evaluated. The method HELM computes the coefficients and from this the voltage Padé approximant is obtained. For a Padé approximant order, for example $[1/1]$, two coefficients of the power series are necessary.

With relation to the RHELM, we perform an initial run to compute a power series coefficients followed by a Padé approximant determination. This result is used to initialize a restarting process and generate an updated germ solution. It is possible to use only two coefficients for the initial run (before the restarting process). From the first restarting, a fixed number of coefficients are always established by the user in function of the highest polynomial degree and a Padé approximant of degree M , $[M/M]$, is calculated. But, the user can select this number of coefficients according to the experiments. The highest order degree of the initial power series coefficients are

designated as N_0 , the restarting number as R_n and the degree order of power series terms per restarting is assigned as N_R . In this simulation, for convenience, six initial power series terms ($N_0 = 6$) and each restart (R_n) with other six coefficients ($N_R = 6$) were kept.

The system was analyzed in its original configuration (case 1 - even for this load level note that the operational point is far from the ideal conditions, say near voltage 1.0 pu) and its condition was evaluated for an absolute tolerance error between the value of voltage V_2 calculated accurately and by the Padé approximation. Up to 35 terms were allowed for each Padé order. For this nominal situation the NR method converged with 6 iterations and the HELM and the RHELM obtained the same voltage solution, reaching a tolerance error of 6.3×10^{-9} and 1.5×10^{-9} , respectively. The Padé order for the HELM was $[32/32]$. The RHELM required only 1 restarting ($R_n = 1$). Then, the orders of Padé for this case were: $[3/3]$ (for the first run); and $[3/3]$ (for the first and single restarting). This means that only 12 coefficients were needed to determine the results, but 6 at a time per polynomials and a single restarting. Therefore, a number very reduced of coefficients were evaluated if compared to the 64 coefficients required for the HELM. Note that just Padé approximant at most order 6 was needed in this evaluation for RHELM.

In the loading level 2 (case 2) the load was increased by 4.0%. In this last operating condition, the system had finite result for the voltage only by the RHELM method, whereas both the original HELM (find results with Padé order $[35/35]$, but with tolerance 1.1×10^{-2}) and the NR methods diverged until 10 iterations. The RHELM obtained the solution with an error of 6×10^{-15} and required only 4 restarting ($[3/3] + 4 \times [3/3]$). Again, only Padé approximant of order $[3/3]$ were adopted and the degree a of polynomial for the power series has order 6. For this case 30 coefficients, which is equivalent to 5 polynomial each one of order 6. The system was also analyzed under a situation of severe overload, for 50% above the load condition from the case 1 (case 3). For this situation no operational voltage was found. In fact, for this condition the term a computed by using (6.9) has a complex value, confirming the lack of real-valued solution for the problem.

The results are summarized in Table 6.4. Column 1 indicates the case analyzed and column 2 the value of the load used. Columns 3 and 4 show the voltage magnitude and angle obtained by the NR/HELM/RHELM solution methods. Column 5 represents the maximum error tolerance specified for the voltage deviation in relation to the

exact value. Column 6 indicates the number of iterations by NR or whether this method diverges (represented by “**DIV**”). Column 7 represents the error obtained by the HELM method. Finally, Columns 8 to 11 represent the initial number of coefficients N_0 before the restarts, the number of coefficients N_R by each restarting of the RHELM, the restarting number R_n , and the error obtained by the RHELM method for this configuration, respectively.

Table 6.4: Convergence results by NR \times HELM \times RHELM for different load levels

| Case | Load $P+jQ$ (pu) | Voltage V_2 | | Max Spec. Error | MTP (NR) It. N° | HELM Error $\ V\ _\infty$ | RHELM | | | |
|------|----------------------------|------------------------|-------------------------|-----------------------|-----------------------|---------------------------------|---------|-------|-------|-------------------------|
| | | <i>Mag</i> (pu) | <i>Ang</i> (deg) | | | | Config. | | | Error $\ V\ _\infty$ |
| | | | | | | | N_0 | N_R | R_n | |
| 1 | 1.00+j0.600 | 0.618 | -13.092 | 1e-8 | 6 | 6.3e-9 | 6 | 6 | 1 | 1.5e-9 |
| 2 | 1.04+j0.624 | 0.522 | -16.211 | 1e-8 | DIV | 1.1e-2 | 6 | 6 | 4 | 6e-15 |
| 3 | 1.50+j0.900 | - | - | 1e-8 | DIV | DIV | 6 | 6 | 9 | DIV |

The Figure 6.4 illustrates graphically the deviation between the exact value of the voltage at bus 2 and the value calculated by the RHELM and HELM as the number of coefficients is increased and the order of a polynomial of the Padé approximation for the three levels of loading. From this point all vertical plot are assumed in \log_{10} (base 10 logarithmic) scale.

The results of Table 6.4 and Figure 6.4 indicate that the RHELM has a better convergence than the original HELM in the original situation (case 1), reaching 1.5×10^{-9} , and the solution coincides with that obtained by the traditional MATPOWER (NR). For case 2, it is observed that the traditional MATPOWER (NR) does not converge for a specified error tolerance of 1×10^{-8} and a limit of 10 iterations. The HELM reached a poor convergence of 1.1×10^{-2} . The RHELM signals that the solution exists and is observed a too much better convergence result, reaching 6×10^{-15} .

In case 3, all methods diverge, confirmed by the exact evaluation previously detected. For the non-iterative methods the results are evidenced for both the HELM and RHELM through oscillations in the rational fraction of Padé approximant as observed in [9], [12].

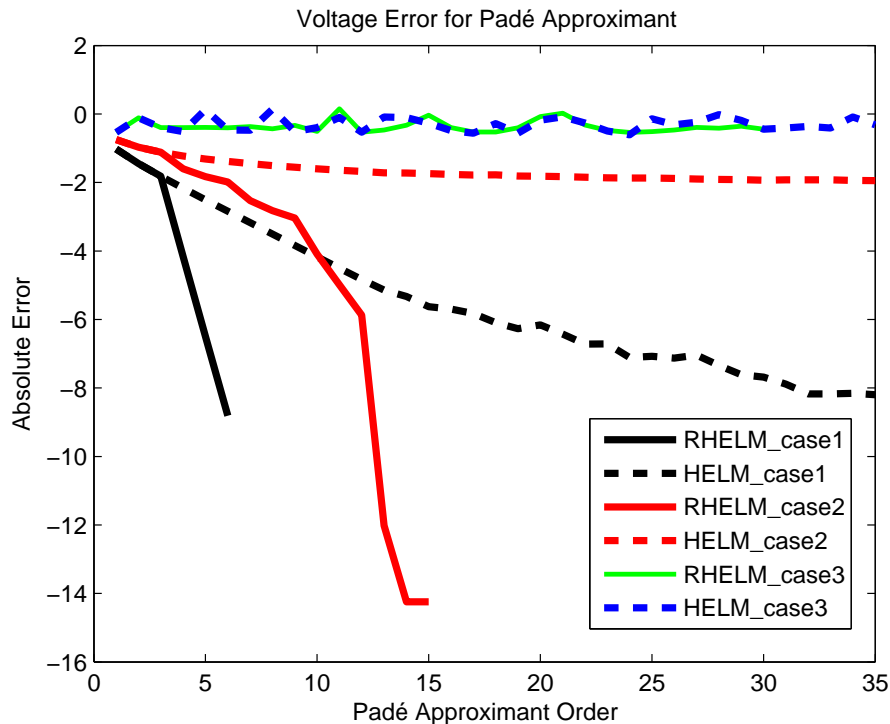


Figure 6.4: Errors obtained for different load levels by the RHELM and HELM for case 1 to 3 for a maximum Padé order $L = M = 35$

6.4.2 Study with Different Parameters for the Interconnection Circuit

In this section the influence of the interconnection circuit impedance Z is evaluated (only the reactance was changed). The load at bus 2 was kept constant with the value $S = 1.0 + j0.60 pu$.

The results are summarized in Table 6.5. Column 1 indicates the case analyzed and column 2 the value of the impedance used. Columns 3 and 4 show the exact voltage magnitude and angle obtained analytically. Column 5 represents the maximum error tolerance specified for the voltage deviation in relation to the exact value. Column 6 indicates the number of iterations by NR or whether this method diverges (represented by “**DIV**”). Column 7 represents the error obtained by the HELM method. Finally, columns 8 to 11 the initial number of coefficients N_0 before the restarting, the number of coefficients N_R by each restarting of the RHELM, the number of restarts R_n , and the error obtained by the RHELM, respectively.

Figure 6.5 illustrates graphically the deviation between the exact value of the voltage at bus 2 and the calculated value by the HELM and RHELM as a function of

Table 6.5: Convergence results by NR \times HELM \times RHELM for different line reactances

| Case | Impedance $R+jX$ (pu) | Voltage V_2 | | Max Spec. Error | MTP (NR) It. N $^\circ$ | HELM Error $\ V\ _\infty$ | RHELM | | | |
|------|---------------------------------|------------------------|-------------------------|-----------------------|-------------------------------|---------------------------------|---------|-------|-------|-------------------------|
| | | <i>Mag</i> (pu) | <i>Ang</i> (deg) | | | | Config. | | | Error $\ V\ _\infty$ |
| | | | | | | | N_0 | N_R | R_n | |
| 1 | 0.1+j0.20000 | 0.618 | -13.092 | 1e-8 | 6 | 6.3e-9 | 6 | 6 | 1 | 1.5e-9 |
| 2 | 0.1+j0.21100 | 0.546 | -16.061 | 1e-8 | 8 | 8.4e-4 | 6 | 6 | 3 | 5.5e-16 |
| 3 | 0.1+j0.21166 | 0.524 | -16.816 | 1e-8 | DIV | 1.0e-2 | 6 | 6 | 4 | 8.1e-15 |

the number of coefficients and the order of the Padé approximant (up to $L = M = 35$) for the three values of impedance Z .

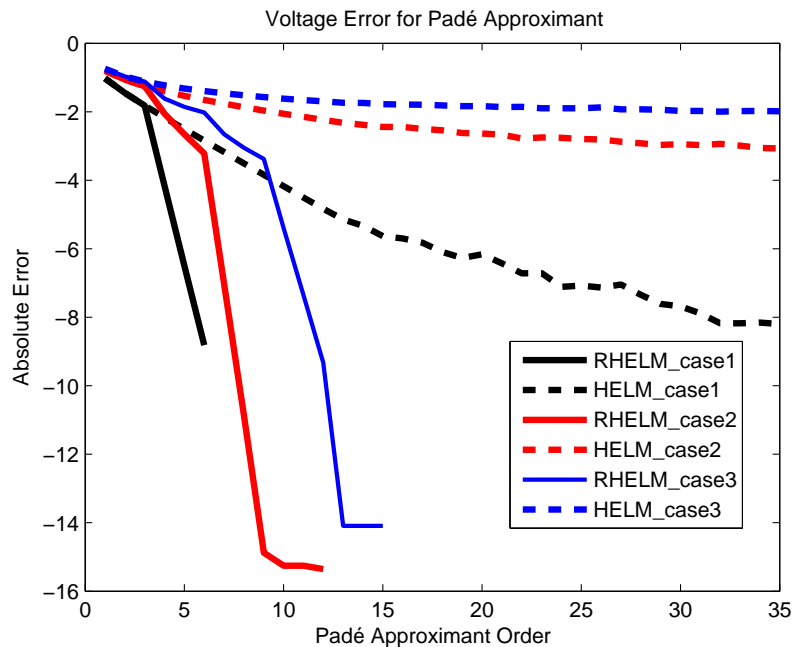


Figure 6.5: Errors obtained for different transmission line configurations by the RHELM and HELM for case 1 to 3 for a maximum Padé approximant order $L = M = 35$

For the case 1 the NR method needed 6 iterations to converge. The HELM and the RHELM obtained the same voltage solution, reaching a tolerance error of 6.3×10^{-9} and 1.5×10^{-9} , respectively. It is important to cite that this case 1 is the same of the previous subsection. So, the Padé order for the HELM was $L = M = 32$ and only 1 restarting was necessary for the RHELM, besides the initial process computation. For the case 2 and considering the tolerance error of 1×10^{-8} , the system had finite result for the voltage by the RHELM and NR. The original HELM did not achieve the required accuracy, since the error obtained for it was 8.4×10^{-4} . The NR methods

required 8 iterations to converge. The RHELM obtained the solution with an error of 5.5×10^{-16} and 3 restarting. The system was also analyzed under a critical situation near the voltage collapse. Even for this new situation, the system had finite result for the voltage only by the RHELM, whereas the original HELM (with an error of 1.0×10^{-2}) and the NR method diverged up to 10 iterations. On the other hand, the RHELM obtained the solution with an error of 8.1×10^{-15} using only 4 restarting.

6.5 ANALYSIS FOR MULTIBUS TEST SYSTEMS

This section aims to extend the investigation considering experiments with larger system models usually adopted as benchmark for tests.

All investigations cover tests involving the accuracy and convergence related to the studied methods. Hence, in order to evaluate the performance of the solution convergence for both the RHELM and HELM, several test system models were evaluated by applying the proposed approach RHELM, the original HELM, and NR method all making use of the own or modified MATPOWER input/output interface [14].

For each test system case analyzed in this section, a graphical result is presented considering the absolute error obtained for the Padé approximant voltage for the RHELM (continuous line) and for the HELM model (dotted) line. Both methods are limited for a 15 Padé approximant order, i.e., the final solution for each method may contain up to $n = 30$ power series degrees. If a tolerance error (1×10^{-8}) is reached, it means that the solution of the non-iterative methods RHELM and/or HELM are both the same. Again this tolerance is computed in relation to the determined voltage solution obtained by MATPOWER (result used as reference voltage). For the RHELM 3 quantities are set: N_0 , which is the initial polynomial degree before the restart, the N_R , which is the the degree order of the polynomial series by each restarting, and the R_n , which is the restarting number with N_R . All initial germ solution for RHELM coincides with those ones adopted as guess for running the case in MATPOWER. For the HELM it is considered the error obtained for a polynomial coefficient until it reaches the tolerance error of (1×10^{-8}) or the error obtained for a limit of a 15 degree Padé approximant order.

6.5.1 9-Bus System

The IEEE 9-bus system consists of 9 buses, 3 generators, 3 power transformers, 6 lines and 3 loads. The convergence results for the RHELM model with an initial quantity of power series degree ($N_0 = 4$) and allowing a number of restarts ($R_n = 1$) with a number ($N_R = 6$) of coefficients for each restart as well the results for the HELM model applied for this system is represented in Figure 6.6.

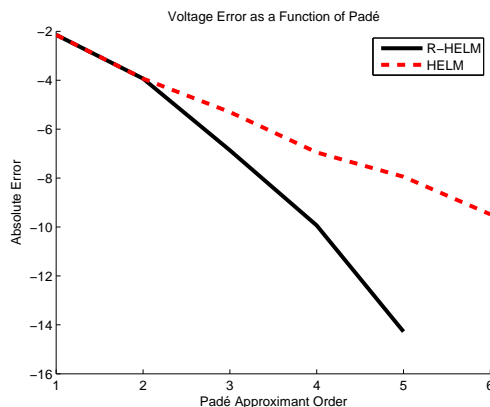


Figure 6.6: Solution convergence results by the RHELM and the original HELM methods for the 9-bus system

For this case the NR method needed 4 iterations to converge. The HELM and the RHELM obtained the same voltage solution, reaching a tolerance error of 3.3×10^{-10} and 5.0×10^{-15} , respectively. The Padé order for the HELM was $[L = M = 6]$.

6.5.2 14-Bus System

The IEEE 14-bus test case has 14 buses, 5 generators, and 11 loads. The convergence results for the RHELM model with a initial quantity of power series terms ($N_0 = 4$) and allowing a number of restarts ($R_n = 1$) with a number ($N_R = 4$) of coefficients for each restart as well the results for the HELM model applied for this system is represented in Figure 6.7.

For this case the NR method needed 4 iterations to converge. The HELM and the RHELM obtained the same voltage solution, reaching a tolerance error of 4.7×10^{-9} and 8.4×10^{-10} , respectively. The Padé order for the HELM was $[L = M = 10]$ and 1 restarting was necessary for the RHELM.

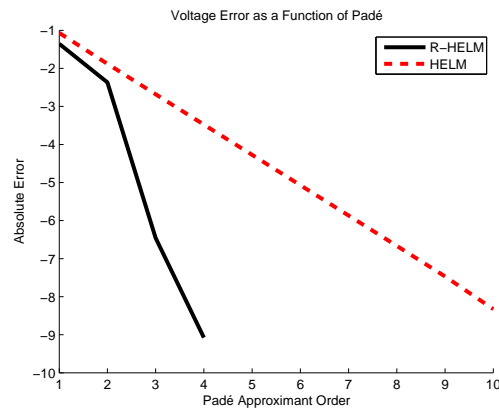


Figure 6.7: Solution convergence results by the RHELM and the original HELM methods for the 14-bus system

6.5.3 39-Bus System

The IEEE 39-bus test system contains 39 buses, 32 transmission lines, 24 transformers and 10 generators. The convergence results for the RHELM model with an initial degree of power series ($N_0 = 2$) as well as the results for the HELM model applied for this system are represented in Figure 6.8. It is important to cite that none restart was necessary for the RHELM in this case.

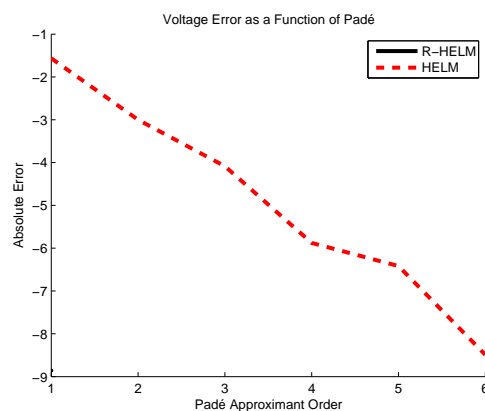


Figure 6.8: Solution convergence results by the RHELM and the original HELM methods for the 39-bus system with $N_0 = 2$, $R_n = 0$ and $N_R = 0$

Only for illustration, the Figure 6.9 represents the situation where for an initial degree of the power series terms ($N_0 = 2$) it was allowed a number of restarts ($R_n = 1$) with a number ($N_R = 2$) of coefficients. For this single restart, it is evident that the solution obtained by the RHELM would be reached without the necessity of any restart.

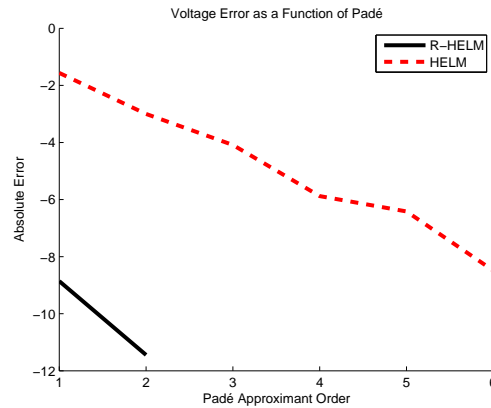


Figure 6.9: Solution convergence results by the RHELM and the original HELM methods for the 39-bus system with $N_0 = 2$, $R_n = 1$ and $N_R = 2$

For this case in both situations the NR method needed 1 iteration to converge and the HELM and RHELM obtained the same voltage solution. The HELM achieved a tolerance error of 3.2×10^{-9} with a Padé order of $[L = M = 6]$. The RHELM in the first situation ($N_0 = 2$) reached a tolerance error of 1.4×10^{-9} and none restarting was necessary, getting a Padé order of $[L = M = 1]$, whereas the starting solution is already the converged solution with the required precision. In the second situation, the RHELM, with a configuration of $N_0 = 2$, $R_n = 1$ and $N_R = 2$, obtained an yet too better performance of 3.6×10^{-12} with a Padé order of $[L = M = 2]$.

6.5.4 118-Bus System

The IEEE 118-bus test system consists of 118 buses, 54 synchronous machines, 20 of which are compensators and 15 motors. The convergence results for the RHELM model with an initial degree of power series terms ($N_0 = 4$) and allowing a number of restarts ($R_n = 1$) with a number ($N_R = 4$) of coefficients for each restart as well as the results for the HELM model applied for this system is illustrated in Figure 6.10.

For this case the NR method needed 4 iterations to converge. The HELM and the RHELM obtained the same voltage solution, reaching a tolerance error of 4.3×10^{-9} and 1.6×10^{-11} , respectively. The Padé order for the HELM was $[L = M = 6]$ and 1 restarting was necessary for the RHELM.

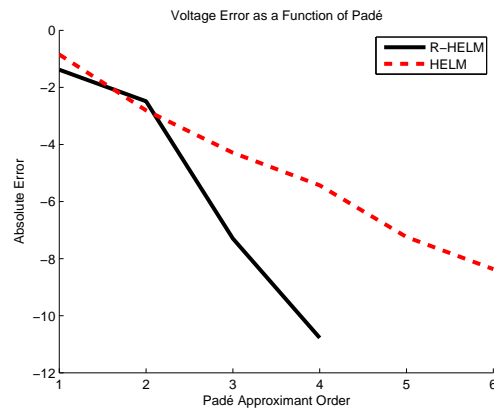


Figure 6.10: Solution convergence results by the RHELM and the original HELM methods for the 118-bus system

6.5.5 300-Bus System

The IEEE 300-bus test system contains 69 generators, 306 transmission lines, 174 transformers and 197 loads. The convergence results for the RHELM model with an initial degree of power series terms ($N_0 = 4$) and allowing a number of restarts ($R_n = 2$) with a number ($N_R = 4$) of coefficients for each restart as well as the results for the HELM model applied for this system is exhibited in Figure 6.11.

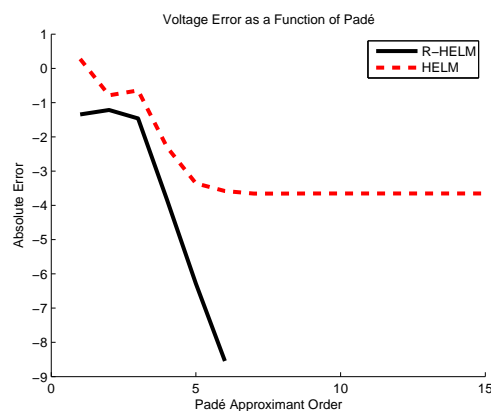


Figure 6.11: Solution convergence results by the RHELM and the original HELM methods for the 300-bus system

For this case the NR method needed 5 iterations to converge. The HELM did not converge, reaching an error of 2.2×10^{-4} which is outside of the limit of 1.0×10^{-8} . The RHELM obtained the same voltage solution of the NR method, reaching a tolerance error of 2.8×10^{-9} with 2 restarts.

6.5.6 1354-Bus System

The network contains 1354 buses, 260 generators, and 1991 branches. The convergence results for the RHELM model with an initial quantity of power series terms ($N_0 = 2$) and allowing a number of restarts ($R_n = 6$) with a number ($N_R = 2$) of coefficients for each restart as well the results for the HELM model applied for this system is represented in Figure 6.12. Concerning the RHELM, note that for this system we have used only 2 terms for the power series, either at first stage before restarting or along the restarting.

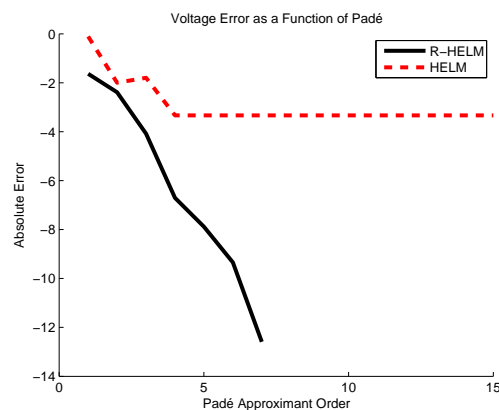


Figure 6.12: Solution convergence results by the RHELM and the original HELM methods for the 1354-bus system

For this case the NR method needed 4 iterations to converge. The HELM did not converge, reaching an error of 4.6×10^{-4} which is outside of the limit of 1.0×10^{-8} . The RHELM obtained the same voltage solution of the NR method, reaching a tolerance error of 2.6×10^{-13} with 6 restarts.

6.5.7 9241-Bus System

The 9241-Bus system represents a more complex European transmission network and it contains 9241 buses, 1445 generators, and 16049 branches. The convergence results for the RHELM model with a initial quantity of power series terms ($N_0 = 2$) and allowing a number of restarts ($R_n = 6$) with a number ($N_R = 2$) of coefficients for each restart as well the results for the HELM model applied for this system is represented in Figure 6.13. Again only polynomials with 2 terms were used for the RHELM.

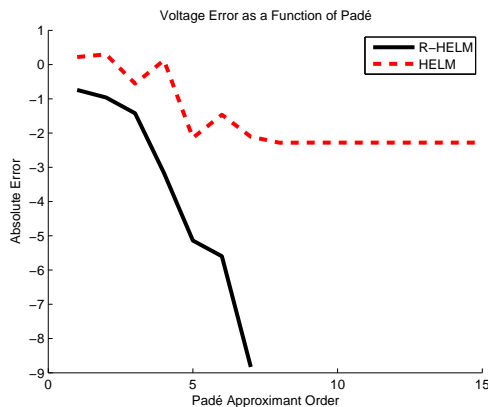


Figure 6.13: Solution convergence results by the RHELM and the original HELM methods for the 9241-bus system

For this case the NR method needed 5 iterations to converge. The HELM did not converge, reaching an error of 5.0×10^{-3} which is outside of the limit of 1.0×10^{-8} . The RHELM obtained the same voltage solution of the NR method, reaching a tolerance error of 1.4×10^{-9} with 6 restarts.

6.5.8 Other Experiments with Smaller Number of Restarting

In this subsection we have done other experiments for the 300-, 1354- and 9241-bus systems in order to investigate how the number of restarting on RHELM cause influence on the performance of the method. Table 6.6 presents two cases (*case 1* and *case 2*), where this evaluation is analyzed.

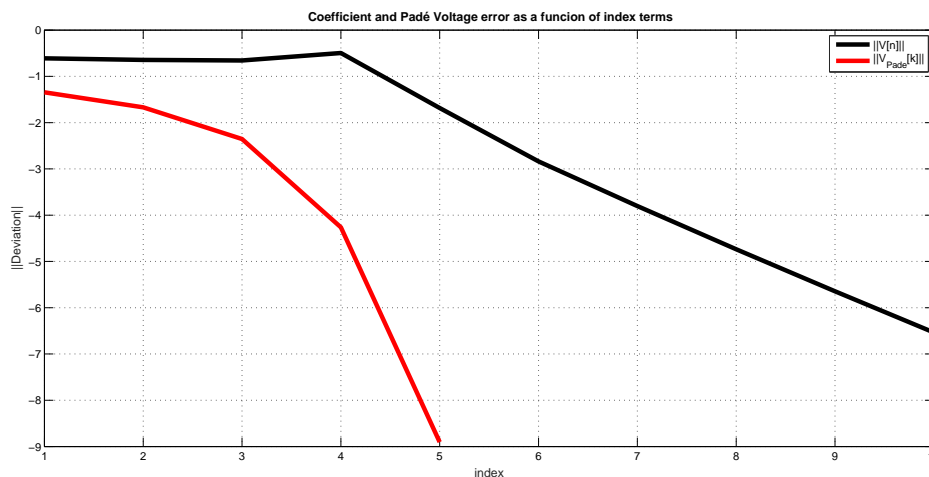
From Table 6.6 in *case 1*, it is observed that there is more restarting than in *case 2*, although the order of the degrees of the polynomials are smaller in *case 1*. However, the RHELM determines the expected solution with error specified in both cases. This fact illustrates the numerical robustness of the method for this flexibility with respect to the amount of restarting and the degrees of the power series polynomials. The smaller the number of restarting, the less number of LU factorization is required in the calculation process. This reduces the computational cost since the execution time in the LU factorization is much higher than the calculation of the coefficients of the power series, as will be shown later.

Figures 6.14, 6.15 and 6.16 illustrate plots on the voltage absolute error for the 300-, 1354- and 9241-bus models, respectively. It is observed that despite the

Table 6.6: Results of experiments for different restarting evaluated on the 300-, 1354- and 9241-bus models

| Model | Case 1 | | | | Case 2 ($N_R = 6$) | | |
|-------|--------|-------|-------|-----------------------|----------------------|-------|-----------------------|
| | N_0 | R_n | N_R | Error | N_0 | R_n | Error |
| 300 | 4 | 2 | 4 | 2.8×10^{-9} | 4 | 1 | 1.8×10^{-9} |
| 1354 | 2 | 6 | 2 | 2.6×10^{-13} | 2 | 1 | 7.1×10^{-9} |
| 9241 | 2 | 6 | 2 | 1.4×10^{-9} | 2 | 2 | 4.8×10^{-10} |

reduced number of restarting along the numerical calculation of the voltage power series coefficients (and consequently the Padé approximant), the RHELM always reaches a correct solution when this exists. Also, the restarting process speed-up the process of convergence characteristic, which is not verified on HELM. Therefore, the flexibility in being able to explore the characteristics of the germ solution is one of the strong points of the proposed method. Another aspect to highlight is that RHELM performed well for all size of system studied in this work. On the contrary, HELM has failed for converging to the specified tolerance error for the three biggest systems studied in this Master's Dissertation.

Figure 6.14: Solution convergence results by the RHELM when $R_n = 1$ for the 300-bus system

It is important to cite that the time convergence is a problem to the original HELM [9]. The code implemented for the RHELM shows to be faster than the HELM. However, both techniques are relatively slower when compared to the NR method. But the advantage of the RHELM is that it demands a few order Padé approximant for reaching the required precision and it preserves the same advantages of the original HELM, ensuring, unequivocally to find a solution if it exists.

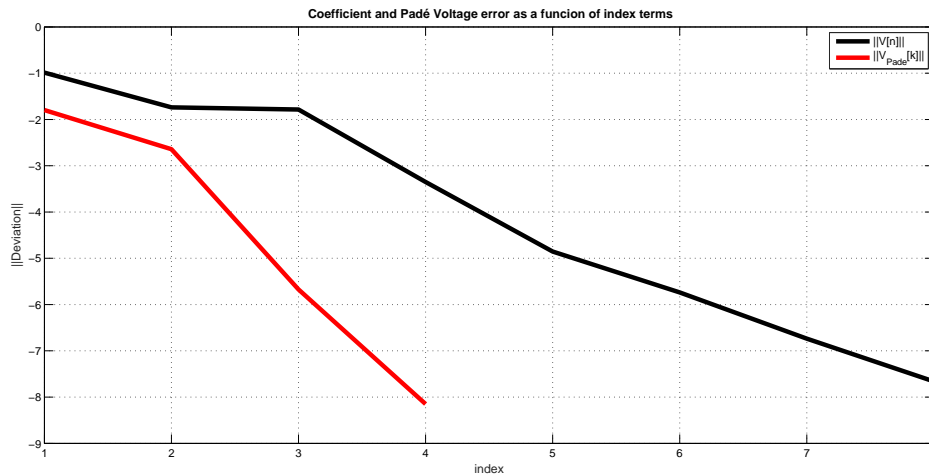


Figure 6.15: Solution convergence results by the RHELM when $R_n = 1$ for the 1354-bus system

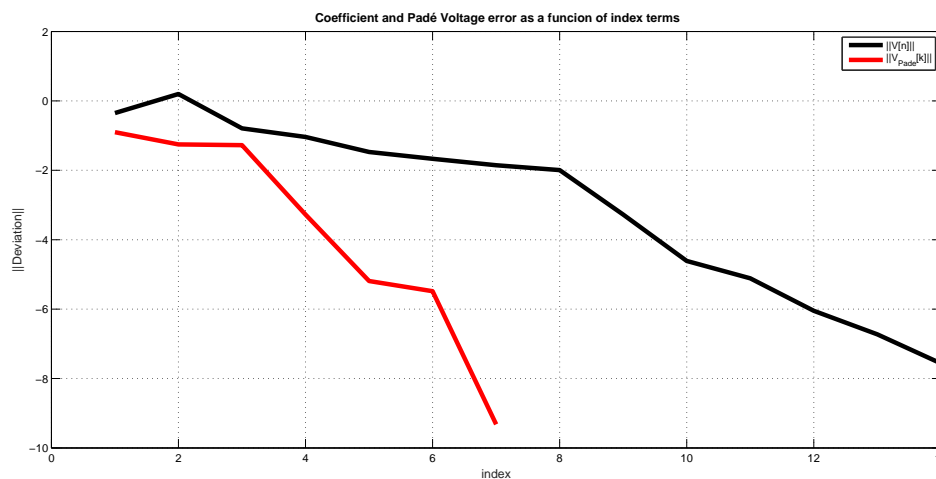


Figure 6.16: Solution convergence results by the RHELM when $R_n = 2$ for the 9241-bus system

6.6 EXECUTION TIME CHARACTERISTICS

In this section the problem of execution time related to specific characteristics of each one of the RHELM, HELM and NR method is evaluated. We have chosen to perform experiments on the 39-, 118-, 300-, 1354- and 9241-bus models. Smaller systems present computation burden very reduced in such way that the computational cost may be neglected. The characteristics of the 39- and 118-bus models were discussed in Subsection 6.5.3 and 6.5.4, respectively. For the bigger systems, we explore the characteristics presented in *case 2* shown in Table 6.6.

All execution times were observed in seconds. The metric to measure these times took into account the execution of specific loops for calculations. These specific loops were considered for those parts with higher calculation burden for each one of the methods. So details on calculations of each method are highlighted. All the calculation were repeated according to the size of the system and taken the mean of the execution time. So the information is already the execution mean time obtained for each method. For the 39-, 118- and 300-bus model, we repeated the calculation 1000 times. But for higher systems as 1354- and 9241-models the repetition was carried out 100 times. All computations were carried out in MATLAB on AMD Intel[®] Core[™] i7 CPU with 2.5 GHz and 16 GB RAM.

Table 6.7 yields the execution time, in seconds, for main partial computational and total burden related to RHELM numerical implementation. The partial parts are called Reduction, LUPQR, Solver and Padé. The last row of the table gives the total execution time for the method. Each partial part are described as follows:

Reduction: process which is carried out to convert systems such as (5.12) into (5.15); the system is reduced from $4N$ unknowns to $2(N-1)$ unknowns;

LUPQR: perform the factorization LUPQR of the matrix of the linear system coefficients;

Solver: perform the solution of a linear system by using the LUPQR factors finding before;

Padé: perform an economy-size computation of the Padé approximants (until 6 degrees are allowed).

Table 6.7: Execution time relative to the computational burden performed by RHELM for the 39-, 118-, 300-, 1354- and 9241-bus systems

| Type | 9241 | 1354 | 300 | 118 | 39 |
|--------------|-------------|--------------------|----------------------|----------------------|----------------------|
| Reduction | 0.4604 | 0.0139 | 0.0031 | 0.00119 | 3.0×10^{-4} |
| LUPQR | 0.2508 | 0.0174 | 0.0037 | 0.00136 | 2.3×10^{-4} |
| Solver | 0.1205 | 0.0085 | 0.0020 | 7.2×10^{-4} | 1.1×10^{-4} |
| Padé | 0.0082 | 9×10^{-4} | 2.7×10^{-4} | 1.3×10^{-4} | 3.1×10^{-5} |
| Total | 0.858 | 0.0408 | 0.0091 | 0.0034 | 6.8×10^{-4} |

Table 6.8 yields the execution time, in seconds, for main partial computational and total burden related to HELM numerical implementation. The partial parts considered for this method are the factorization LUPQR, the solver and Padé computations. Again, the last row of the table gives the total execution time required by the method.

Table 6.8: Execution time relative to the computational burden performed by HELM for the 39-, 118-, 300-, 1354- and 9241-bus systems

| Type | 9241 | 1354 | 300 | 118 | 39 |
|--------------|-------------|-------------|------------|----------------------|----------------------|
| LUPQR | 0.0859 | 0.0095 | 0.0017 | 7.2×10^{-4} | 2.5×10^{-4} |
| Solver | 0.202 | 0.0113 | 0.0032 | 2.6×10^{-4} | 1.7×10^{-4} |
| Padé | 27.55 | 3.003 | 0.6924 | 0.0099 | 0.00494 |
| Total | 28.044 | 3.023 | 0.6974 | 0.0109 | 0.00537 |

Finally, Table 6.9 yields the execution time, in seconds, for main partial computational and total burden related to NR numerical implementation on MATPOWER. Now, the partial parts considered for this method are the mismatch, Jacobian construction and solver computations. Again, the last row of the table gives the total execution time.

Table 6.9: Execution time relative to the computational burden performed by NR method for the 39-, 118-, 300-, 1354- and 9241-bus systems

| Type | 9241 | 1354 | 300 | 118 | 39 |
|--------------|----------------------|----------------------|-----------------------|----------------------|-----------------------|
| Mismatch | 4.4×10^{-3} | 3.3×10^{-4} | 1.54×10^{-4} | 6.1×10^{-5} | 1.5×10^{-5} |
| Solver | 0.4595 | 0.03066 | 0.0067 | 0.00211 | 2.0×10^{-4} |
| Jacobian | 0.0708 | 0.00719 | 0.0017 | 5.6×10^{-4} | 9.4×10^{-5} |
| Total | 0.5347 | 0.03817 | 0.0086 | 0.00273 | 3.12×10^{-4} |

Table 6.10 exhibits the ratio of the execution time with relation to the execution time of the NR method. The RHELM require cost computational almost similar to the NR method. So we can consider it as competitive at this level with NR. Besides it has the characteristics of the HELM solution. The HELM, on the other hand is very intensive for large-scale systems. A hard cost is demanded to compute the Padé approximant.

From these results it is demonstrated the high efficiency of the RHELM performance compared to the original HELM. Considering only the biggest system

Table 6.10: Ratio of the execution time with relation to the execution time of the NR method

| Method | 9241 | 1354 | 300 | 118 | 39 |
|---------------|-------------|-------------|------------|------------|-----------|
| RHELM | 1.60 | 1.07 | 1.06 | 1.25 | 2.17 |
| HELM | 52.4 | 79.19 | 81.0 | 3.99 | 17.2 |

(9241-bus model), we observe that the ratio of the total execution time between the RHELM and NR method is about 1.6. On the other hand, when this ratio is for the HELM this figure goes to 52.4. This last result agrees with high intensive computational cost reported in [9] for HELM and the high computational cost to determine the Padé approximant. In that paper a ratio of 55.8 for the 300-bus model and 8.5 for the 118-bus model was found. The authors in [9] reported an improving on the Padé implementation for the HELM results, but it reduced the ratio for 12.3 and 5.0, respectively.

It is important to cite that the time convergence is a problem to the original HELM [9]. The code implemented for the RHELM shows to be considerably faster than the HELM. But the advantage of the RHELM is that it demands just a few order Padé approximant for reaching the required precision and it preserves the same advantages of the original HELM, ensuring, unequivocally to find a solution if it exists.

6.7 CONCLUSION OF THE CHAPTER

In this chapter experiments implemented to assess the performance of RHELM was assessed. Several results show the superior performance compared to HELM. Evaluation of execution mean time has demonstrated that the RHELM is competitive with NR method and presents the HELM benefit characteristics.

It is demonstrated that the RHELM accelerates the solution convergence when compared with the HELM. Thus it is necessary less terms of the voltage power series and, consequently, a low order Padé approximant to get the same solution that would be obtained by the HELM and NR methods. Exactly, the proposed scheme of restarting the HELM presented in this work, has a great impact on the convergence process.

It was also demonstrated the advantages of the HELM and, consequently, the new approach RHELM, which maintains the same advantages in addition to have the faster

convergence property. Thus, it was showed that the non-iterative methods guarantees the existence of the solution if one exists and signals unequivocally if no solution exists.

Chapter 7 CONCLUSION

7.1 GENERAL CONCLUSIONS

This work presented the basic formulation for the general power flow problem, some conventionally adopted solution for iterative methods and also a recently non-iterative method based on an Holomorphic Embedding Method (HEM). This technique consists on embedding a given set of equation through a variable known as embedding parameter, α . The problem is formulated in such way that for the equivalent problem evaluated for an unitary value of α we recover the solution of the original problem.

The HEM application to the power flow problem was called HELM [7]. This method treats the power flow representation in two steps: firstly, a power series for approximating the voltage is calculated. But, in general these power series has very small convergence radius at the value of the embedding parameter. Then, due to the need to expand the radius of convergence, a transformation is sought by analytic continuation technique. Hence, in a second stage the power series is converted into a rational fraction of polynomials denominated Padé approximant. Therefore, the approximated numerical solution is verified when the embedding parameter is set in the unit.

The HELM is based on the computation of the power series from a single germ solution. This solution is equivalent to have the same slack-bus voltage replicated for all bus, since no shunt connection and no load are assumed to be connected to the buses. For systems with high level of loading the coefficients of the voltage power series can stagnate in a very small absolute value. This fact also contributes to a stagnation of the analytic function for the embedding parameter unitary without a specified error tolerance being achieved. Some works need to extend the precision of the floating-point mantissa numbers besides the double-precision usually dealt with in MATLAB to get adequate results [39].

In this work we propose to modify the HELM by including initial values associated to a germ solution and restarting the process with an updated germ solution which

has better information about the desired solution. This way we called this alternative method as Restarted HELM (RHELM). The change in HELM has provided a significant improvement in the convergence process for the solution of interest of the problem and maintains the characteristic of the HELM when it is verified that the problem has no real solution. A mark of our proposal is to work with power series of very low order. So, the computations are carried out only on the MATLAB environment without needing to extend the double-precision accuracy adopted by this tool.

In the RHELM a first germ solution is used to generate a power series in general quadratic or no more than bi-quadratic. Differently of HELM approach, the germ solution is applied to a network which allows the computation of an initial current at each bus (in the original HELM all currents are zero, since initially the problem is treated at no load). This first germ solution can be generated by applying the own conventional HELM. So, in our approach each germ solution is initial value dependent. The closer the initialization is to the solution, the better the convergence process. This means less number of restarting or even none. Still for the initial germ solution, after calculating the voltages power series, then a rational fraction based on a Padé approximant is computed for this power series. The result for an embedding parameter unitary allows to generate a first approximation of the bus voltages. Then this result of voltages is used as initial values for a first restarting process, where an updated power series is determined. The same determination for the Padé approximant is verified and also the computation of the approximated bus voltage by fixing again the new embedding parameter at unit. The process continues in restarting until a prescribed error tolerance is reached.

RHELM offers advantages and possibilities to reach the required solution precision with a few terms of the Padé approximant (differently of HELM) and a very reduced number of restarting. The proposed method always presents convergence for the solution when it exists. Also, presents similar characteristics to the HELM when the power flow has no real-valued solution. The method was tested for system of low- and large-scale size and always presented fast and robust characteristic of convergence, even for operations near the point of voltage collapse.

The description of the information in the manuscript was gathered in some chapters with the theoretical basis on the subject and a chapter in which experiments are presented for demonstrating the effectiveness of the proposed methodology.

The Chapter 1 presented the contextualization of the power flow study importance, the existing solution methods, the motivation and objectives for the approach proposed in this work.

The Chapter 2 described the power flow problem formulation and some methods applied for solving it, since the traditional well known iterative methods, as Gauss Seidel (GS) method, Newton-Raphson (NR) method and Fast Decoupled Load Flow (FDLF) method, until a non iterative method (Series Load Flow), which did not have success for real power systems magnitude. Some inherent problems associated with the iterative methods were exposed. These conventional methods perform reliably for the meshed system operating at near nominal conditions, but they are initial estimate dependent, and they face convergence issues when the system is under contingency or heavily loaded.

The Chapter 3 described the formulation based on the non iterative, but recursive technique, Holomorphic Embedding Method (HEM), which applied to the load flow problem (HELM). For a better understanding of the problem solution using the HEM, the description based on a simple three-bus electric system was presented. It was also demonstrated how to obtain Padé approximant, an analytical continuation technique which is a process to enlarge greatly the radius of convergence of the power series for HELM. This is a required procedure to obtain the final solution to the problem, unless a tolerance error. They have explained the advantages of the HELM, which is not dependent on an initial solution guess and guarantees to find the operational solution if it exists and unequivocally signals if the problem does not have this solution.

The Chapter 4 presented a bibliographical review on works related to progress on HELM. A detailed description of references covering works published since 2012 is presented. It was inferred with this literature review that the HELM still motivate investigations on the theme.

The Chapter 5 presented in details the improving technique proposed in this work. The proposed method aims to accelerate the convergence of the holomorphic embedding power flow model, called Restarted HELM (RHELM). The alternative method was denominated Restarted HELM, because despite to use the conventional HELM approach, it has a characteristic of allowing updating the germ (initial seed) solution. It was demonstrated that this specific updating of partial solution provides characteristics to the method for optimizing the convergence process.

The Chapter 6 presented the implementation results, discussion emphasizing performance comparisons involving the proposed RHELM, HELM and Newton-Raphson methods. It was demonstrated that the RHELM accelerates the solution convergence when compared with the HELM. Thus it is necessary less terms of the voltage power series and, consequently, a low order Padé approximant to get the same solution that would be obtained by the HELM and NR methods. Several test systems were employed for carrying out experiments aiming to demonstrate the performance of the proposed technique.

7.2 FUTURE WORK SUGGESTIONS

The HELM method was launched recently and has several investigations for getting new approaches to improve this novel non-iterative technique for solving the power flow problem. Therefore, some research still deserves attention. The technique proposed in this work (RHELM) aims to accelerate the convergence using a low order Padé approximant to the original HELM. But this new approach is also HELM-based and demands some improvements, among which it is cited:

- The inclusion of different type of load modeling, since in this work only the constant power model was assumed;
- The consideration of the operational limits to the reactive power sources and other devices;
- The assessment of other analytic continuation techniques for providing higher precision to decrease the round-off errors during the calculation of the voltage power series;
- The study for applying the RHELM and HELM to aid the identification of the weakest bus of the power system, aiming to estimate the voltage collapse point; and also,
- The inclusion of the HVDC modeling and implementations for power flow analysis on direct current systems.

Bibliography

- [1] Empresa de Pesquisa Energética - “Brazilian Energy Balance 2017, Year 2016,” Rio de Janeiro: EPE, 2017
- [2] A. B. M. S. Ali. “Smart Grids: Opportunities, Developments, and Trends.” Springer London, 2013.
- [3] J.J. Grainger and W.D. Stevenson, “Power Systems Analysis,” McGraw-Hill, New York, Jan. 1994.
- [4] Y. Feng, “Solving for the Low-Voltage/Large-Angle Power-Flow Solutions by using the Holomorphic Embedding Method,” Doctoral Dissertation, Arizona State University, Jul. 2015.
- [5] S. Iwamoto and T. Tamura, “A Load Flow Calculation Method for Ill-Conditioned Power Systems,” IEEE Transactions on Power Apparatus and Systems, Apr. 1981, vol. PAS-100, no. 4, pp. 1736-1743.
- [6] P. Sauer, “Explicit Load-Flow Series and Functions,” IEEE Transactions on Power Apparatus and Systems, 1981, vol. PAS-100, no. 8, pp. 3754-3763.
- [7] A. Trias, “The Holomorphic Embedding Load-Flow Method,” Power and Energy Society General Meeting, pp. 1-8, July 2012.
- [8] G. Baker, P. Graves-Morris, “Padé approximants,” Series: Encyclopedia of Mathematics and its applications, Cambridge University Press, 1996.
- [9] S. Rao, Y. Feng, D. J. Tylavsky and M. K. Subramanian, “The Holomorphic Embedding Method Applied to the Power-Flow Problem,” in IEEE Transactions on Power Systems, vol. 31, no. 5, pp. 3816-3828, Sept. 2016.
- [10] A. Trias, “Fundamentals of the Holomorphic Embedding Load-Flow Method,” ArXiv e-prints, no. 1509.02421, Sep. 2015.

-
- [11] M. K. Subramanian, Y. Feng and D. Tylavsky, "PV Bus Modeling in a holomorphically Embedded Power-Flow Formulation," North American Power Symposium (NAPS), Manhattan, KS, 2013.
- [12] Shruti D. Rao, Daniel J. Tylavsky, and Yang Feng, "Estimating the Saddle-node Bifurcation Point of Static Power Systems Using the Holomorphic Embedding Method," International Journal of Electrical Power and Energy Systems, vol. 84, pp. 1-12, 2017.
- [13] A. Trias and J. L. Marín, "The Holomorphic Embedding Loadflow Method for DC Power Systems and Nonlinear DC Circuits," IEEE Trans. Circuits Syst. I, Reg. Papers, vol. 63, no. 2, pp. 322-333, Feb. 2016.
- [14] R. D. Zimmerman, C. E. Murillo-Sánchez, and R. J. Thomas, "MATPOWER: Steady-State Operations, Planning and Analysis Tools for Power Systems Research and Education," IEEE Trans. Power Syst., vol.26, no. 1, pp. 12-19, Feb. 2011.
- [15] P. Murty, "Power Systems Analysis." Hyderabad, India: BSP, 2007.
- [16] J. Arrillaga and C. P. Arnold, "Computer Analysis of Power Systems." Christchurch, New Zealand: John Wiley & Sons, 1990.
- [17] Expósito, A.G.; Gomez, E.A.; Conejo, A.J.; Canizares, C. "Electric Energy Systems: Analysis and Operation." CRC Press: Boca Raton, FL, USA, 2009.
- [18] G. W. Stagg A. El-Abiad "Computer Methods in Power System Analysis." in New York: McGraw-Hill 1968.
- [19] L. L. Grigsby "Power Systems." in New York: CRC Press 2006.
- [20] Carvalho, A. G. "Solução das Equações de Fluxo de Carga a Partir de Aproximações de Padé de Tensões Nodais de Barra." Departamento de Engenharia Elétrica, Universidade de Brasília, Brasília, DF, 53p. 2017.
- [21] H. Saadat, "Power System Analysis." McGraw-Hill, 2010.
- [22] B. Stott, "Review of Load-Flow Calculation Methods," Proceedings of the IEEE, vol. 62, No. 7, pp. 916-929, Jul. 1974.
- [23] J. D. Glover, M. S. Sarma and T. J. Overbye, "Power System Analysis and Design 5th Edition," Cengage Learning, Stamford, 2011.

-
- [24] A. Göran “Power System Analysis.” EEH - Power Systems Laboratory, ETH Zürich, Sep. 2012.
- [25] Afolabi, O.A., Ali, W.H., Cofie, P., Fuller, J., Obiomon, P. and Kolawole, E.S. “Analysis of the Load Flow Problem in Power System Planning Studies.” *Energy and Power Engineering*, vol. 7, pp. 509-523, Sep. 2015.
- [26] Y. Li, “Effect of Various Holomorphic Embeddings on Convergence Rate and Condition Number as Applied to the Power Flow Problem.” Master Thesis, Arizona State University, Nov. 2015.
- [27] S.P. Suetin, “Padé Approximants and the Effective Analytic Continuation of a Power Series,” *Russian Math. Surveys*, 57:1 (2002), 43-141.
- [28] I.J.Nagrath D.P.Kothari “Modern Power System Analysis.” Tata Mcgraw-Hill Newdelhi India 2003.
- [29] W. Xu, Y. Liu, J. C. Salmon, T. Le and G. W. K. Chang, “Series Load Flow: A Novel Non-Iterative Load Flow Method,” in *IEEE Proceedings - Generation, Transmission and Distribution*, vol. 145, no. 3, pp. 251-256, May 1998.
- [30] Ahlfors L.V., “Complex Analysis: an Introduction to the Theory of Analytic Functions of One Complex Variable,” McGraw-Hill, 1979.
- [31] Golub, G.H. and Von Loan, C.F., “Matrix Computations,” The Johns Hopkins University Press, Third Edition, London, UK, 1996.
- [32] A. C. Santos, F. D. Freitas and L. F. J. Fernandes, “Holomorphic Embedding Approach as an Alternative Method for Solving the Power Flow Problem,” 2017 in *Workshop on Communication Networks and Power Systems (WCNPS)*, Brasília, Brazil, 2017, pp. 1-4.
- [33] M. K. Subramanian, “Application of Holomorphic Embedding to the Power-Flow Problem,” Thesis Presented in Partial Fulfillment of the Requirements for the Degree Master of Science, pp. 13, Arizona State University, Jul. 2014.
- [34] S. Rao and D. Tylavsky, “Theoretical Convergence Guarantees Versus Numerical Convergence Behavior of the Holomorphically Embedded Power Flow Method.” In: *International Journal of Electrical Power and Energy Systems*. 2018 ; Vol. 95. pp. 166-176
- [35] H. Stahl, “The convergence of Padé Approximants to Functions with Branch Points,” *J. Approximation Theory*, vol. 91, no. 2, pp. 139-204, 1997.

-
- [36] A. C. Santos, F. D. Freitas and L. F. J. Fernandes, "Load Flow Problem Formulation as a Holomorphic Embedding Method," 2018 in *VII Simpósio Brasileiro de Sistemas Elétricos (SBSE)*, Niterói, Brazil, 2018, pp. 1-6.
- [37] A. Trias, "System and Method for Monitoring and Managing Electrical Power Transmission and Distribution Networks," U.S. Patent 7,519,506 and 7,979,239, Apr. 14, 2009, and Jul. 12, 2011.
- [38] Y. Feng and D. Tylavsky, "A Novel Method to Converge to the Unstable Equilibrium Point for a Two-Bus System," 2013 in North American Power Symposium (NAPS), Manhattan, KS, pp. 1-6, Nov. 2013.
- [39] B. Schmidt, "Implementation and Evaluation of the Holomorphic Embedding Load Flow Method," Master Thesis, Technical Univ. Munchen, Mar. 2015.
- [40] S. S. Baghsorkhi, S. P. Suetin, "Embedding AC Power Flow in the Complex Plane Part I: Modelling and Mathematical Foundation," arXiv:1604.03425v2, Jul. 2016
- [41] I. Wallace et al., "Alternative PV Bus Modelling with the Holomorphic Embedding Load Flow Method," arXiv:1607.00163v1, Jul. 2016.
- [42] S. Rao and D. Tylavsky, "Nonlinear Network Reduction for Distribution Networks Using the Holomorphic Embedding Method," 2016 in North American Power Symposium (NAPS), Denver, CO, pp. 1-6, Sep. 2016.
- [43] A. Shukla, S. Kesharwani and S. N. Singh, "Efficient Holomorphic Based Approach for Unit Commitment Problem," 2016 in National Power Systems Conference (NPSC), Bhubaneswar, pp. 1-6, Dec. 2016.
- [44] P. S. Sauter, C. A. Braun, M. Kluwe and S. Hohmann, "Comparison of the Holomorphic Embedding Load Flow Method with Established Power Flow Algorithms and a New Hybrid Approach," 2017 Ninth Annual IEEE Green Technologies Conference (GreenTech), Denver, CO, 2017, pp. 203-210, Mar. 2017.
- [45] B. Wang, C. Liu and K. Sun, "Multi-Stage Holomorphic Embedding Method for Calculating the Power-Voltage Curve," in *IEEE Transactions on Power Systems*, vol. PP, no. 99, pp. 1-1, Jun. 2017.
- [46] C. Liu, B. Wang, F. Hu, K. Su, and C. Leth, "Real-Time Voltage Stability Assessment for Load Areas Based on the Holomorphic Embedding Method," arXiv:1702.01464v2, Jun. 2017.

-
- [47] S. Rao, "Exploration of a Scalable Holomorphic Embedding Method Formulation for Power System Analysis Applications." Doctoral Dissertation, Arizona State University, Jul. 2017.
- [48] Y. Zhu, D. Tylavsky and S. Rao, "Nonlinear Structure-Preserving Network Reduction Using Holomorphic Embedding," in IEEE Transactions on Power Systems, vol. PP, no. 99, pp. 1-1, Aug. 2017.
- [49] M. Basiri-Kejani and E. Gholipour, "Holomorphic Embedding Load-Flow Modeling of Thyristor-Based FACTS Controllers," in IEEE Transactions on Power Systems, vol. 32, no. 6, pp. 4871-4879, Nov. 2017.
- [50] C. Liu, B. Wang, X. Xu, K. Su, D. Shi and C. Leth, "A Multi-Dimensional Holomorphic Embedding Method to Solve AC Power Flows," Accepted by IEEE Access (10.1109/ACCESS.2017.2768958) Oct. 2017.